

©[2013]

YAO CHENG

ALL RIGHTS RESERVED

A General Birnbaum-Saunders Model and its  
Application in ALT Models

by

Yao Cheng

A thesis submitted to the

Graduate School-New Brunswick

Rutgers, the State University of New Jersey

in partial fulfillment of the requirements

for the degree of

Master of Science

Graduate Program in Industrial and Systems Engineering

written under the direction of

Dr. Elsayed A. Elsayed

and approved by

---

---

---

---

New Brunswick, New Jersey

January 2013

# ABSTRACT OF THE THESIS

## A General Birnbaum-Saunders Model and its Application in ALT Models

by

Yao Cheng

Thesis Director:

Elsayed A. Elsayed

Fatigue, recognized as one of the main causes of failures of mechanical and electrical components, is a class of structural damage that occurs when material is exposed to cyclic application of stress with varying or constant amplitudes. It is necessary to develop suitable lifetime distributions to predict the reliability and useful life of components or systems which experience fatigue failure due to random or constant amplitude loading during their usage.

Birnbaum and Saunders (1968) propose the standard Birnbaum-Saunders (SB-S) distribution which belongs to the normal distribution family to fit the fatigue failure data to a life distribution. This model has a single dominant crack which appears and grows as the structure experiences repeated load cycles up to the

point that the crack is sufficiently long to cause failure.

The underlying assumptions, derivations, probability density function (*pdf*), cumulative density function (*cdf*), hazard function, reliability function, characteristics and properties of SB-S distribution have been investigated. The hazard function of SB-S distribution is shown to be always upside-down, which is limited because it fails to cover other types of failure conditions.

In this thesis, we overcome the limitations of the SB-S distribution in modeling different types of failure rates and generalize the SB-S to be generalized Birnbaum-Saunders (GB-S) distribution. We present the characteristics of the distribution and the sufficient and necessary conditions that enable it to model multiple failure conditions. We also verify that the GB-S distribution provides better fit to failure data and propose new methodologies for the estimation of the parameters of the GB-S distribution for different sample sizes and shape parameters.

An accelerated life testing (ALT) model can utilize the accelerated failure data to predict the reliability and lifetime of components or systems under normal environments. In this research, we develop the GB-S based ALT models, and deal with the inference procedure. We compare the performance of GB-S accelerated model with other ALT models. We also develop the GB-S based accelerated life testing plans for reliability performance prediction since a properly designed ALT plan makes the reliability estimation and prediction more efficient.



## **ACKNOWLEDGEMENT**

I would like to express my deep gratitude to my advisor Professor Elsayed A. Elsayed for his patience, support, and inspiration through this research. Professor Elsayed's knowledge of the field and his personality has a profound influence upon my graduate and general education. Without his patient encouragement, this thesis could not have been accomplished.

My sincere thanks are extended to Professor Kang Li, Professor Hoang Pham for serving on my committee and providing valuable suggestions.

I also take this opportunity to thank Ms Cindy Ielmini for her support.

## TABLE OF CONTENTS

ABSTRACT OF THE THESIS .....	ii
ACKNOWLEDGMENT .....	iv
CHAPTER 1 INTRODUCTION.....	1
1.1 Background and Motivation of Research.....	1
1.2 Problem Statement.....	6
1.3 Thesis Organization.....	10
CHAPTER 2 LITERATURE REVIEW.....	12
2.1 Properties and Characteristics of SB-S Distribution.....	12
2.2 Parameters' Estimation Methodologies.....	17
2.3 GB-S Distribution and SB-S Related Distributions.....	20
2.4 SB-S Accelerated Model.....	23
2.4.1 ALT Models.....	23
2.4.2 SB-S Distribution Based ALT Model.....	24
2.5 Conclusion.....	26
CHAPTER 3 STANDARD BIRNBAUM-SAUNDERS (SB-S)	
DISTRIBUTION.....	28
3.1 Assumptions and Derivation of SB-S Distribution.....	28
3.1.1 Assumptions of the SB-S Distribution.....	29
3.1.2 Derivation of the SB-S Distribution.....	30
3.2 Maximum Likelihood Estimation (MLE) and Modified Moment Estimation	
(MME) of SB-S Distribution.....	33

3.2.1 MLE of SB-S Distribution.....	33
3.2.2 MME of SB-S Distribution.....	35
3.2.2.1 Moment Estimation (ME) of SB-S Distribution.....	36
3.2.2.2 Modified Moment Estimation (MME) of SB-S Distribution.....	36
3.3 Hazard Function of SB-S Distribution.....	38
3.3.1 Shape of the Hazard Function.....	38
3.3.2 Change Point of SB-S Distribution's Hazard Function.....	41
3.4 Conclusion.....	43
CHAPTER 4 GENERALIZED BIRNBAUM-SAUNDERS (GB-S)	
DISTRIBUTION.....	44
4.1 Characteristics and Properties of GB-S Distribution.....	44
4.1.1 GB-S Distribution.....	45
4.1.2 Characteristics and Properties of GB-S Distribution.....	47
4.1.2.1 Characteristics of GB-S Distribution.....	47
4.1.2.2 Properties of GB-S Distribution.....	51
4.2 Hazard Function of GB-S Distribution.....	52
4.3 Simulation Study.....	66
4.4 Conclusion.....	70
CHAPTER 5 GB-S DISTRIBUTION'S PARAMETER	
ESTIMATION.....	71
5.1 Maximum Likelihood Estimation (MLE).....	71
5.1.1 The Estimation Function.....	72

5.1.2 Fisher Information Matrix and Variance-Covariance Matrix.....	73
5.2 Modified Maximum Likelihood Estimation (MMLE).....	76
5.3 Simulation Study.....	80
5.3.1 Computation Procedure.....	80
5.3.2 Simulation Results.....	82
5.4 Conclusion.....	85
CHAPTER 6 GB-S ACCELERATED LIFE MODEL.....	86
6.1 GB-S and Other Accelerated Models.....	87
6.1.1 The Inverse Power Law Accelerated Models.....	87
6.1.2 General Log-linear Acceleration Form.....	89
6.2 Parameter Estimation.....	91
6.2.1 Estimation of Inverse Power Law Accelerated Models' Parameters.....	91
6.2.2 Estimation of General Accelerated Models' Parameters.....	97
6.3 ALT Models Comparison.....	97
6.4 An Accelerated Life Testing Plan.....	102
6.4.1 GB-S ALT Plan with Constant Stress.....	103
6.4.1.1 Variance of Reliability Estimate.....	104
6.4.1.2 Mean Time to First Failure or Quantile Failure.....	109
6.4.1.2.1 Quantile Failure.....	109
6.4.1.2.2 Mean Time to First Failure.....	111
6.4.1.3 Numerical Example.....	113
6.4.2 GB-S ALT Plan with Step Stress.....	114

6.4.2.1 Cumulative Damage Model.....	115
6.4.2.2 Likelihood Functions.....	116
6.4.2.3 Formulating Optimal Problems.....	117
6.4.2.3.1 Variance of Reliability Estimate.....	117
6.4.2.3.2 Quantile Failure and Mean Time to First Failure.....	118
6.4.2.4 Numerical Example.....	119
6.5 Conclusion.....	120
CHAPTER 7 CONCLUSION AND FUTURE WORK.....	122
REFERENCES.....	125
APPENDIX A.....	128
APPENDIX B.....	130

## LIST OF FIGURES

Figure 2.1 Hazard rate of SB-S distribution with $\alpha=1,2,3$ and $\beta=1$ .....	16
Figure 3.1 Hazard rate for $\alpha=1,2,3$ and $\beta=1$ .....	41
Figure 4.1 Kurtosis of GB-S distribution with different $\alpha$ and $\lambda$ when $\beta=1$ .....	50
Figure 4.2 GB-S density function with different $\lambda$ .....	51
Figure 4.3 GB-S hazard function with different $\lambda$ .....	65
Figure 4.4 Theoretical and predicted hazard rate by SB-S and GB-S when $\alpha=1, \beta=1.5$ .....	67
Figure 4.5 Theoretical and predicted hazard rates by SB-S and GB-S when $\alpha=0.5, \beta=4$ .....	68
Figure 4.6 Theoretical and predicted hazard rates by SB-S and GB-S when $\alpha=3, \beta=1$ .....	69
Figure 6.1 Predicted <i>cdf</i> (Data sets 1 and 2) of three inverse power law models and theoretical <i>cdf</i> .....	99
Figure 6.2 Predicted <i>cdf</i> (Data sets 1 and 2) of three general models and theoretical <i>cdf</i> .....	99
Figure 6.3 Predicted <i>cdf</i> (Data sets 2 and 3) three inverse power law models and theoretical <i>cdf</i> .....	101
Figure 6.4 Predicted <i>cdf</i> (Data sets 2 and 3) of three general models and theoretical <i>cdf</i> .....	101
Figure 6.5 Constant-stress test.....	104

Figure 6.6 Simple step-stress test.....	115
-----------------------------------------	-----

## LIST OF TABLES

Table 4.1 Roots condition of $s'(x)$ and shape of GB-S hazard rate.....	63
Table 4.2 Parameters of SB-S and GB-S distribution.....	66
Table 4.3 SSE of SB-S and GB-S distribution's hazard rate estimates.....	70
Table 5.1 Sample sizes and values of the shape parameters.....	81
Table 5.2 Means of the estimates of parameters when $n=10$ .....	83
Table 5.3 Means of the estimates of parameters when $n=50$ .....	83
Table 5.4 Means of the estimates of parameters when $n=100$ .....	83
Table 5.5 Variances of the estimates of parameters when $n=10$ .....	84
Table 5.6 Variances of the estimates of parameters when $n=50$ .....	84
Table 5.7 Variances of the estimates of parameters when $n=100$ .....	85
Table 6.1 Estimated Parameters and SSEs of each accelerated model (Sets 1 and 2).....	98
Table 6.2 Estimated Parameters and SSEs of each accelerated model (Sets 2 and 3).....	100
Table 6.3 Optimal solutions to different objectives with constant stress.....	114
Table 6.4 Optimal solutions to different objectives with step stress.....	120



# CHAPTER 1

## INTRODUCTION

### 1.1 Background and Motivation of Research

Fatigue is a class of structural damage that occurs when a material is exposed to cyclic application of stress with varying or constant amplitudes. Fatigue failure, which is thought to be unsearchable because the fatigue could not be seen or observed, is firstly observed in 19<sup>th</sup> century and has received increasing attention since. The fatigue problem is identified in the axles of carriages and wagons in the early 1800s and fatigue is also responsible for airplane crashes affecting British cargo planes in the 1950s (Diaz-Garcia and Leiva-Sanchez2002). Besides, failure caused by fatigue in metallic structures is a pervasive phenomenon and failure of structural materials under cyclic application of stress or strain is now a problem of increasing interests of industry because most of the mechanical components work under cyclic stresses with varying or constant amplitudes during their lifetime of operation. The fatigue phenomenon and the final dominant failure of the mechanical components are created by these varying or constant stresses. The stress does not only refer to the mechanical force but also includes any other type of “stress”, such as humidity, voltage, temperature, etc. Previous research has shown that a single static stress or strain, which is far below the threshold of the structure and causes no damage to the structure

if applied once, could induce fatigue failure if applied repeatedly. This noteworthy result emphasizes the importance of fatigue because it can induce the final failure with lower amplitude of loading.

Recognized as one of the main causes for the failure of mechanical and some electrical components, fatigue has led to a need for developing more precise approaches or suitable lifetime distributions to predict the reliability and useful life of components which are subjected to fatigue due to random or constant amplitude loading during their operations. To model such a failure, which eventually happens when the dominant crack surpasses the threshold, researchers utilize the normal distribution family to provide an accurate description. Similar to these distributions, Birnbaum and Saunders (1968) propose a lifetime distribution, called standard Birnbaum-Saunders (SB-S) distribution, which belongs to normal distribution family, to fit the fatigue failure data. This model has a single dominant crack which appears and grows as the structure experiences repeated loads up to the point that the crack is sufficiently long to cause failure. It is assumed that for each stage of loading, the increment of dominant crack is non-negative and independent. A large number of small increases accumulate in length before failure occurs. Moreover, the total crack length follows a normal distribution. Internal and external environments determine the distribution of the number of cycles necessary to cause the failure. If the loads occur more or less regularly in time, one can replace the probability that the structure will fail by a certain number of cycles with the probability it fails within a certain time.

The distribution of the failure time can then be used to determine the magnitude and behavior of the failure rate. Commonly the hazard rate is utilized since it is referred to as the instantaneous failure rate. Hazard rate expression of lifetime is of greatest importance for system engineers, designers, and repair and maintenance of a system. The failure rate expression is helpful to estimate mean time to failure, the reliability or availability of the components or systems, and the warranty policy (Elsayed 2012). Likewise, it helps to study the failure behavior, like expected number of failures in a certain period by obtaining the cumulative hazard function of the system. Sufficient conditions are obtained to show that a lifetime density has a general bathtub-shaped failure rate which starts with a high rate at the beginning of the system operation, mainly because of the weak units, design and installation and operating errors. Then the failure rate decreases gradually until it reaches a constant rate with the remove of the failed components, which is the second stage of the system. In the following third stage, called the wear out region, the hazard rate starts to significantly increase until the final failure occurs. Of course the failure may happen randomly during any of the stages. Besides this most common failure rate, in some other situations, failure rate can be increasing, decreasing, down-upside, upside-down or multimodal.

The rapid rate of advances in technology and global competition has emphasized the increasing need for the accurate estimation of reliability of a product, component or system (Zhang 2005). Statistical models for processes of fatigue failure enable us to describe the random variation of failure times exposed to fatigue due to different

patterns or levels of cyclic forces (Diaz-Garcia and Leiva-Sanchez 2002). Nevertheless, predicting reliability using fatigue data at normal operating conditions might not be feasible due to the extensive time and resource needed. Therefore, testing units at accelerated conditions and utilizing the failure times that observed at high levels of stress to predict the lifetime at operating levels of stress is an appropriate alternative approach. This type of test is termed an accelerated life test (ALT). A model which relates reliability and lifetime under severe conditions to normal environments is called an ALT model.

ALT models are classified mainly into several groups: statistic-based model (parametric or non-parametric), physics-experimental-based models and physics-statistics-based models (Elsayed 2012).

Parametric models assume that failure time at different stress levels are related to each other by a common failure distribution with different parameters (usually a mean or scale parameters). The life-stress function, which is the function of applied stress, substitutes the scale parameters as different levels of stresses applied while the shape parameter remains the same. Accelerated failure time (AFT) model is one of typical parametric models.

Non-parametric models appear to be a more suitable model when the failure data does not fit any failure distribution accurately. Cox' proportional hazards (PH) model and

the linear model are typical non-parametric models.

Physics-experimental-based models are used when time to failure can be explained based on the physics of the failure mechanism by either the development of a theoretical or experimental method. Some classic models used to predict time to failure are electromigration model, humidity dependence failures model and fatigue failures model.

Physics-statistics-based models explain the relationship between applied stress and failure rate by utilizing the parameters of the physics of the device in conjunction with the statistical parameters to obtain the realistic models. The general log-linear relationship is a general life-stress relationship which incorporates other models, for example, the Arrhenius model, the inverse-power model and the Eyring relationship.

Most of the previous work related to the SB-S distribution investigates its characteristics, properties, inference procedure and the application of SB-S distribution in some specific life-stress relationship-based ALT models. For example, the properties and characteristics of SB-S distribution are presented (Kundu 2010) and the hazard function of SB-S distribution is proven to be always upside-down (Kundu 2008). Ng *et al* (2003) provide the modified moment estimation (MME) and other modified estimation methodologies to obtain an unbiased estimation of SB-S distribution's parameters. Power-law life-stress relationship is applied to SB-S

distribution to develop an accelerated SB-S life model(Owen and Padgett 2000). These contributions are discussed in more details in the next chapter.

Since the hazard function of SB-S distribution is unimodal for all values of the shape parameter, its application in modeling products with different failure modes requires a more flexible fatigue life distribution involving varied failure types. This requirement can be achieved by generalizing the SB-S distribution. In this thesis we investigate a generalized B-S (GB-S) distribution. We present its properties, characteristics and the shape of its hazard function. It is also important to examine when this GB-S distribution fits failure data better than the SB-S distribution. Additionally, since ALT models can increase the fatigue failure of a specimen, it is interesting to apply ALT models to GB-S distribution and design an optimal ALT plan so that reliability and lifetime of components and systems using accelerated failure data can be accurately predicted at normal operating conditions.

## **1.2 Problem Statement**

It is proven the hazard function of SB-S distribution is restricted to be only upside-down. Owen (2004, 2006) presents GB-S distributions to improve the flexibility of the SB-S in terms of fitting different failure rate models.

This thesis investigates one of the GB-S distributions in order to facilitate its

applicability for other types of hazard functions. More specifically, the thesis investigates GB-S distribution and the shape of its hazard function as well as its accuracy of fitting failure data. The thesis also develops expressions for the characteristics of the GB-S distribution. We begin by presenting the probability density function (*pdf*) and the hazard function of SB-S distribution. The *pdf* of SB-S distribution is given by Eq. (1.1) as:

$$f(t; a, \beta) = \frac{1}{2\sqrt{2\pi}at} \left[ \left( \frac{t}{\beta} \right)^{\frac{1}{2}} + \left( \frac{\beta}{t} \right)^{\frac{1}{2}} \right] e^{\left\{ -\frac{1}{2a^2} \left[ \left( \frac{t}{\beta} \right) + \left( \frac{\beta}{t} \right) - 2 \right] \right\}} \quad (1.1)$$

Where  $T$ , denotes the lifetime,  $t$  is the realization of  $T$ , and  $\alpha$  and  $\beta$  are the parameters of SB-S distribution. The SB-S hazard function is given as:

$$h(t; a, \beta) = \frac{f(t; a, \beta)}{R(t; a, \beta)} = \frac{\frac{1}{2\sqrt{2\pi}at} \left[ \left( \frac{t}{\beta} \right)^{\frac{1}{2}} + \left( \frac{\beta}{t} \right)^{\frac{1}{2}} \right] e^{\left\{ -\frac{1}{2a^2} \left[ \left( \frac{t}{\beta} \right) + \left( \frac{\beta}{t} \right) - 2 \right] \right\}}}{1 - \Phi \left\{ \frac{1}{a} \left[ \left( \frac{t}{\beta} \right)^{\frac{1}{2}} - \left( \frac{\beta}{t} \right)^{\frac{1}{2}} \right] \right\}} \quad (1.2)$$

As stated earlier, Kundu (2008) establishes that the hazard function of SB-S distribution is unimodal and presents its change point (the point at which the distribution changes from increasing to decreasing hazards) which is the major

limitation of SB-S distribution.

Generalized forms of SB-S distribution (Owen 2004, 2006) are proposed by introducing another shape parameter. We investigate one of the GB-S distributions and discuss the necessary and sufficient conditions that enable the GB-S distribution to model different failure rate shapes.

The thesis also compares the performances of SB-S and GB-S distribution by applying them to groups of simulated failure data.

The characteristics and properties of the GB-S distribution are also investigated in this thesis. Utilizing the relationship between GB-S distribution's lifetime  $T$  and standard normal variable  $Z$ , we present the moments, expected failure time, variance, skewness, kurtosis and other statistical properties of  $T$ .

We develop efficient methodologies to estimate GB-S distribution's parameters. Although the maximum likelihood estimator (MLE) provides accurate estimation in most cases, exceptions may occur when sample size is small. Ng *et al* (2003) propose the modified moment estimators (MMEs) of SB-S distribution which are easy to compute, but biased for large shape parameters and small sample size cases. Simulation results of other proposed biased-reduction estimators of SB-S distribution reveal that they have advantages and limitations, respectively. Those estimators are



discussed in next chapter.

Providing a satisfactory estimation methodology of the GB-S distribution's parameters is one of the problems to be investigated in this thesis. We examine the MLE and employ the modified MLE (MMLE) that alleviates most of the limitations previously encountered (Cohen 1980). This new methodology substitutes one of the local maximum estimation equations with Eq. (1.3):

$$E\left(F\left(X_k\right)\right)=F\left(x_k\right) \quad (1.3)$$

We perform a simulation study to compare the performance of both MLE and MMLE for different sample size and shape parameters.

Power-law life-stress relationship is applied to SB-S distribution to build SB-S accelerated life model (Owen and Padgett 2000). The (inverse) power-law model has applications to fatigue studies in metals where failure tends to be crack-induced. We intend to utilize the ALT models to obtain the GB-S accelerated life model. We apply accelerated failure time (AFT) model to GB-S distribution and we also develop other ALT models. Those models are used to predict the reliability and lifetime under any operating condition by using the accelerated data and their performances are compared. To obtain an accurate and efficient prediction of the reliability, we design an ALT plan of GB-S distribution which aims to optimize the objective functions

under time and budget constraints.

In summary, the SB-S distribution has wide applications but is limited due to its inability to model different shapes of failure rate functions. The thesis intends to investigate the GB-S distribution to overcome the limitation. Studying the properties and characteristics as well as the parameter estimation methodologies of GB-S distribution are also investigated. Finally, we generalize the ALT models and apply them to GB-S distribution. We also intend to design ALT plans to predict life and reliability accurately under normal stresses.

### **1.3 Thesis Organization**

The thesis is organized as follows. Chapter 2 provides a thorough review of literature of SB-S distribution. We introduce the work related to SB-S distribution, the properties, inference procedure, SB-S distribution related distributions, generalization work based on SB-S distribution and its application in ALT models. In chapter 3, the thesis introduces the SB-S distribution, the assumptions and derivation, the properties, characteristics, several observations, inference procedures and its hazard rate in details. Chapter 4 deals with the GB-S distribution that Owen (2004) proposes. We investigate the characteristics, properties and observations of the distribution. We also examine the various types of failure rate shapes of GB-S distribution. We also perform extensive simulation in order to verify that GB-S distribution provides “better”

fit to fatigue failure data than the SB-S distribution. Chapter 5 focuses on the parameter estimation of GB-S distribution utilizing MLE and MMLE; the computational simulation indicates that for different sample sizes and different values of shape parameters, the results of MLE and MMLE are significantly different. Chapter 6 presents the application of GB-S distribution to ALT models. We propose GB-S based ALT models as well as other AFT models. Those models' performances are compared based on experiment accelerated data. Also, we provide an approach for the design of optimum ALT plans when the GB-S distribution is utilized in fitting the failure data at accelerated stress conditions. Consequently, the reliability performances under any operating stress can be obtained.

## **CHAPTER 2**

### **LITERATURE REVIEW**

In this chapter we provide a detailed overview of SB-S distribution and related distributions. We also discuss the use of SB-S distribution in accelerated life testing (ALT) and reliability prediction. We begin this chapter with basic properties, characteristics, observations and the hazard function of SB-S distribution in section 2.1. We then present a view of different parameter estimation methods of SB-S distribution's parameters in section 2.2. The advantages and disadvantages of such methods are also discussed. In section 2.3 we present a review of the literature of GB-S distributions and SB-S related distributions. The review indicates that these distributions fail to relax the limitation of hazard function of SB-S distribution. In section 2.4, power-law accelerated SB-S model is reviewed. The review shows that the use of B-S distribution in ALT for life prediction at normal conditions is limited to SB-S distribution. However, the use of B-S distribution in ALT model can be further generalized by the GB-S distribution.

#### **2.1 Properties and Characteristics of SB-S Distribution**

SB-S distribution (Birnbaum and Saunders 1968) is a widely accepted distribution for modeling fatigue failure of specimens, products or systems when a dominant crack,

which is caused by cyclic or continuous stresses and strains, either time-varying or constant, surpasses a predetermined crack length threshold. In this section, we provide the basic properties, characteristics, observations and the hazard function of SB-S distribution.

The SB-S distribution is derived based on the assumption that crack extension for the  $i$ th cycle is determined by the applied loading in this cycle only. It is also assumed that the crack extension for each cycle is non-negative and mutually independent.

Desmond (1985) notes that a variety of distributions describing crack extension size can still result in an SB-S distribution for estimating the fatigue lifetime. It is also observed that the fatigue failure life still follows the SB-S distribution when the basic assumption of the SB-S distribution regarding the crack growth is relaxed. In other words, the SB-S distribution can be used to model the fatigue failure life when the crack increment in a certain cycle not only depends on the current loading but also is affected by the total crack size caused by previous cycles.

Birnbaum and Saunders (1968) present the probability density function (*pdf*), expected failure time, variance, skewness  $\chi_1(T)$  and kurtosis  $\chi_2(T)$  respectively as follows:

The *pdf* of the SB-S distribution is:

$$f(t; a, \beta) = \frac{1}{2\sqrt{2\pi}at} \left[ \left( \frac{t}{\beta} \right)^{\frac{1}{2}} + \left( \frac{\beta}{t} \right)^{\frac{1}{2}} \right] e^{\left\{ -\frac{1}{2a^2} \left[ \left( \frac{t}{\beta} \right) + \left( \frac{\beta}{t} \right) - 2 \right] \right\}}$$

The expected time to failure is:

$$E(T) = \beta \left( 1 + \frac{\alpha^2}{2} \right)$$

The variance of the time to failure is:

$$Var(T) = (\alpha\beta)^2 \left( 1 + \frac{5\alpha^2}{4} \right)$$

The skewness and kurtosis, respectively are:

$$\chi_1(T) = \frac{16\alpha^2 (11\alpha^2 + 6)}{(5\alpha^2 + 4)^3}$$

$$\chi_2(T) = \frac{6\alpha^2 (93\alpha^2 + 41)}{(5\alpha^2 + 4)^2} + 3$$

Generally, the  $k$ th moment of  $T$  can be derived (Kundu 2010) as:

$$\begin{aligned}
E(T^k) &= \int_0^\infty t^k f(t) dt = \int_0^\infty \frac{t^{k-1}}{\sqrt{2\pi\alpha}} \left[ \left( \frac{t}{\beta} \right)^{\frac{1}{2}} - \left( \frac{\beta}{t} \right)^{\frac{1}{2}} \right] \exp \left\{ \frac{1}{\alpha^2} \left[ \left( \frac{t}{\beta} \right) - \left( \frac{\beta}{t} \right) - 2 \right] \right\} dt \\
&= \beta^k \sum_{j=0}^k \sum_{i=0}^j \frac{(2k-2j+2i)}{2^{k-j+i} (k-j+i)!} \left( \frac{\alpha}{2} \right)^{k-j+i}
\end{aligned}$$

Moreover, if  $T$  belongs to SB-S distribution with parameters  $\alpha$  and  $\beta$ ,  $T^{-1}$  also belongs to SB-S distribution with the corresponding parameters  $\alpha$  and  $\beta^{-1}$ , respectively (Ng *et al* 2003). Therefore, we readily have:

$$E(T^{-1}) = \beta^{-1} \left( 1 + \frac{\alpha^2}{2} \right)$$

$$Var(T^{-1}) = \alpha^2 \beta^{-2} \left( 1 + \frac{5\alpha^2}{4} \right)$$

The basic properties of SB-S distribution show that the mode of lifetime  $T$  is obtained by solving a non-linear equation in  $\alpha$ . Again for all  $\alpha$ , the median is always  $\beta$ . For all values of the shape parameter, the shape of *pdf* is unimodal. Kundu (2008) observes that once  $\alpha$  approaches zero, the shape of the *pdf* of the SB-S distribution becomes symmetric with respect to  $t=\beta$ , however, SB-S distribution is mainly used to model the skewed data so it is not common to have  $\alpha$  close to zero in real life applications.

To obtain the moments of  $T$  more generally, Rieck (1999) proposes the moment

generating function (MGF) and obtains the  $k$ th moment of SB-S distribution, where  $k$  can be either integer or fractional.

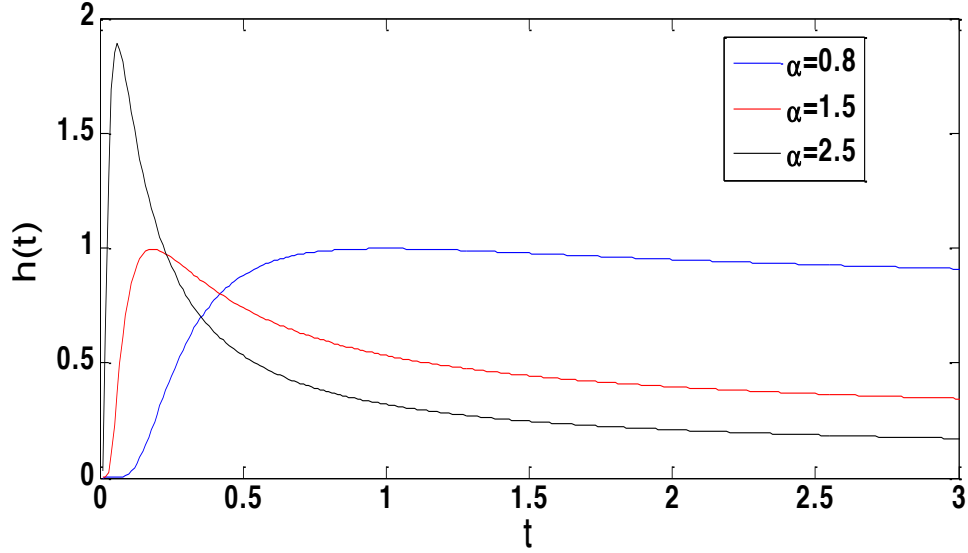


Figure 2.1 Hazard rate of SB-S distribution with  $\alpha=0.8, 1.5, 2.5$  and  $\beta=1$

From Figure 2.1 we observe that larger shape parameters cause the change point (up to down) to be more evident for the same value of scale parameter, i.e., larger shape parameter results in a sharper peak of the hazard function.

Kundu (2008) discusses the change point of the SB-S distribution's hazard function by defining the changing point as  $c(\alpha)$ . The change point can be obtained by utilizing different estimation methods and is a decreasing function of  $\alpha$ . However there is no closed-form expression of  $c(\alpha)$ . Kundu (2008) obtains a functional approximation of  $c(\alpha)$  as:



$$c(a) = \frac{1}{(1.8417\alpha - 0.4604)^2}. \quad (2.1)$$

It is observed that for  $\alpha > 0.6$ , the approximation in Eq. (2.1) works very well. However,  $c(\alpha)$  does not exist at  $\alpha = 0.249986$  and the approximation gives unreasonable values in the range of  $0.25 < \alpha < 0.5$ .

## 2.2 Parameters' Estimation Methodologies

In this section, we provide a review of different parameters' estimation methodologies for SB-S distribution and their advantages and disadvantages. The maximum likelihood estimator (MLE) for SB-S distribution is also discussed originally by Birnbaum and Saunders (1968). Apparently, moment estimator (ME) can be applied to this distribution; however, this estimator is biased. In addition, when the sample coefficient of variation ( $CV$ ) is larger than  $\sqrt{5}$ , the ME is no longer available. Even if the  $CV$  is smaller than  $\sqrt{5}$ , the estimator of the scale parameter  $\beta$  is not unique (Ng *etal*2003). To obtain the MLE of  $\beta$ , it is necessary to set a non-linear equation of  $\beta$  which might result in computational round off errors and potential inaccuracies. Although two iterative schemes for the non-linear equation of  $\beta$  are suggested by Birnbaum and Saunders (1968), one of them is only applicable for small  $\alpha$  and the other procedure is not available for some sample space (Ng *etal*2003). In addition, since exact distributions of the MLEs are not available, their asymptotic distributions are obtained by Engelhardt *et al* (1981) for constructing confidence intervals of the

parameters. Again, Ng *et al*(2003) mention that the behavior of the confidence interval is not certain when sample size is small. Above all, the MLE of  $\alpha$  is biased, especially when the sample size is small or when the data is incomplete (Ng *et al* 2003).

As we stated earlier, ME and MLE both have application limitations as well as computational difficulties. To improve the estimation of conventional estimators, Ng *et al*(2003) propose the modified moment estimator (MME) which always provides unique estimation of  $\beta$ . Two modified estimators which improve both ME and MLE, called Bias-reduced estimator and Jackknife estimator, are also proposed (Ng *etal*2003).

Monte Carlo simulation is used to compare the results of these estimators (Ng *etal*2003). The simulation results show that the performances of the MLE and MME are almost identical regardless of the sample size as long as the shape parameter  $\alpha$  is not large. The results also show that the MLE and the MME obtain large standard deviations for small sample sizes. When shape parameter is large, Jackknife MLE and Jackknife ME provide identical results which have less bias but larger standard deviations than Bias-reduced MLE and Bias-reduced ME. Ng *et al* (2003) also prove that in terms of computation procedure, when sample size is large, Bias-reduced MLE and Bias-reduced ME are simple while the Jackknife MLE and Jackknife ME take longer computation time. The asymptotic confidence intervals do not work very well

when the sample size is less than 20.

A simple bias-corrected estimator of  $\alpha$  by using a regression curve fitted to the bias of the MLE of  $\alpha$  based on Monte Carlo simulations is provided (Ng *et al* 2003). This technique is proposed and applied to set a bias correction formula for the MLE of a two-parameter Weibull distribution. Reick (1999) also proposes the approximation for a small shape parameter  $\alpha$  with moment generating function (MGF).

Tang and Chang (1993) obtain the coverage probability, change point and reliability bound of the SB-S distribution, both point and interval. To achieve this, they construct a 100 $p$ th percentile confidence interval and use the two-sided tolerance limits for the estimation. Dupuis and Mills (1998) obtain the robust estimation of the parameters and quantiles of SB-S distribution since in practice the collected data does not always follow the SB-S model. The robust estimation technique is based on the optimal bias-robust estimator (OBRE) which is similar but better than MLE. This procedure considers the weight of each observation and shows that low weights are not suitable for fitting the SB-S model. Also, robust confidence interval can be used to estimate the change point of the hazard rate function. Rieck (1999) derives the inference procedure for the SB-S distribution with symmetrically incomplete data since in practice it is common to end a life testing before all items under test fail. Therefore, estimation procedures need to be developed to model the censored data. This

estimator can be applied for the parameters of SB-S distribution and extends its applicability for both complete samples and Type 2 censored samples.

Although different methods are proposed to estimate SB-S distribution's parameters, there is no widely accepted estimation method that provides a convincing approximation of the shape parameter, especially when the sample size is small and the shape parameter is large.

### **2.3 GB-S Distribution and SB-S Related Distributions**

Since SB-S distribution is considered as one of the normal distribution family and its relationship with similar distributions is discussed. Desmond (1985) discusses the relationship between SB-S distribution and the Inverse Gaussian (IG) distribution. The SB-S distribution can be written as a combination of an IG distribution and the reciprocal of an IG distribution. The hazard functions of the two distributions are very similar. Desmond (1985) compares the two distributions and the result shows that SB-S distribution is more flexible than IG distribution, whereas the IG distribution seems to have applications for incomplete data but SB-S distribution has difficulty in incorporating such data.

Kundu (2010) describes properties of the length biased version of SB-S distribution (LBBS) which can be easily established where the LB distributions are defined as particular cases of the weighted SB-S distribution. The properties of LBBS can be

obtained by utilizing SB-S distribution. For example, the *pdf* of LBBS can be easily obtained using the standard transformation method. The cumulative distribution function (*cdf*) of LBBS can also be obtained in terms of  $\Phi(g)$ .

Similarly, the *pdf* of the mixture of two SB-S distributions (MSB-S) distribution can be either unimodal or bimodal. The moments of the MSB-S distribution can be obtained in terms of the moments of the two SB-S distributions. Likewise, the hazard function of the MSB-S distribution can be expressed by the mixture of two SB-S hazard functions (Kundu, 2010).

Owen (2004, 2006) presents two GB-S distributions by introducing a second shape parameter. One of the GB-S distributions considers the effect of sequence of loading and the crack extension thus the crack extension is modeled as a memory process. MLE is proposed to estimate the parameters of the distribution. The hazard function of this GB-S distribution covers the increasing hazard rate as well. However, this relaxation is not general enough when compared with another form of the GB-S distributions. In the other GB-S distribution, Owen (2004, 2006) generalizes the SB-S distribution by building the relationship between lifetime  $T$  and standard normal variable  $Z$  as:

$$Z = \frac{1}{a} \left[ \left( \frac{T}{\beta} \right)^\lambda - \left( \frac{\beta}{T} \right)^\lambda \right] \quad (2.2)$$

Here  $\lambda$  and  $\alpha$  are the shape parameters and  $\beta$  is the scale parameter of this GB-S distribution.  $T$  is lifetime of the GB-S distribution and  $Z$  is the standard normal variable. Therefore, the *pdf* of lifetime  $T$  is given in Eq. (2.3) as:

$$f(t; a, \beta, \lambda) = \frac{\lambda}{\sqrt{2\pi a t}} \left[ \left( \frac{t}{\beta} \right)^{\lambda} + \left( \frac{\beta}{t} \right)^{\lambda} \right] \exp \left\{ -\frac{1}{2a^2} \left[ \left( \frac{t}{\beta} \right)^{2\lambda} + \left( \frac{\beta}{t} \right)^{2\lambda} - 2 \right] \right\} \quad (2.3)$$

Including the GB-S distribution above, Diaz-Garcia and Dominguez-Molina (2005) present a more general form of the SB-S distribution by providing univariate and multivariate extensions; for example, sinh-normal distribution of spherical type. Diaz-Garcia and Leiva-Sanchez (2002) extend SB-S distribution to an elliptically contoured distribution. From this type of distribution they derive several specific Elliptic distributions such as Pearson Type VII,  $t$ , Cauchy, Normal, Laplace and Logistic distributions. This generalization makes this family of distributions effective in covering a wide range of life conditions. Desmond (1985) also uses a biological model to provide a more general derivation of SB-S distribution. His generalized derivation yields an SB-S distribution family which incorporates lognormal and other distributions.

The GB-S distribution as described in Eq. (2.3) has not been thoroughly investigated. In other words, the characteristics of the distribution and the conditions that enable it to model upside-down hazard rate function and monotonically increasing hazard rate

function or their combination which may be useful in modeling the rollercoaster failure rate of electronic systems (roller coaster failure rate means that the failure rate is multimodal as advocated by Wong (1989)) are the subject of investigation of this thesis. We also present the characteristics, properties and inference procedure of this GB-S distribution. Furthermore, methods for providing unbiased estimation methods of the GB-S distribution's parameters are investigated.

## 2.4 SB-S Accelerated Model

### 2.4.1 ALT Models

ALT models can be divided into several types. Each model has underlying assumptions and builds relationship between different reliability measures. AFT models assume that the covariates act multiplicatively on the failure time. Expressing the stress function as  $\exp(aZ)$ , a typical AFT model is defined by  $R(t; Z) = R_0 [\exp(aZ)t]$ . Cox's proportional hazards (PH) model is the most widely used non-parametric ALT model because it relaxes the requirement of the failure time distribution's form. It is mainly based on the assumption that the ratio of the hazard rates of two identical units under two stress levels is constant, i.e.,  $h(t; Z) = h_0(t) \exp(aZ)$ . For the proportional odds (PO) model, the stress function  $\exp(aZ)$  builds relationship between the odds functions under different stress levels, where the odds function  $\theta(t)$  is defined as:  $\theta(t) = \frac{F(t; Z)}{1 - F(t; Z)}$ . Therefore, the PO

model is written as  $\frac{F_s(t;Z)}{1-F_s(t;Z)} = e^{aZ} \frac{F_0(t)}{1-F_0(t)}$ . It states that the odds of failure are proportional to the applied stress levels.

These ALT models along several others such as the extended linear hazards regression models and the proportional mean residual life models are normally used to relate the units' lives at accelerated conditions to their lives at normal operating conditions. Although, the B-S distribution model is widely used in fatigue analysis, its application to ALT models is limited. In this section, we review the use of SB-S distribution as an ALT prediction model. Later in the thesis, we intend to explore and generalize its use by using the GB-S distribution.

#### 2.4.2 SB-S Distribution Based ALT Model

The inverse power law model is commonly used for non-thermal accelerated stresses and is given as:

$$h(S) = \gamma \cdot S^{-\eta}, \gamma > 0, \eta > 0 \quad (2.4)$$

Where

$h(S)$  is a quantifiable life measure, such as mean life, characteristic life, etc

$S$  represents the stress level

$\gamma, \eta$  are model parameters.



Owen and Padgett (2000) develop the inverse power law accelerated form of the SB-S distribution and explore the corresponding inference procedures. By substituting the scale parameter  $\beta$  with the accelerated life model  $h(S)$ , the accelerated B-S model can be written as:

$$f(t; a, h(S)) = \frac{1}{2\sqrt{2\pi}at} \left[ \left( \frac{t}{h(S)} \right)^{\frac{1}{2}} + \left( \frac{h(S)}{t} \right)^{\frac{1}{2}} \right] e^{\left\{ -\frac{1}{2a^2} \left[ \left( \frac{t}{h(S)} \right) + \left( \frac{h(S)}{t} \right) - 2 \right] \right\}} \quad (2.5)$$

Where

$$h(S) = \gamma \cdot S^{-\eta}, \quad \gamma > 0, \eta > 0$$

The MLE of the unknown model parameters in (2.5) can be obtained by minimizing the likelihood function:

$$L(\alpha, \gamma, \eta; t_{ij}, S_i) = \prod_{i=1}^k \prod_{j=1}^{n_i} \frac{1}{2\sqrt{2\pi}at_{ij}} \left[ \left( \frac{t_{ij}}{\gamma S_i^{-\eta}} \right)^{\frac{1}{2}} + \left( \frac{\gamma S_i^{-\eta}}{t_{ij}} \right)^{\frac{1}{2}} \right] e^{\left\{ -\frac{1}{2a^2} \left[ \left( \frac{t_{ij}}{\gamma S_i^{-\eta}} \right) + \left( \frac{\gamma S_i^{-\eta}}{t_{ij}} \right) - 2 \right] \right\}} \quad (2.6)$$

Where

$k$  is the number of accelerated stress levels

$t_{ij}$  is observed cycle-to-failure of stress level or type  $i$  at the observed time index  $j$

$j$  is index for failure times observed for  $S_j \quad j=1,2,\dots,n$

$n_j$  is number of items tested at stress  $S_j$

Owen and Padgett (2000) also utilize the model to estimate lower distribution percentiles for any value of the acceleration factor. This SB-S model implies the applicability of ALT models to GB-S distribution. Therefore, we intend to investigate the use of GB-S distribution in ALT.

## 2.5 Conclusion

In this chapter, the literature concerning the SB-S distribution is reviewed in details. GB-S distribution and SB-S distribution families are proposed but they all fail to cover a wide range of failure rate functions. There are different methods proposed to estimate SB-S distribution's parameters but little research is conducted to provide estimates of the parameters of the GB-S distribution, especially when the sample size is small. The inverse power law model is applied to SB-S distribution to relate failure times at accelerated conditions to those at normal operating conditions. A thorough review of the literature shows that GB-S accelerated model has not been investigated. In this thesis we investigate the GB-S distribution by presenting its characteristics and properties. We also examine the GB-S distribution's hazard function and its applicability in industry. Moreover, we compare the performances of MMLE and

MLE using extensive simulation studies. Finally, we present a generalized ALT model and discuss different GB-S based ALT models. We also intend to investigate the development of optimal accelerated life testing plans for the GB-S based ALT model.

## CHAPTER 3

### STANDARD BIRNBAUM-SAUNDERS (SB-S) DISTRIBUTION

In chapter 2, we present the probability density function (*pdf*), expected failure time, variance, skewness, kurtosis and some properties of SB-S distribution. We also introduce different methods for the SB-S distribution's parameters estimation and highlight the fact that the hazard rate function of SB-S distribution is restricted to be only unimodal (Kundu 2008). In this chapter, we provide a detailed discussion of the SB-S distribution before we introduce and investigate the GB-S distribution in chapter 4.

We begin this chapter by stating the underlying assumptions of the SB-S distribution. In section 3.2 we present details of the parameter estimation methodologies of the SB-S distribution and then examine the shape and the change point of the hazard function of SB-S distribution in section 3.3.

#### 3.1 Assumptions and Derivation of SB-S Distribution

Birnbaum and Saunders (1968) propose the SB-S distribution to model fatigue failure time of units when a dominant crack, which is caused by cyclic or other types of stresses, surpasses or reaches a predetermined crack length threshold. To utilize SB-S

model, the stress is not only restricted to mechanical loading but also refers to any stress due to environmental conditions, such as humidity, temperature, electric field, etc. In this section, we briefly present the assumptions and derivation of SB-S distribution.

### 3.1.1 Assumptions of the SB-S Distribution

Usually, “loading” is expressed as a function that represents the amount of stresses acting on the specimen at any given moment in time. To derive SB-S distribution, the following assumptions are necessary:

1. A cycle contains  $m$  types of applied loadings, for example, temperature, humidity, electric field, shock, vibration, etc. Each application of the  $j$ th loading type in the  $i$ th cycle results in a random crack extension. The distribution for this random variable depends on the actual crack extension caused by applied loadings in this cycle only.
2. Let  $X_{ij}$  represent the crack extensions caused by the  $j$ th loading in the  $i$ th cycle, which are non-negative and mutually independent and  $X_i$  represent the accumulated crack extensions caused by  $m$  types of loadings in the  $i$ th cycle. Let  $X$  represent the dominant crack at the end of the  $n$ th cycle. The relationship

among  $X_{ij}$ ,  $X_i$  and  $X$  can be expressed as: 
$$X = \sum_{i=1}^n X_i = \sum_{i=1}^n \sum_{j=1}^m X_{ij}$$

3. The dominant crack at the end of  $n$ th cycle  $X$  is approximately normally distributed with mean  $n\mu$  and variance  $n\sigma^2$ . Where  $\mu$  and  $\sigma$  are the mean and standard deviation of the crack that occurs in one cycle, respectively.
4. The fatigue failure happens when the dominant crack length  $X$  reaches or surpasses the threshold  $\omega$  expressed as:

$$X = \sum_{i=1}^n X_i = \sum_{i=1}^n \sum_{j=1}^m X_{ij} \geq \omega \quad (3.1)$$

It is also observed that the fatigue life still follows the SB-S distribution when the basic assumptions of the SB-S distribution regarding the crack growth are relaxed. More specifically, the SB-S distribution can be adopted for modeling the fatigue life when the crack increment in a certain cycle depends not only on the current but also on previous loadings. In addition, Desmond (1985) notes that a variety of distributions describing crack extension size can still result in an SB-S distribution for estimating the fatigue lifetime.

### 3.1.2 Derivation of the SB-S Distribution

The failure threshold of a given product is determined by its own conditions and the operating environment. Based on the assumptions mentioned above, the SB-S

distribution is derived as follows:

The probability that the crack does not exceed the threshold length  $\omega$  is obtained as:

$$\Phi\left(\frac{\omega - n\mu}{\sigma\sqrt{n}}\right) = \Phi\left(\frac{\omega}{\sigma\sqrt{n}} - \frac{\mu\sqrt{n}}{\sigma}\right)$$

Similarly, if  $T$  denotes a specimen's lifetime (expressed in number of cycles), the cumulative density function (*cdf*) of  $T$  is approximately given by:

$$\Pr(T \leq t) = 1 - \Phi\left(\frac{\omega}{\sigma\sqrt{t}} - \frac{\mu\sqrt{t}}{\sigma}\right) = \Phi\left(\frac{\mu\sqrt{t}}{\sigma} - \frac{\omega}{\sigma\sqrt{t}}\right) = \Phi\left[\frac{1}{\alpha}\left(\sqrt{\frac{t}{\beta}} - \sqrt{\frac{\beta}{t}}\right)\right] \quad (3.2)$$

Where

$$\alpha = \frac{\sigma}{\sqrt{\omega\mu}}, \quad \beta = \frac{\omega}{\mu}, \quad \alpha > 0, \beta > 0$$

The random variable  $T$ , denoting the lifetime, follows SB-S distribution. The parameters  $\alpha$  and  $\beta$  are shape and scale parameters of SB-S distribution, respectively.

The reliability function, the *pdf*, and the hazard rate function, respectively, are:

$$R(t; a, \beta) = 1 - \Phi(t; a, \beta) = 1 - \Phi \left[ \frac{1}{\alpha} \left( \sqrt{\frac{t}{\beta}} - \sqrt{\frac{\beta}{t}} \right) \right] \quad (3.3)$$

$$f(t; a, \beta) = \frac{1}{2\sqrt{2\pi}at} \left[ \left( \frac{t}{\beta} \right)^{\frac{1}{2}} + \left( \frac{\beta}{t} \right)^{\frac{1}{2}} \right] e^{\left\{ -\frac{1}{2a^2} \left[ \left( \frac{t}{\beta} \right) + \left( \frac{\beta}{t} \right) - 2 \right] \right\}} \quad (3.4)$$

$$h(t; a, \beta) = \frac{f(t; a, \beta)}{R(t; a, \beta)} = \frac{\frac{1}{2\sqrt{2\pi}at} \left[ \left( \frac{t}{\beta} \right)^{\frac{1}{2}} + \left( \frac{\beta}{t} \right)^{\frac{1}{2}} \right] e^{\left\{ -\frac{1}{2a^2} \left[ \left( \frac{t}{\beta} \right) + \left( \frac{\beta}{t} \right) - 2 \right] \right\}}}{1 - \Phi \left\{ \frac{1}{a} \left[ \left( \frac{t}{\beta} \right)^{\frac{1}{2}} - \left( \frac{\beta}{t} \right)^{\frac{1}{2}} \right] \right\}} \quad (3.5)$$

We observe that the derivation of SB-S distribution is similar to a known model called Miner's Rule, which is one of the most widely used cumulative damage models for failures caused by fatigue. Miner's Rule deals with the case that the unit is subjected to different types of loadings with multiple levels. Of course, this general model incorporates single type of stress or stress with constant magnitude as a special case. For a given unit, the  $j$ th type of loading in the  $i$ th cycle, represented by  $S_{ij}$ , produces a fatigue life of  $N_{ij}$  cycles. The number of cycles representing the damage accumulated at stress  $S_{ij}$  is  $n_{ij}$ . Assessing the proportion of life  $p_{ij} = \frac{n_{ij}}{N_{ij}}$  consumed at each stress level and adding the proportions together, the failure occurs when the sum of proportions equals to one. Assuming the failure happens at the end of the  $n$ th cycle, Miner's Rule can then be expressed by Eq. (3.6) as:



$$\sum_{i=1}^n \sum_{j=1}^m p_{ij} = 1 \quad (3.6)$$

This is similar to Eq. (3.1). Thus, when Miner's Rule is appropriate to model the fatigue failure, the SB-S model can also be properly used for life prediction.

### 3.2 Maximum Likelihood Estimation (MLE) and Modified Moment Estimation (MME) of SB-S Distribution

In chapter 2, we present several estimation methodologies of SB-S distribution's parameters. However, we just mention their advantages and disadvantages. In this section, we estimate the parameters  $\alpha$  and  $\beta$  by utilizing MLE and MME.

#### 3.2.1 MLE of SB-S Distribution

Placing the failure time data of a random sample with size  $n$  in an increasing order  $t_1 \leq t_2 \leq \dots \leq t_n$ , we readily have the sample arithmetic mean  $s$  and harmonic mean  $r$  given by Eq. (3.7) and (3.8) respectively:

$$s = \frac{1}{n} \sum_{i=1}^n t_i \quad (3.7)$$

$$r = \left[ \sum_{i=1}^n t_i^{-1} \right]^{-1} \quad (3.8)$$

Generally, the harmonic mean function  $K(x)$  can be further defined as:

$$K(x) = \left[ \sum_{i=1}^n (x+t_i)^{-1} \right]^{-1}, \text{ for } x \geq 0 \quad (3.9)$$

Where  $x$  is a positive variable.

We obtain the likelihood function for the sample as given in Eq. (3.10):

$$L(t_i; \alpha, \beta) = \frac{\prod_{i=1}^n \left[ \left( \frac{t_i}{\beta} \right)^{\frac{1}{2}} + \left( \frac{t_i}{\beta} \right)^{-\frac{1}{2}} \right]}{(2\sqrt{2\pi})^n \alpha^n \prod_{i=1}^n t_i} \exp \left\{ \sum_{i=1}^n \left[ \left( \frac{t_i}{\beta} \right) + \left( \frac{t_i}{\beta} \right)^{-1} \right] - 2n \right\} \quad (3.10)$$

We obtain the log-likelihood function by taking logarithm of Eq. (3.10). Setting the partial derivatives of the log-likelihood function with respect to  $\alpha$  and  $\beta$  equal to zero respectively, we obtain  $\alpha(\beta)$  that maximizes the likelihood function with

$$\alpha(\beta) = \left( \frac{s}{\beta} + \frac{\beta}{s} - 2 \right)^{\frac{1}{2}} \text{ for a given } \beta. \text{ The estimation of } \beta \text{ can be obtained by solving}$$

Eq. (3.11):

$$\beta^2 - \beta [2r + K(\beta)] + r [s + K(\beta)] = 0 \quad (3.11)$$

Eq. (3.11) is a non-linear equation of  $\beta$  which might result in computational round off errors and potential inaccuracies. Birnbaum and Saunders (1968) suggest two

iterative schemes for solving this non-linear equation. However, one is only applicable for small  $\alpha$  and the other is not available for some sample space (Ng *et al* 2003).

In addition, since exact distributions of the MLEs are not available, Engelhardt *et al* (1981) obtain the asymptotic distribution of parameters  $\alpha$  and  $\beta$ , which is a bivariate normal, to construct confidence intervals of the parameters as given in (3.12):

$$\begin{pmatrix} \alpha \\ \beta \end{pmatrix} \sim N \left( \begin{pmatrix} \alpha \\ \beta \end{pmatrix}, \begin{pmatrix} \frac{\alpha^2}{2} & 0 \\ 0 & \frac{\beta}{n[0.25 + \alpha^2 + I(\alpha)]} \end{pmatrix} \right) \quad (3.12)$$

Where

$$I(\alpha) = 2 \int_0^\infty \left\{ [1 + g(\alpha x)]^{-1} - 0.5 \right\}^2 d\Phi(x)$$

$$g(y) = 1 + \frac{y^2}{2} + y \left( 1 + \frac{y^2}{4} \right)^{\frac{1}{2}}$$

Again, Ng *et al* (2003) state that the behavior of the confidence interval is not certain when the sample size is small.

### 3.2.2 MME of SB-S Distribution

#### 3.2.2.1 Moment Estimation (ME) of SB-S Distribution

Using conventional ME to estimate the parameters of the SB-S distribution, we set Eq.

(3.13) and (3.14) as:

$$E[T] = \frac{\sum_{i=1}^n t_i}{n} = \beta \left(1 + \frac{\alpha^2}{2}\right) \quad (3.13)$$

$$E[T^2] - \{E[T]\}^2 = \frac{\sum_{i=1}^n t_i^2}{n} - \left(\frac{\sum_{i=1}^n t_i}{n}\right)^2 = (\alpha\beta)^2 \left(1 + \frac{5\alpha^2}{4}\right) \quad (3.14)$$

The corresponding ME of  $\alpha$  and  $\beta$  can then be obtained as solutions of  $\alpha$  and  $\beta$  of the two equations. As stated earlier, conventional ME is biased when the sample size is small. In addition, when the sample coefficient of variation ( $CV$ ) is larger than  $\sqrt{5}$ , the ME is no longer available. Moreover, when the  $CV$  is smaller than  $\sqrt{5}$ , the estimator of the scale parameter  $\beta$  is not unique (Ng *et al* 2003).

### 3.2.2.2 Modified Moment Estimation (MME) of SB-S Distribution

Instead of using the first and second population moments, Ng *et al* (2003) propose an MME by replacing Eq. (3.14) with Eq. (3.15):

$$r^{-1} = \frac{\sum_{i=1}^n t_i^{-1}}{n} = \beta^{-1} \left(1 + \frac{\alpha^2}{2}\right) \quad (3.15)$$

Thus MME can be utilized to obtain  $\alpha$  and  $\beta$  by providing Eq. (3.15) and (3.16):

$$s = \beta \left( 1 + \frac{\alpha^2}{2} \right) \quad (3.16)$$

Solving Eq. (3.15) and (3.16) for  $\alpha$  and  $\beta$ , we obtain  $\alpha$  and  $\beta$  as Eq.(3.17) and (3.18):

$$\alpha = \left\{ 2 \left[ \left( \frac{s}{r} \right)^{\frac{1}{2}} - 1 \right] \right\}^{\frac{1}{2}} \quad (3.17)$$

$$\beta = (rs)^{\frac{1}{2}} \quad (3.18)$$

Again, the asymptotic joint distribution of  $\alpha$  and  $\beta$  is bivariate normal given by:

$$\begin{pmatrix} \alpha \\ \beta \end{pmatrix} \sim N \left( \begin{pmatrix} \alpha \\ \beta \end{pmatrix}, \begin{pmatrix} \frac{\alpha^2}{2n} & 0 \\ 0 & \frac{\alpha^2 \beta^2}{n} \left( \frac{1 + \frac{3}{4} \alpha^2}{\left( 1 + \frac{1}{2} \alpha^2 \right)^2} \right) \end{pmatrix} \right) \quad (3.19)$$

Besides MLE and MME, Ng *et al* (2003) propose other modified estimation methods such as bias-reduced estimator and Jackknife estimator to estimate SB-S distribution's

parameters. Comparison among these estimation methods indicates that there is no widely accepted estimation method that provides a convincing approximation of  $\alpha$ , especially when  $\alpha$  is large.

### **3.3 Hazard Function of SB-S Distribution**

Commonly, the hazard rate is utilized to determine the magnitude and behavior of the failure rate since it is referred to as the instantaneous failure rate. Sometimes, distributions with monotone or constant hazard function are used to model failure time data. However, it can be often observed that the hazard rate increases to a point and then decreases (upside-down) or starts by decreasing from a high rate to a point and then rises (down-upside). The hazard rate can be even more complicated with multiple ups and downs (roller coaster (Wong 1989)). Generally, bathtub-shaped failure rate and roller coaster failure rate can be adopted to model most of the life conditions.

#### **3.3.1 Shape of the Hazard Function**

To investigate the shape of the hazard function of GB-S distribution in the next chapter, it is necessary to examine the shape of the hazard function of SB-S distribution which is originally provided by Kundu (2008).

Set

$$\varepsilon(t) = t^{\frac{1}{2}} - t^{-\frac{1}{2}},$$

$$\varepsilon'(t) = \frac{1}{2} \left( t^{-\frac{1}{2}} + t^{-\frac{1}{2}} \right)$$

$$\varepsilon''(t) = \frac{-1}{2t^2} \left[ \frac{1}{2} t^{\frac{1}{2}} + \frac{3}{2} t^{-\frac{1}{2}} \right]$$

$$\varepsilon^2(t) = t + t^{-1} - 2$$

Then the *pdf* and the hazard function of SB-S distribution can be written as Eq. (3.20)

and (3.21), respectively:

$$f(t) = \frac{1}{\sqrt{2\pi}\alpha} \varepsilon'(t) \exp \left\{ -\frac{1}{2\alpha^2} \varepsilon(t) \right\} \quad (3.20)$$

$$h(t) = \frac{f(t)}{1-F(t)} = \frac{\frac{1}{\sqrt{2\pi}\alpha} \varepsilon'(t) \exp \left\{ -\frac{1}{2\alpha^2} \varepsilon(t) \right\}}{\Phi \left\{ -\frac{\varepsilon(t)}{\alpha} \right\}} \quad (3.21)$$

The shape of the hazard function is not clear by observing Eq. (3.21). Investigating the shape of  $h(t)$  by examining whether  $h'(t)$  is positive or not does not work well because of its computational difficulty. Kundu (2008) utilizes a lemma (Glaser 1980) to establish the main result regarding the shape of the hazard function. The lemma adopted by Kundu (2008) is similar to the lemmas that we utilize when discussing the shape of hazard function of GB-S distribution in Chapter 4.

The Lemma states that  $f(t)$ , for  $t > 0$ , is the *pdf* of a positive real-valued continuous

random variable, and defines  $\eta(t) = \frac{f'(t)}{f(t)}$ . If there exists a time  $t_0$  such that  $\eta'(t) > 0 \forall t \in (0, t_0)$ ,  $\eta'(t_0) = 0$  and  $\eta'(t) < 0 \forall t \in (t_0, \infty)$ . The hazard function corresponding to  $f(t)$  is either an upside-down or a decreasing function of  $t$ . Furthermore, if  $\zeta = \lim_{t \rightarrow 0} f(t)$  exists, possibly equal to 0 or  $\infty$ , the hazard function is decreasing if  $\zeta = \lim_{t \rightarrow 0} f(t) = \infty$  and is upside-down if  $\zeta = \lim_{t \rightarrow 0} f(t) = 0$ .

For SB-S distribution,  $\eta(t)$  and  $\eta'(t)$  can be investigated more specifically as:

$$\eta(t) = -\left[ \frac{\varepsilon''(t)}{\varepsilon'(t)} - \frac{\varepsilon'(t)\varepsilon(t)}{\alpha^2} \right] = \frac{t^{\frac{1}{2}} + \frac{3}{2}t^{-\frac{1}{2}}}{2\left(t^{\frac{1}{2}} + t^{-\frac{1}{2}}\right)} + \frac{\left(t^{\frac{1}{2}} - t^{-\frac{3}{2}}\right)}{2\alpha^2}$$

and

$$\eta'(t) = \frac{-\alpha^2 t^3 + (-6\alpha^2 + 2)t + (-3\alpha^2 + 4)t + 2}{2(t+1)^2 \alpha^2 t^3}$$

Kundu (2008) shows that for SB-S distribution, there indeed exists a time  $t_0$  such that  $\eta'(t) > 0 \forall t \in (0, t_0)$ ,  $\eta'(t_0) = 0$  and  $\eta'(t) < 0 \forall t \in (t_0, \infty)$ . Thus, the hazard function of SB-S distribution is either upside-down or decreasing.

Furthermore, Kundu (2008) proves that  $\lim_{t \rightarrow 0} h(t; \alpha) = 0$ . Since  $\lim_{t \rightarrow 0} R(t; \alpha) = 1$ , we readily



have that  $\lim_{t \rightarrow 0} f(t; \alpha) = 0$ . Therefore, the hazard function of SB-S distribution is established as an upside-down function of  $t$

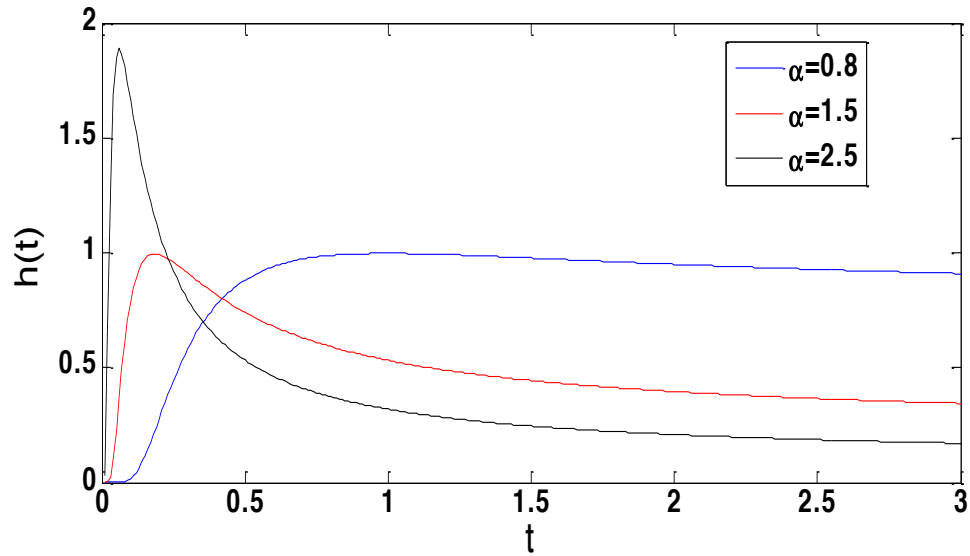


Figure 3.1 GB-S hazard rate with  $\alpha = 0.8, 1.5, 2.5$  and  $\beta = 1$

From Figure 3.1 we observe that larger shape parameters cause the change point to be more evident for the same value of scale parameter, i.e., for SB-S distribution, larger shape parameter results in a sharper peak hazard function.

### 3.3.2 Change Point of SB-S Distribution's Hazard Function

Kundu (2008) discusses the change point of the hazard function of the SB-S distribution by defining the change point as  $c(\alpha)$ , which is a decreasing function of  $\alpha$  and is obtained by solving Eq. (3.23):

$$\Phi\left(-\frac{1}{\alpha}\varepsilon(t)\right)\left\{-\left(\varepsilon'(t)\right)^2\varepsilon(t)+\alpha^2\varepsilon''(t)\right\}+\alpha\phi\left(-\frac{1}{\alpha}\varepsilon(t)\right)\left(\varepsilon'(t)\right)^2=0\quad(3.23)$$

Eq. (3.23) results in acceptable estimates of the parameter  $\alpha$  when  $\alpha$  is large but is difficult to obtain the estimates when  $\alpha$  is small. Kundu (2008) observes that when  $\alpha$  approaches zero,  $c(\alpha)$  approaches infinity. Particularly, the numerical solution of (3.23) is unstable when  $\alpha < 0.5$ .

Kundu (2008) proposes a functional approximation of  $c(\alpha)$  given as:

$$c(a)=\frac{1}{(1.8417\alpha-0.4604)^2}\quad(3.24)$$

Again, for  $\alpha > 0.6$ , the approximation in Eq. (3.24) provides a satisfying result. However,  $c(\alpha)$  does not exist at  $\alpha = 0.249986$  and the approximation gives unreasonable values in the range of  $0.25 < \alpha < 0.5$ .

Kundu (2008) proposes the MME and other bias-reduced estimation methods to estimate the change point. He also conducts Monte Carlo simulations to compare the performances of the estimation methods. The result shows that when sample size decreases, both bias and variance of all estimation methodologies increase. Moreover, in general, all the methods overestimate  $c(\alpha)$ .

### 3.4 Conclusion

In this chapter, we present the assumptions and the derivation of SB-S distribution; then we utilize MLE and MME to estimate the parameters of the distribution. We also introduce the procedure of examining the shape of SB-S distribution's hazard function. Since the hazard function is an upside-down function of  $t$ , it is obviously limited because it fails to cover othertypes of failure conditions. One of the GB-S distributions families that Owen (2004) proposes is investigated in depth in Chapter 4. We investigate the necessary conditions that result in a wider range of failure rate shapes for the GB-S distribution.

## CHAPTER 4

### GENERALIZED BIRNBAUM-SAUNDERS (GB-S)

### DISTRIBUTION

In chapter 3, we show that the hazard function of SB-S distribution is restricted to be only unimodal which fails to cover a wide range of failure rates such as increasing, constant or decreasing. In this chapter, we investigate in depth one of the generalized B-S (GB-S) distributions that Owen (2004) proposes and determine the necessary and sufficient conditions to have a wide range of practical failure rates. In section 4.1, we introduce the *pdf*, the *cdf*, the reliability function and the hazard function of GB-S distribution; we also investigate its characteristics and basic properties. The conditions that enable the GB-S distribution to model upside-down hazard rate function and monotonically increasing hazard rate function or their combination which may be useful in modeling the rollercoaster failure rate of electronic systems (roller coaster failure rate means that the failure rate is multimodal as advocated by Wong (1989)) are the subject of investigation of section 4.2. In section 4.3, we compare the performance of SB-S and GB-S distribution using simulation of failure time data.

#### 4.1 Characteristics and Properties of GB-S Distribution

In this section, we start with the relationship between GB-S distribution's failure time  $T$  and standard normal random variable  $Z$ . We present the *pdf*, the reliability function, the *cdf* and the hazard function of GB-S distribution. We investigate its characteristics and basic properties in this section.

#### 4.1.1 GB-S Distribution

The relationships between SB-S distribution's variable  $T$  and standard normal variable  $Z$  are:

$$Z = \frac{1}{a} \left[ \left( \frac{t}{\beta} \right)^{\frac{1}{2}} - \left( \frac{\beta}{t} \right)^{\frac{1}{2}} \right] \quad (4.1)$$

$$T = \beta \left[ \frac{aZ}{2} + \sqrt{\left( \frac{aZ}{2} \right)^2 + 1} \right]^2 \quad (4.2)$$

Where  $T$  is the time to failure.

Similar to (4.1) and (4.2), the relationships between GB-S distribution's variable  $T$  and the standard normal random variable  $Z$  are:

$$Z = \frac{1}{a} \left[ \left( \frac{t}{\beta} \right)^{\lambda} - \left( \frac{\beta}{t} \right)^{\lambda} \right] \quad (4.3)$$

$$T = \beta \left[ \frac{aZ}{2} + \sqrt{\left( \frac{aZ}{2} \right)^2 + 1} \right]^{\frac{1}{\lambda}} \quad (4.4)$$

Where  $\alpha$ ,  $\beta$  and  $\lambda$  are corresponding parameters of GB-S distribution. The parameters  $\alpha$  and  $\lambda$  are the shape parameters of the GB-S distribution and  $\beta$  is the scale parameter. The SB-S distribution is a special case of GB-S when  $\lambda=0.5$ .

The density function of  $T \sim GB-S(\alpha, \beta, \lambda)$  is given by (Owen 2004):

$$f(t; \alpha, \beta, \lambda) = \frac{\lambda}{\sqrt{2\pi\alpha t}} \left[ \left( \frac{t}{\beta} \right)^{\lambda} + \left( \frac{\beta}{t} \right)^{\lambda} \right] e^{\left\{ -\frac{1}{2\alpha^2} \left[ \left( \frac{t}{\beta} \right)^{2\lambda} + \left( \frac{\beta}{t} \right)^{2\lambda} - 2 \right] \right\}}, \quad 0 < t < \infty, \alpha > 0, \beta > 0, \lambda > 0 \quad (4.5)$$

We obtain the corresponding reliability function, the *pdf*, and the hazard function.

The *cdf* is expressed as:

$$F(t; \alpha, \beta, \lambda) = \Phi \left\{ \frac{1}{\alpha} \left[ \left( \frac{t}{\beta} \right)^{\lambda} - \left( \frac{\beta}{t} \right)^{\lambda} \right] \right\} \quad (4.6)$$

The reliability function is:

$$R(t; \alpha, \beta, \lambda) = 1 - F(t; \alpha, \beta, \lambda) = 1 - \Phi \left\{ \frac{1}{\alpha} \left[ \left( \frac{t}{\beta} \right)^{\lambda} - \left( \frac{\beta}{t} \right)^{\lambda} \right] \right\} \quad (4.7)$$

The hazard rate is:

$$h(t; \alpha, \beta, \lambda) = \frac{f(t; \alpha, \beta, \lambda)}{R(t; \alpha, \beta, \lambda)} = \frac{\frac{\lambda}{\sqrt{2\pi}\alpha t} \left[ \left( \frac{t}{\beta} \right)^\lambda + \left( \frac{\beta}{t} \right)^\lambda \right] e^{\left\{ -\frac{1}{2\alpha^2} \left[ \left( \frac{t}{\beta} \right)^{2\lambda} + \left( \frac{\beta}{t} \right)^{2\lambda} - 2 \right] \right\}}}{1 - \Phi \left\{ \frac{1}{\alpha} \left[ \left( \frac{t}{\beta} \right)^\lambda - \left( \frac{\beta}{t} \right)^\lambda \right] \right\}} \quad (4.8)$$

Other reliability characteristics can be easily obtained using the above expressions.

#### 4.1.2 Characteristics and Properties of GB-S Distribution

The characteristics and properties of SB-S distribution are presented in Chapter 3. In this section, we obtain the moments, mean time to failure, variance, skewness, and kurtosis of the GB-S distribution. We also provide additional properties of GB-S distribution.

##### 4.1.2.1 Characteristics of GB-S Distribution

We utilize Eqs.(4.1) and (4.2) to explore the characteristics of SB-S distribution. Similarly, we investigate the moments of GB-S distribution by considering Eqs. (4.3) and (4.4) which are repeated below.

$$Z = \frac{1}{\alpha} \left[ \left( \frac{T}{\beta} \right)^\lambda - \left( \frac{\beta}{T} \right)^\lambda \right]$$

$$T = \beta \left[ \frac{\alpha Z}{2} + \sqrt{\left( \frac{\alpha Z}{2} \right)^2 + 1} \right]^{\frac{1}{\lambda}}$$

Using the above transformations, we obtain, as shown in Appendix A, that:

$$\text{For } Z = -\frac{2}{\alpha} \text{ or } \frac{2}{\alpha}, \quad \left( \frac{T}{\beta} \right)^\gamma = \sum_{k=0}^{\infty} \binom{\frac{r}{\lambda}}{k} 2^{\frac{r}{2\lambda} - \frac{k}{2}} \left( \frac{\alpha Z}{2} \right)^k \quad (4.9)$$

$$\text{For } -\frac{2}{\alpha} < Z < \frac{2}{\alpha}, \quad \left( \frac{T}{\beta} \right)^\gamma = \sum_{k=0}^{\infty} \sum_{s=0}^{\infty} \binom{\frac{r}{\lambda}}{k} \binom{\frac{r}{2\lambda} - \frac{k}{2}}{s} \left( \frac{\alpha}{2} \right)^{2s+k} Z^{2s+k} \quad (4.10)$$

$$\text{For } Z < -\frac{2}{\alpha} \text{ or } Z > \frac{2}{\alpha}, \quad \left( \frac{T}{\beta} \right)^\gamma = \sum_{k=0}^{\infty} \sum_{s=0}^{\infty} \binom{\frac{r}{\lambda}}{k} \binom{\frac{r}{2\lambda} - \frac{k}{2}}{s} \left( \frac{\alpha}{2} \right)^{\frac{r}{\lambda} - 2s} Z^{\frac{r}{\lambda} - 2s} \quad (4.11)$$

Then we obtain the  $r$ th moment of  $T$  as:

$$E(T^r) = \beta^r \sum_{k=0}^{\infty} \sum_{s=0}^{\infty} \binom{\frac{r}{\lambda}}{k} \binom{\frac{r}{2\lambda} - \frac{k}{2}}{s} \cdot (I_1 + I_2) \quad (4.12)$$

Where



$$I_1 = \left(\frac{\alpha}{2}\right)^{2s+k} \int_{-\frac{\alpha}{2}}^{\frac{\alpha}{2}} z^{2s+k} \exp\left(-\frac{z^2}{2}\right) dz \quad (4.13)$$

$$I_2 = \left(\frac{a}{2}\right)^{\frac{r}{\lambda}-2s} \cdot \left( \int_{-\infty}^{\frac{2}{\alpha}} z^{\frac{r}{\lambda}-2s} \exp\left(-\frac{z^2}{2}\right) dz + \int_{\frac{2}{\alpha}}^{\infty} z^{\frac{r}{\lambda}-2s} \exp\left(-\frac{z^2}{2}\right) dz \right) \quad (4.14)$$

Equations (4.13) and (4.14) can be written as:

$$I_1 = 2^{\frac{-2s-k-1}{2}} \left[ \Gamma\left(\frac{2s+k+1}{2}\right) - \Gamma\left(\frac{2s+k+1}{2}, \frac{2}{a^2}\right) \right] \left[ (-1)^{2s+k} + 1 \right]$$

$$I_2 = \frac{\alpha^{\frac{r}{\lambda}-2s}}{2^{\frac{\frac{r}{\lambda}-2s+1}{2}}} \left[ (-1)^{\frac{r}{\lambda}-2s} + 1 \right] \Gamma\left(\frac{\frac{r}{\lambda}-2s+1}{2}, \frac{2}{\alpha^2}\right)$$

It is worth noting that the moments of GB-S distribution do not exist when  $Z < -\frac{2}{\alpha}$ .

Once we obtain the  $r$ th moment of  $T$ , we investigate the expected time to failure  $E(T)$ ,

the variance  $Var(T)$ , the coefficients of skewness  $\gamma_1(T)$  and the kurtosis  $\gamma_2(T)$  as

follows:

$$E(T) = \beta \sum_{k=0}^{\infty} \sum_{s=0}^{\infty} \left( \frac{1}{\lambda} \right) \binom{\frac{1}{2\lambda} - \frac{k}{2}}{s} \cdot (I_1 + I_2)$$

$$Var(T) = \beta^2 \sum_{k=0}^{\infty} \sum_{s=0}^{\infty} \binom{\frac{2}{\lambda}}{k} \binom{\frac{1}{\lambda} - \frac{k}{2}}{s} \cdot (I_1 + I_2) - [E(T)]^2$$

$$\gamma_1(T) = \frac{E(T^3)}{Var^{1.5}(T)} = \frac{\beta^3 \sum_{k=0}^{\infty} \sum_{s=0}^{\infty} \binom{\frac{3}{\lambda}}{k} \binom{\frac{3}{2\lambda} - \frac{k}{2}}{s} \cdot (I_1 + I_2)}{Var^{1.5}(T)}$$

$$\gamma_2(T) = \frac{E(T^4)}{Var^2(T)} - 3 = \frac{\beta^4 \sum_{k=0}^{\infty} \sum_{s=0}^{\infty} \binom{\frac{4}{\lambda}}{k} \binom{\frac{2}{\lambda} - \frac{k}{2}}{s} \cdot (I_1 + I_2)}{Var^2(T)} - 3$$

It is observed that the skewness and kurtosis are not affected by the scale parameter  $\beta$ .

Kurtosis, a measure of the shape of a probability distribution, is an important statistics as higher kurtosis means the variance is the result of infrequent extreme deviations, as opposed to frequent modestly sized deviations.

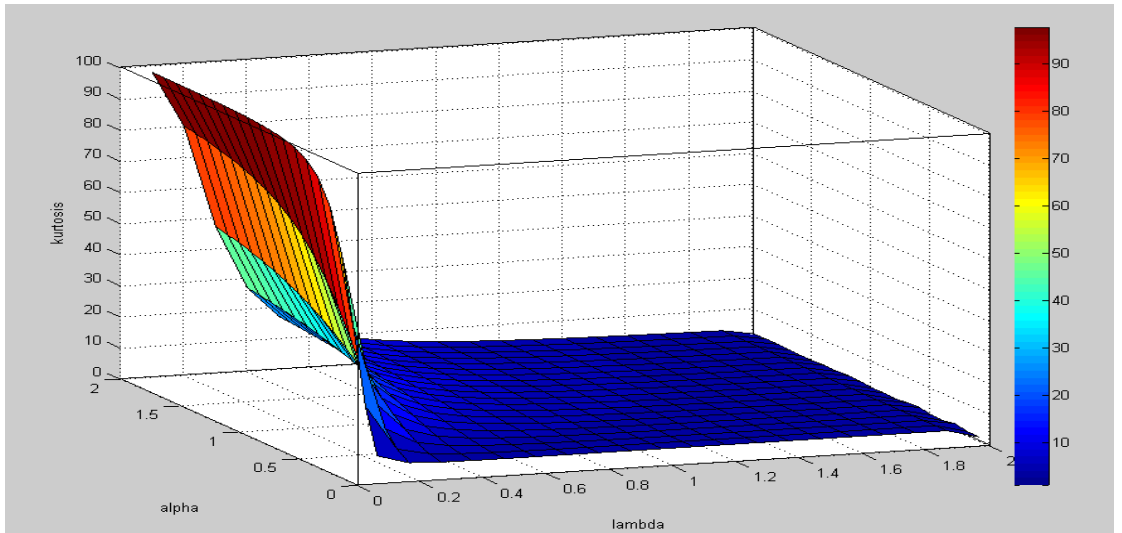


Figure 4.1 Kurtosis of GB-S distribution with different  $\alpha$  and  $\lambda$  when  $\beta=1$

In Figure 4.1, we set  $\beta=1$  since the scale parameter has no influence on the kurtosis. We observe that when  $\lambda$  becomes smaller, the kurtosis increases sharply. In other words, for a GB-S distribution with constant  $\alpha$ , the smaller the parameter  $\lambda$  the higher the contribution of infrequent extreme deviations; when  $\lambda$  is large, the GB-S distribution has more frequent modestly sized deviations.

#### 4.1.2.2 Properties of GB-S Distribution

Since the reliability function of GB-S distribution is always monotonously decreasing from 1 to 0 and the *cdf* of GB-S distribution is increasing from 0 to 1, we only examine that the *pdf* of GB-S distribution as a unimodal function of  $t$ . Figure 4.2 shows that the *pdf* of GB-S distributions are all unimodal for different values of  $\lambda$ .

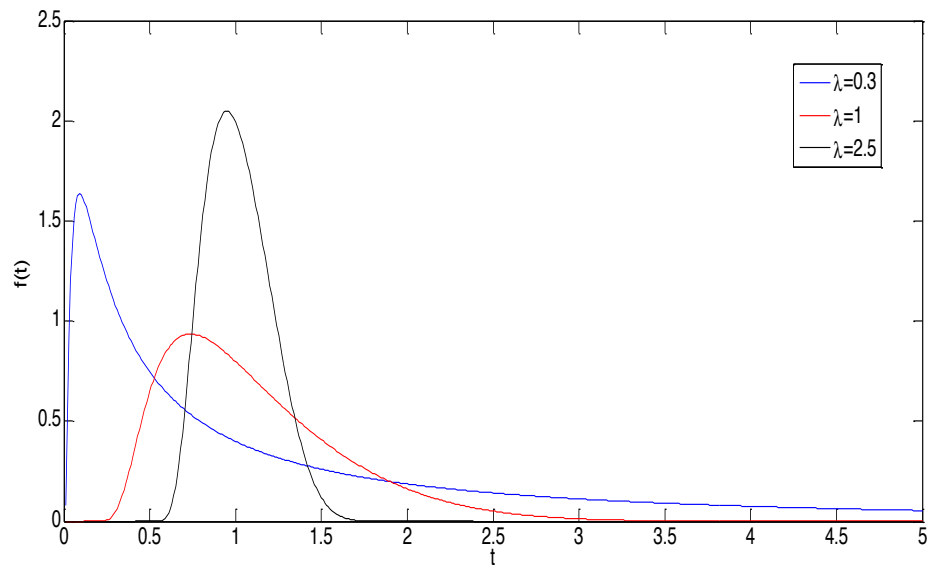


Figure 4.2 GB-S density function with different  $\lambda$

Another important observation about the inverse of  $T$  is that: if  $T$  belongs to GB-S distribution with parameters  $\alpha, \beta$  and  $\lambda$ , then  $T^{-1}$  also belongs to GB-S distribution with the corresponding parameters  $\alpha, \beta^{-1}$  and  $\lambda$ , respectively. Therefore, we readily have:

$$E(T^{-1}) = \frac{1}{\beta} \sum_{k=0}^{\infty} \sum_{s=0}^{\infty} \binom{\frac{1}{\lambda}}{k} \binom{\frac{1}{2\lambda} - \frac{k}{2}}{s} \cdot (I_1 + I_2)$$

and

$$Var(T^{-1}) = \beta^{-2} \sum_{k=0}^{\infty} \sum_{s=0}^{\infty} \binom{\frac{2}{\lambda}}{k} \binom{\frac{1}{\lambda} - \frac{k}{2}}{s} \cdot (I_1 + I_2) - [E(T^{-1})]^2$$

Since the skewness and kurtosis are only affected by the shape of the distribution, the skewness and kurtosis of  $T^{-1}$  are the same as the skewness and kurtosis of  $T$ . Thus,

$$\gamma_1(T^{-1}) = \frac{E(T^{-3})}{Var^{1.5}(T^{-1})} = \frac{\beta^{-3} \sum_{k=0}^{\infty} \sum_{s=0}^{\infty} \binom{\frac{3}{\lambda}}{k} \binom{\frac{3}{2\lambda} - \frac{k}{2}}{s} \cdot (I_1 + I_2)}{Var^{1.5}(T^{-1})}$$

$$\gamma_2(T^{-1}) = \frac{E(T^{-4})}{Var^2(T^{-1})} - 3 = \frac{\beta^{-4} \sum_{k=0}^{\infty} \sum_{s=0}^{\infty} \binom{\frac{4}{\lambda}}{k} \binom{\frac{2}{\lambda} - \frac{k}{2}}{s} \cdot (I_1 + I_2)}{Var^2(T^{-1})} - 3$$

## 4.2 Hazard Function of GB-S Distribution

As we discuss earlier in chapter 3, the hazard function of SB-S distribution is upside down for all  $t$ . In this section, we utilize a similar methodology to that adopted in chapter 3 to investigate the shape of GB-S distribution's hazard function. Again, without loss of generality we set  $\beta=1$ . We also set:

$$\varepsilon(t) = t^\lambda - t^{-\lambda} \quad (4.15)$$

$$\varepsilon'(t) = \lambda(t^{\lambda-1} + t^{-\lambda-1}) \quad (4.16)$$

$$\varepsilon''(t) = \frac{-\lambda}{t^2} [(1-\lambda)t^\lambda + (1+\lambda)t^{-\lambda}] \quad (4.17)$$

$$\varepsilon^2(t) = t^{2\lambda} + t^{-2\lambda} - 2 \quad (4.18)$$

Then the *pdf* and the hazard function of SB-S distribution can be written as Eqs. (4.19)

and (4.20), respectively as:

$$f(t) = \frac{1}{\sqrt{2\pi\alpha}} \varepsilon'(t) \exp \left\{ -\frac{1}{2\alpha^2} \varepsilon^2(t) \right\} \quad (4.19)$$

$$h(t) = \frac{f(t)}{1-F(t)} = \frac{\frac{1}{\sqrt{2\pi\alpha}} \varepsilon'(t) \exp\left\{-\frac{1}{2\alpha^2} \varepsilon^2(t)\right\}}{\Phi\left\{-\frac{\varepsilon(t)}{\alpha}\right\}} \quad (4.20)$$

Similar to the SB-S distribution's hazard function, we discuss the shape of the hazard function of GB-S distribution by utilizing similar Lemmas to the ones that Kundu (2008) adopts when investigating the hazard function of SB-S distribution.

The following Lemmas (Glaser 1980) are necessary for studying the shape of the hazard function of GB-S distribution:

Lemma 1: Suppose  $f(t)$ , for  $t > 0$ , is the *pdf* of a positive real-valued continuous random variable, and defines  $\eta(t) = -\frac{f'(t)}{f(t)}$ . If there exists a  $t_0$  such that  $\eta'(t) > 0 \forall t \in (0, t_0)$ ,  $\eta'(t_0) = 0$  and  $\eta'(t) < 0 \forall t \in (t_0, \infty)$ . The hazard function corresponding to  $f(t)$  is either an upside-down or a decreasing function of  $t$ .

Lemma 2: If  $\eta'(t) > 0 \forall t \in (0, \infty)$ , the hazard function is an increasing function of  $t$ .

Lemma 3: If Lemma 1 holds and  $\varsigma = \lim_{t \rightarrow 0} f(t)$  exists, possibly equal to 0 or  $\infty$ , the hazard function is decreasing if  $\varsigma = \lim_{t \rightarrow 0} f(t) = \infty$  and is upside-down if  $\varsigma = \lim_{t \rightarrow 0} f(t) = 0$ .

More specifically, for GB-S distribution, we obtain:

$$\eta(t) = -\frac{f'(t)}{f(t)} = -\left[ \frac{\varepsilon''(t)}{\varepsilon'(t)} - \frac{\varepsilon'(t)\varepsilon(t)}{\alpha^2} \right] = \frac{(1-\lambda)t^\lambda + (1+\lambda)t^{-\lambda}}{t^{1+\lambda} + t^{1-\lambda}} + \frac{\lambda(t^{2\lambda-1} - t^{-2\lambda-1})}{\alpha^2} \quad (4.21)$$

$$\eta'(t) = \frac{s(t)}{\alpha^2 (t^{1+\lambda} + t^{1-\lambda})^2 t^{4\lambda}} \quad (4.22)$$

Where

$$\begin{aligned} s(t) = & (2\lambda^2 - \lambda)t^{8\lambda} + \left[ (\alpha^2 + 4)\lambda^2 - 2\lambda - \alpha^2 \right] t^{6\lambda} - (4\lambda^2 - 2\alpha^2)t^{4\lambda} \\ & + \left[ 4\lambda^2 + (\alpha^2 - 2)\lambda + \alpha^2 \right] t^{2\lambda} + (2\lambda^2 + \lambda) \end{aligned} \quad (4.23)$$

According to the Lemmas mentioned above, we study the shape of the GB-S distribution's hazard function by examining  $\eta'(t)$ . Since

$$\alpha^2 (t^{1+\lambda} + t^{1-\lambda})^2 t^{4\lambda} > 0 \quad \forall t \in (0, \infty), \text{ we only need to investigate } s(t)$$

With the substitution method, we set  $x = t^{2\lambda}$ :

$$s(t) = s(x) = ax^4 + bx^3 + cx^2 + dx + e \quad (4.24)$$

and

$$s'(x) = 4ax^3 + 3bx^2 + 2cx + d = Ax^3 + Bx^2 + Cx + D \quad (4.25)$$

Where

$$a = 2\lambda^2 - \lambda$$

$$b = (\alpha^2 + 4)\lambda^2 - 2\lambda - \alpha^2$$

$$c = 4\lambda^2 - 2\alpha^2$$

$$d = 4\lambda^2 + (\alpha^2 - 2)\lambda + \alpha^2$$

$$e = 2\lambda^2 + \lambda$$

and

$$A = 4a \quad (4.26)$$

$$B = 3b \quad (4.27)$$

$$C = 2c \quad (4.28)$$

$$D = d \quad (4.29)$$

Now we can examine the shape of GB-S distribution's hazard function by investigating the root conditions of  $s'(x)$ .

The discriminant  $\Delta$  of a cubic polynomial can be utilized to obtain the information about its roots. According to Shengjin's formula (1988), we obtain the discriminant of a cubic polynomial  $Ax^3 + Bx^2 + Cx + D$  as:



$$\Delta = B'^2 - 4A'C' \quad (4.30)$$

Where

$$A' = B^2 - 3AC \quad (4.31)$$

$$B' = BC - 9AD \quad (4.32)$$

$$C' = C^2 - 3BD \quad (4.33)$$

So the discriminant  $\Delta$  of a cubic polynomial is:

$$\Delta = B'^2 - 4A'C' = -3B^2C^2 - 54ABCD + 81A^2D^2 + 12AC^3 + 12B^3D \quad (4.34)$$

Then, we obtain the discriminant and the roots conditions in Appendix B. The discriminant and the roots conditions have the following relationship:

If  $\Delta > 0$ , the cubic polynomial has one root as:

$$x_{11} = \frac{-B - \sqrt[3]{Y_1} - \sqrt[3]{Y_2}}{3A} \quad (4.35)$$

Where

$$Y_{1,2} = A'B + \frac{3A(-B' \pm \sqrt{B'^2 - 4A'C'})}{2}$$

If  $\Delta = 0$ , the cubic polynomial has two roots as:

$$x_{21} = -\frac{B}{A} + \frac{B'}{A'}$$

$$x_{22} = \frac{B'}{2A'}$$

If  $\Delta < 0$ , the cubic polynomial has three roots as:

$$x_{31} = \frac{(-B - 2\sqrt{A'})\cos\left(\frac{\theta}{3}\right)}{3A}$$

$$x_{32,33} = \frac{(-B + \sqrt{A'})\left(\cos\frac{\theta}{3} \pm \sqrt{3}\sin\frac{\theta}{3}\right)}{3A}$$

Where

$$\theta = \arccos\left(\frac{2A'B - 3AB'}{2A^{1.5}}\right)$$

More specifically, upon substituting Eqs. (4.26) - (4.29) into Eq. (4.34), we obtain the discriminant of  $s'(x)$  as:

$$\Delta = -108b^2c^2 - 1296(abcd - a^2d^2) + 384ac^3 + 324b^3d \quad (4.36)$$

For  $\Delta < 0$ ,  $s'(x)$  has three roots which are placed in order of  $x_{31}' < x_{32}' < x_{33}'$ , then we have  $t_{31} < t_{32} < t_{33}$ , where  $t_{31} = \sqrt[2\lambda]{x_{31}'}$ ,  $t_{32} = \sqrt[2\lambda]{x_{32}'}$ ,  $t_{33} = \sqrt[2\lambda]{x_{33}'}$ . Similarly, when  $\Delta = 0$ ,  $s'(x)$  has two roots and we have  $t_{21} < t_{22}$ , where  $t_{21} = \sqrt[2\lambda]{x_{21}'}$ ,  $t_{22} = \sqrt[2\lambda]{x_{22}'}$ . When  $\Delta > 0$ ,  $s'(x)$  has only one root  $x_{11}$  and we have  $t_{11} = \sqrt[2\lambda]{x_{11}'}$ . The details of the roots can be found in Appendix B.

It is observed that  $\varsigma = \lim_{t \rightarrow 0} f(t; \alpha, \beta, \lambda) = 0$ . We also investigate  $s(0) = 2\lambda^2 + \lambda > 0 \forall t \in (0, \infty)$ . When  $\lambda < 0.5$ ,  $s(\infty) = -\infty$  and when  $\lambda > 0.5$ ,  $s(\infty) = \infty$ . Following are the different conditions that enable  $\eta'(t)$  to be positive or negative; we can determine the conditions that result in different shapes of GB-S distribution

1. When  $\Delta < 0$  and  $\lambda < 0.5$ , for  $0 < x_{31}' < x_{32}' < x_{33}'$  and  $x_{31}' < 0 < x_{32}' < x_{33}'$ , if  $s(t_{32}) > 0$ , there exists a  $t_0$  such that  $s'(t) > 0 \forall t \in (0, t_0)$ ,  $s'(t_0) = 0$  and  $s'(t) < 0 \forall t \in (t_0, \infty)$ , according to Lemma 1 and Lemma 3, the hazard function of GB-S distribution is an upside-down function; if  $s(t_{32}) \leq 0$ , the hazard function is a roller coaster hazard function.

2. When  $\Delta < 0$  and  $\lambda < 0.5$ , for  $x_{31}' < x_{32}' < 0 < x_{33}'$  and  $x_{31}' < x_{32}' < x_{33}' < 0$ ,

according to Lemma 1 and Lemma 3, the hazard function is upside-down function because there always exists a  $t_0$  such that  $s'(t) > 0 \forall t \in (0, t_0)$ ,  $s'(t_0) = 0$  and  $s'(t) < 0 \forall t \in (t_0, \infty)$

3. When  $\Delta = 0$  and  $\lambda < 0.5$ , whether  $x_{21}' < x_{22}' < 0$  or  $0 < x_{21}' < x_{22}'$  or  $x_{21}' < 0 < x_{22}'$ , there always exists a  $t_0$  such that  $s'(t) > 0 \forall t \in (0, t_0)$ ,  $s'(t_0) = 0$  and  $s'(t) < 0 \forall t \in (t_0, \infty)$ . According to Lemma 1 and Lemma 3, the hazard function is always an upside-down function.

4. When  $\Delta > 0$  and  $\lambda < 0.5$ , for either  $x_{11}' < 0$  or  $0 < x_{11}'$ , there always exists a  $t_0$  such that  $s'(t) > 0 \forall t \in (0, t_0)$ ,  $s'(t_0) = 0$  and  $s'(t) < 0 \forall t \in (t_0, \infty)$ . So the hazard function is an upside-down function according to Lemma 1 and Lemma 3.

5. When  $\Delta < 0$  and  $\lambda > 0.5$ , for  $0 < x_{31}' < x_{32}' < x_{33}'$ , if  $s(t_{31}) > 0$  and  $s(t_{33}) > 0$ , we observe that  $s'(t) > 0 \forall t \in (0, \infty)$ , according to Lemma 2, the hazard function of GB-S distribution is an increasing function; if  $s(t_{31}) \leq 0$  or  $s(t_{33}) \leq 0$ , the hazard function of GB-S distribution is a roller coaster function.

6. When  $\Delta < 0$  and  $\lambda > 0.5$ , for  $x_{31}' < 0 < x_{32}' < x_{33}'$  or  $x_{31}' < x_{32}' < 0 < x_{33}'$ , if  $s(t_3) > 0$ , we observe that  $s'(t) > 0 \forall t \in (0, \infty)$ , according to Lemma 2, the hazard function of GB-S distribution is an increasing function; if  $s(t_3) \leq 0$ , the hazard function of GB-S distribution is a roller coaster function.

7. When  $\Delta < 0$  and  $\lambda > 0.5$ , for  $x_{31}' < x_{32}' < x_{33}' < 0$ , it always holds that  $s'(t) > 0 \forall t \in (0, \infty)$ , according to Lemma 2, the hazard function of GB-S distribution is an increasing function.
8. When  $\Delta = 0$  and  $\lambda > 0.5$ , for  $0 < x_{21}' < x_{22}'$  and  $s'(x) < 0$  for any  $x \in (x_{21}, x_{22})$ , according to Lemma 2, the hazard function of GB-S distribution is an increasing function if  $s(t_2) > 0$  and the hazard function is a roller coaster function if  $s(t_2) \leq 0$ .
9. When  $\Delta = 0$  and  $\lambda > 0.5$ , for  $0 < x_{21}' < x_{22}'$  and  $s'(x) > 0$  for any  $x \in (x_{21}, x_{22})$ , according to Lemma 2, the hazard function of GB-S distribution is an increasing function if  $s(t_1) > 0$  and the hazard function is a roller coaster function if  $s(t_1) \leq 0$ .
10. When  $\Delta = 0$  and  $\lambda > 0.5$ , for  $x_{21}' < 0 < x_{22}'$  and  $s'(x) < 0$  for any  $x \in (x_{21}, x_{22})$ , the hazard function of GB-S distribution is an increasing function if  $s(t_2) > 0$  and the hazard function is a roller coaster function if  $s(t_2) \leq 0$ .
11. When  $\Delta = 0$  and  $\lambda > 0.5$ , for  $x_{21}' < 0 < x_{22}'$  and  $s'(x) > 0$  for any  $x \in (x_{21}, x_{22})$ , it always holds that  $s'(t) > 0 \forall t \in (0, \infty)$ . So according to Lemma 2, the hazard function of GB-S distribution is an increasing function.
12. When  $\Delta = 0$  and  $\lambda > 0.5$ , for  $x_{21}' < x_{22}' < 0$ , it always holds that  $s'(t) > 0 \forall t \in (0, \infty)$ . So the hazard function of GB-S distribution is an increasing function.

13. When  $\Delta > 0$  and  $\lambda > 0.5$ , for  $x_{11} > 0$ , if  $s(t_1) > 0$ , we observe that  $s'(t) > 0 \forall t \in (0, \infty)$ , according to Lemma 2, the hazard function of GB-S distribution is an increasing function; if  $s(t_1) \leq 0$ , the hazard function of GB-S distribution is a roller coaster function.
14. When  $\Delta > 0$  and  $\lambda > 0.5$ , for  $x_{11} < 0$ , we observe that  $s'(t) > 0 \forall t \in (0, \infty)$ , according to Lemma 2, the hazard function of GB-S distribution is an increasing function.
15. When  $\lambda = 0.5$ , the distribution is SB-S distribution and the hazard function is always an upside down function (Kundu 2008).

Table 4.1 is a summary of the conditions which make the hazard function of the GB-S distribution to be increasing, upside-down and roller coaster.

Table 4.1 Roots condition of  $s'(x)$  and shape of GB-S hazard rate

$\lambda$	$\Delta$	Roots Conditions of $s'(x)$	Shape of $h(t)$
$\lambda < 0.5$	$\Delta < 0$	$0 < x_{31}' < x_{32}' < x_{33}'$ or $x_{31}' < 0 < x_{32}' < x_{33}'$ $s(t_{32}) > 0$	upside-down
		$0 < x_{31}' < x_{32}' < x_{33}'$ or $x_{31}' < 0 < x_{32}' < x_{33}'$	rollercoaster

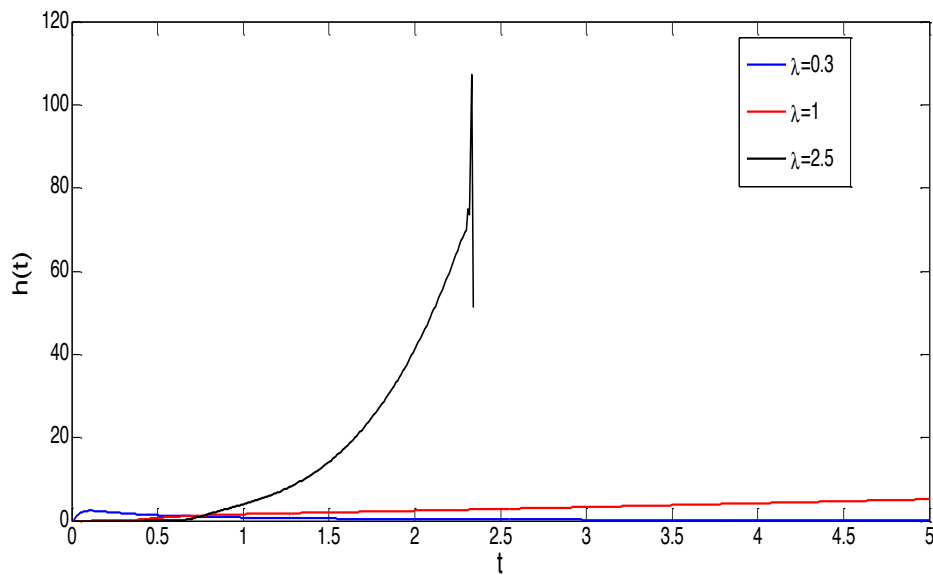
$\lambda < 0.5$	$\Delta < 0$	$s(t_{32}) \leq 0$	
$\lambda < 0.5$	$\Delta < 0$	$x_{31}' < x_{32}' < 0 < x_{33}'$ or $x_{31}' < x_{32}' < x_{33}' < 0$	upside-down
$\lambda < 0.5$	$\Delta = 0$	$x_{21}' < x_{22}' < 0$ or $0 < x_{21}' < x_{22}'$ or $x_{21}' < 0 < x_{22}'$	upside-down
$\lambda < 0.5$	$\Delta > 0$	$0 < x_{11}'$ or $x_{11}' < 0$	upside-down
$\lambda > 0.5$	$\Delta < 0$	$0 < x_{31}' < x_{32}' < x_{33}'$ $s(t_{31}) > 0$ and $s(t_{33}) > 0$	increasing
$\lambda > 0.5$	$\Delta < 0$	$0 < x_{31}' < x_{32}' < x_{33}'$ $s(t_{31}) \leq 0$ or $s(t_{33}) \leq 0$	rollercoaster
$\lambda > 0.5$	$\Delta < 0$	$x_{31}' < 0 < x_{32}' < x_{33}'$ or $x_{31}' < x_{32}' < 0 < x_{33}'$ $s(t_3) > 0$	increasing
$\lambda > 0.5$	$\Delta < 0$	$x_{31}' < 0 < x_{32}' < x_{33}'$ or $x_{31}' < x_{32}' < 0 < x_{33}'$ $s(t_3) \leq 0$	rollercoaster
$\lambda > 0.5$	$\Delta < 0$	$x_{31}' < x_{32}' < x_{33}' < 0$	increasing
$\lambda > 0.5$	$\Delta = 0$	$0 < x_{21}' < x_{22}'$ $s'(x) < 0$ for any $x \in (x_{21}, x_{22})$ , $s(t_2) > 0$	increasing
$\lambda > 0.5$	$\Delta = 0$	$0 < x_{21}' < x_{22}'$	roller

		$s'(x) < 0$ for any $x \in (x_{21}, x_{22})$ , $s(t_2) \leq 0$	coaster
$\lambda > 0.5$	$\Delta = 0$	$0 < x_{21}' < x_{22}'$ $s'(x) > 0$ for any $x \in (x_{21}, x_{22})$ , $s(t_1) > 0$	increasing
$\lambda > 0.5$	$\Delta = 0$	$0 < x_{21}' < x_{22}'$ $s'(x) > 0$ for any $x \in (x_{21}, x_{22})$ , $s(t_1) < 0$	roller coaster
$\lambda > 0.5$	$\Delta = 0$	$x_{21}' < 0 < x_{22}'$ and $s'(x) < 0$ for any $x \in (x_{21}, x_{22})$ , $s(t_2) > 0$	increasing
$\lambda > 0.5$	$\Delta = 0$	$x_{21}' < 0 < x_{22}'$ and $s'(x) < 0$ for any $x \in (x_{21}, x_{22})$ , $s(t_2) \leq 0$	rollercoaster
$\lambda > 0.5$	$\Delta = 0$	$x_{21}' < 0 < x_{22}'$ and $s'(x) > 0$ for any $x \in (x_{21}, x_{22})$	increasing
$\lambda > 0.5$	$\Delta = 0$	$x_{21}' < x_{22}' < 0$	increasing
$\lambda > 0.5$	$\Delta > 0$	$x_{11} > 0$ , $s(t_1) > 0$	increasing
$\lambda > 0.5$	$\Delta > 0$	$x_{11} > 0$ , $s(t_1) \leq 0$	rollercoaster
$\lambda > 0.5$	$\Delta > 0$	$x_{11} < 0$	increasing
$\lambda = 0.5$	$\Delta > 0$ $\Delta = 0$	any	upside-down



	$\Delta < 0$		
--	--------------	--	--

So far, we discuss all possibilities of the shape of GB-S distribution's hazard function by investigating the nature of roots of  $s'(x)$ . In general, the hazard function of GB-S distribution covers three types of failure conditions: the hazard function can be either



an increasing or a roller coaster function of  $t$  when  $\lambda > 0.5$ ; the hazard function can be either an upside-down or a roller coaster function of  $t$  when  $\lambda < 0.5$  and the hazard function is always an upside down function of  $t$  when  $\lambda = 0.5$ .

Figure 4.3 GB-S hazard function when  $\alpha=1,5$  and  $\beta=1$  with different  $\lambda$

The GB-S distribution covers a wider range of hazard functions than the SB-S distribution. Figure 4.3 presents three types of failure modes that the GB-S

distribution covers. The generalization enables the B-S distribution to be more flexible to model increasing hazard rate which is common when a component experiences wear-out or deterioration. The B-S distribution can also model the roller coaster failure rate of an electronic system

### 4.3 Simulation Study

We have shown that the GB-S distribution can model different types of failure rates. We have also shown that the SB-S distribution is a special case of the GB-S distribution and verify this by fitting failure data with both distributions. In this section, we utilize simulation data to compare the performance of GB-S distribution and SB-S distribution. We use MATLAB to generate the simulation data with given distribution parameters.

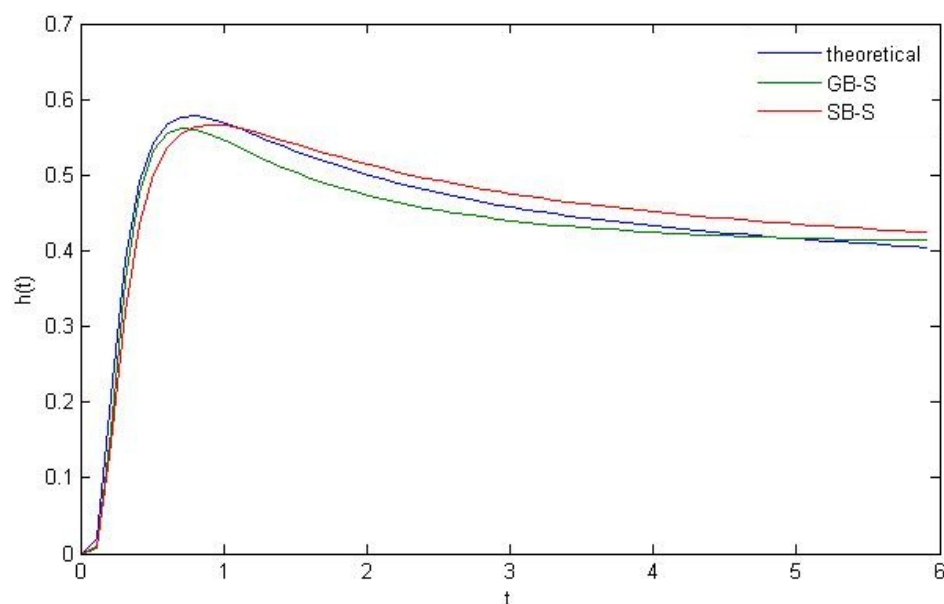
Without loss of generality, we set  $\lambda = 0.5$  and generate four groups of simulated data with different  $\alpha$  and  $\beta$  as shown in Table 4.2.

Table 4.2 Parameters of SB-S and GB-S distribution

	Group 1	Group 2	Group 3
$\alpha$	1	0.5	3

$\beta$	1.5	4	1
---------	-----	---	---

After generating the random failure data we fit both the SB-S and GB-S distribution to the three groups of data, respectively. We use the Maximum Likelihood Estimation



(MLE) approach to estimate the parameters. When generating the failure data,  $\lambda$  is fixed at 0.5. We just estimate  $\alpha$  and  $\beta$  for SB-S distribution while  $\alpha$ ,  $\beta$  and  $\lambda$  are all estimated for the GB-S distribution. Since the failure data are generated with the given parameters, we can obtain the theoretical hazard rate functions and compare them with the estimated hazard rate functions.

Figure 4.4 Theoretical and predicted hazard rate by SB-S and GB-S when

$$\alpha=1, \beta=1.5$$

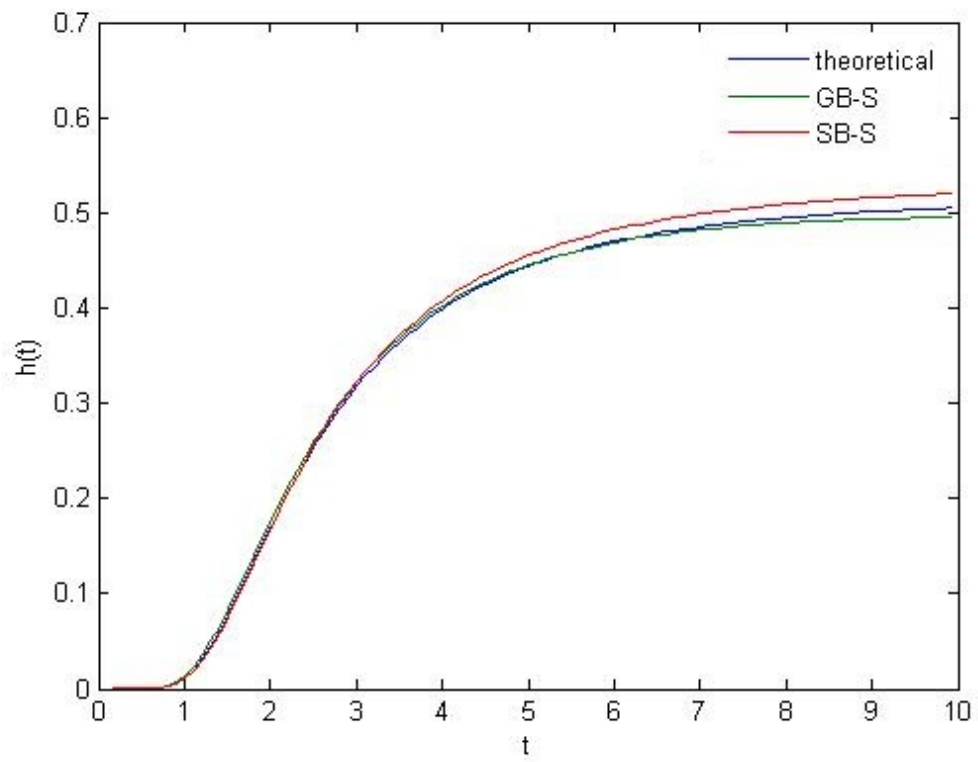


Figure 4.5 Theoretical and predicted hazard rate by SB-S and GB-S when

$$\alpha = 0.5, \beta = 4$$

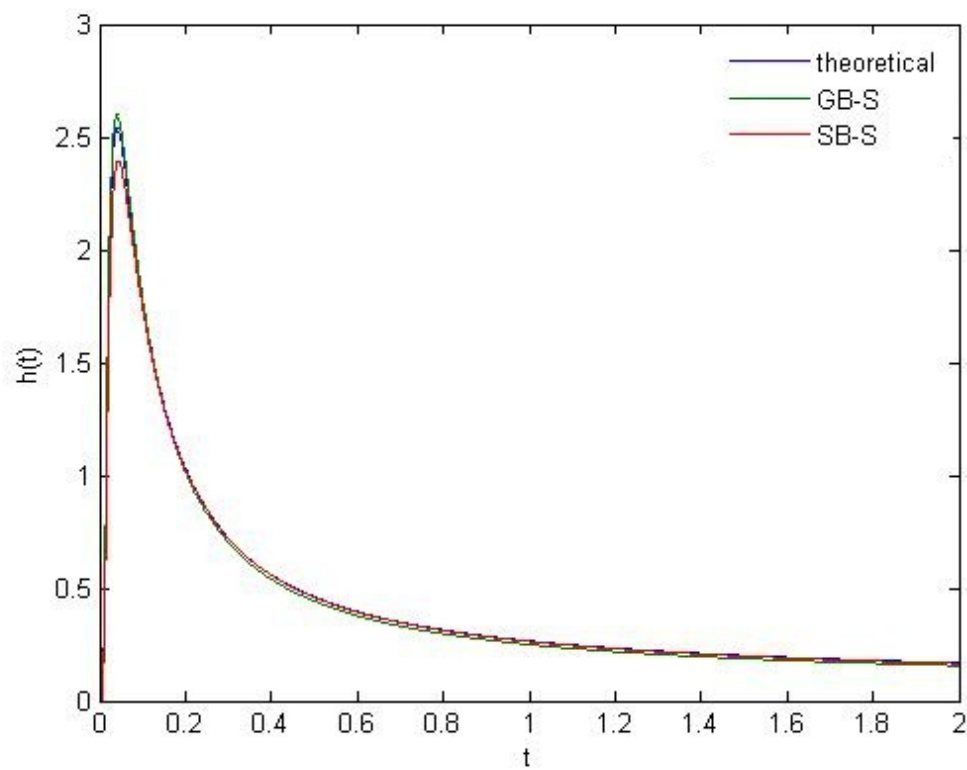


Figure 4.6 Theoretical and predicted hazard rate by SB-S and GB-S when

$$\alpha = 3, \beta = 1$$

Figures 4.4 to 4.6 present the theoretical and estimated hazard rates with different values of  $\alpha$  and  $\beta$ . We summarize the sum of squared errors (SSE) of those estimations in Table 4.3.

Table 4.3 SSE of SB-S and GB-S distribution's hazard rate estimates

	GB-S	SB-S
Group 1	.0192	.0298
Group 2	.0024	.0108
Group 3	.5811	1.5834

The simulation results show that the GB-S distribution provides more accurate hazard rate estimation than SB-S distribution.

#### 4.4 Conclusion

In this chapter, we investigate the GB-S distribution and obtain its characteristics and properties. We also investigate the effect of the distribution parameters on the shape of the GB-S distribution's hazard function. The proposed GB-S distribution is more flexible than the SB-S distribution as it exhibits increasing, roller coaster and upside-down hazard rate functions. Furthermore, we explore the necessary conditions that enable GB-S distribution to model these failure rate functions. We show that indeed the GB-S distribution provides better fit to fatigue failure data than the SB-S distribution.

## **CHAPTER 5**

### **GB-S DISTRIBUTION'S PARAMETER ESTIMATION**

In chapter 4, we investigate the shape of GB-S distribution's hazard function and obtain its characteristics and properties. We show the necessary and sufficient conditions that enable the GB-S distribution to model different failure conditions. In this chapter, we deal with the estimation of GB-S distribution's parameters. In section 5.1, we estimate the parameters by utilizing the traditional Maximum Likelihood Estimation (MLE) methodology which in most cases is considered to be reasonable in comparison with other estimation methodologies. However, in case of insufficient sample, MLE is highly biased and the variance obtained by constructing the Fisher information matrix is large. In section 5.2, a modified MLE (MMLE) method (Cohen and Whitten 1980) is utilized to see whether the modification can improve the estimation's accuracy in case of small sample size. To validate the MMLE, we apply both MLE and MMLE to several groups of random failure time data and compare the performances of the two methodologies. The detailed computational procedure and results of the simulation are discussed in section 5.3.

#### **5.1 Maximum Likelihood Estimation (MLE)**

### 5.1.1 The Estimation Function

The MLE of SB-S distribution is discussed originally by Birnbaum and Saunders (1968). However, obtaining the MLE of  $\beta$  by setting a non-linear equation of  $\beta$  might result in computational round off errors and potential inaccuracies. Now we investigate the application of MLE to GB-S distribution's parameters.

The likelihood function for a sample of size  $n$  from GB-S distribution is

$$\begin{aligned}
 L(\alpha, \beta, \lambda; t_i) &= \prod_{i=1}^n f(t_i; \alpha, \beta, \lambda) = \prod_{i=1}^n \frac{\lambda}{\sqrt{2\pi}at_i} \left[ \left( \frac{t_i}{\beta} \right)^\lambda + \left( \frac{\beta}{t_i} \right)^\lambda \right] e^{\left\{ -\frac{1}{2a^2} \left[ \left( \frac{t_i}{\beta} \right)^{2\lambda} + \left( \frac{\beta}{t_i} \right)^{2\lambda} - 2 \right] \right\}} \\
 &= \frac{\prod_{i=1}^n \left[ \left( \frac{t_i}{\beta} \right)^\lambda + \left( \frac{t_i}{\beta} \right)^{-\lambda} \right] \lambda^n}{(\sqrt{2\pi})^n \alpha^n \prod_{i=1}^n t_i} e^{\left\{ -\frac{1}{2\alpha^2} \left[ \sum_{i=1}^n \left[ \left( \frac{t_i}{\beta} \right)^{2\lambda} + \left( \frac{t_i}{\beta} \right)^{-2\lambda} \right] - 2n \right] \right\}} \quad (5.1)
 \end{aligned}$$

The logarithm of the likelihood function is

$$\begin{aligned}
 l(\alpha, \beta, \lambda; t_i) &= n \log \lambda - \sum_{i=1}^n \log \sqrt{2\pi}at_i + \sum_{i=1}^n \log \left[ \left( \frac{t_i}{\beta} \right)^\lambda + \left( \frac{\beta}{t_i} \right)^\lambda \right] \\
 &\quad - \frac{\sum_{i=1}^n \left( \frac{t_i}{\beta} \right)^{2\lambda}}{2a^2} - \frac{\sum_{i=1}^n \left( \frac{\beta}{t_i} \right)^{2\lambda}}{2a^2} + \frac{n}{a^2} \quad (5.2)
 \end{aligned}$$



Taking the derivatives of (5.2) with respect to  $\alpha, \beta$  and  $\lambda$  and equating the resultants to zero respectively, we obtain

$$\frac{\partial l}{\partial \alpha} = \frac{-a^2 n + \sum_{i=1}^n \left(\frac{t_i}{\beta}\right)^{2\lambda} + \sum_{i=1}^n \left(\frac{\beta}{t_i}\right)^{2\lambda} - 2n}{a^3} = 0 \quad (5.3)$$

$$\frac{\partial l}{\partial \beta} = -\frac{\lambda}{\beta} \sum_{i=1}^n \frac{\left[\left(\frac{t_i}{\beta}\right)^{\lambda} - \left(\frac{t_i}{\beta}\right)^{-\lambda}\right]}{\left[\left(\frac{t_i}{\beta}\right)^{\lambda} + \left(\frac{t_i}{\beta}\right)^{-\lambda}\right]} + \frac{\lambda}{\alpha^2 \beta} \sum_{i=1}^n \left[\left(\frac{t_i}{\beta}\right)^{2\lambda} - \left(\frac{t_i}{\beta}\right)^{-2\lambda}\right] = 0 \quad (5.4)$$

$$\frac{\partial l}{\partial \lambda} = \frac{n}{\lambda} + \sum_{i=1}^n \ln\left(\frac{t_i}{\beta}\right) \frac{\left(\frac{t_i}{\beta}\right)^{\lambda} - \left(\frac{\beta}{t_i}\right)^{\lambda}}{\left(\frac{t_i}{\beta}\right)^{\lambda} + \left(\frac{\beta}{t_i}\right)^{\lambda}} - \frac{1}{\alpha^2} \sum_{i=1}^n \ln\left(\frac{t_i}{\beta}\right) \left[\left(\frac{t_i}{\beta}\right)^{2\lambda} - \left(\frac{\beta}{t_i}\right)^{2\lambda}\right] = 0 \quad (5.5)$$

To obtain the estimates of the parameters, we solve the above non-linear equations using standard iterative procedures. Simple trial-and-error techniques coupled with linear interpolation are also adequate. In this chapter, we perform extensive simulation and estimate the mean and standard deviation of the simulation results.

The simulation details are presented in section 5.3.

### 5.1.2 Fisher Information Matrix and Variance-Covariance Matrix

One of the major benefits of utilizing MLE is that the logarithm of the likelihood function can be utilized to construct the Fisher information matrix  $\mathbf{I}$ . Then the variance-covariance matrix  $\mathbf{I}^{-1}$  can be easily obtained by taking the inverse of the Fisher information matrix.

The covariance matrix of the GB-S distribution can be written as:

$$\begin{pmatrix} \text{Var}(\hat{\alpha}) & \text{Cov}(\hat{\alpha}, \hat{\beta}) & \text{Cov}(\hat{\alpha}, \hat{\lambda}) \\ \text{Cov}(\hat{\alpha}, \hat{\beta}) & \text{Var}(\hat{\beta}) & \text{Cov}(\hat{\beta}, \hat{\lambda}) \\ \text{Cov}(\hat{\alpha}, \hat{\lambda}) & \text{Cov}(\hat{\beta}, \hat{\lambda}) & \text{Var}(\hat{\lambda}) \end{pmatrix}$$

To obtain  $\mathbf{I}^{-1}$ , we construct the Fisher information matrix  $\mathbf{I}$  first. The  $(ij)$ th element of the information matrix  $\mathbf{I}$  is:

$$I_{ij} = E \left[ -\frac{\partial^2 l}{\partial i \partial j} \right] \quad (5.6)$$

More specifically, for the GB-S distribution, the Fisher information matrix  $\mathbf{I}$  is constructed as:

$$\mathbf{I} = \begin{pmatrix} I_{11} & I_{12} & I_{13} \\ I_{21} & I_{22} & I_{23} \\ I_{31} & I_{32} & I_{33} \end{pmatrix}$$

Where

$$I_{11} = E \left[ -\frac{\partial^2 l}{\partial \alpha^2} \right] = \frac{2\alpha^2 n + 3 \left( \alpha^2 n + \sum_{i=1}^n \left( \frac{t_i}{\beta} \right)^{2\lambda} + \sum_{i=1}^n \left( \frac{\beta}{t_i} \right)^{2\lambda} - 2n \right)}{-\alpha^4} \quad (5.7)$$

$$I_{22} = E \left[ -\frac{\partial^2 l}{\partial \beta^2} \right] = \frac{-n\lambda}{\beta^2} \sum_{i=1}^n \frac{\left[ \left( \frac{t_i}{\beta} \right)^\lambda - \left( \frac{t_i}{\beta} \right)^{-\lambda} \right]}{\left[ \left( \frac{t_i}{\beta} \right)^\lambda + \left( \frac{t_i}{\beta} \right)^{-\lambda} \right]} - \frac{4\lambda^2}{\beta^2 \left[ \left( \frac{t_i}{\beta} \right)^\lambda + \left( \frac{t_i}{\beta} \right)^{-\lambda} \right]^2} + \frac{\lambda}{\alpha^2 \beta^2} \sum_{i=1}^n \left[ \left( \frac{t_i}{\beta} \right)^{2\lambda} - \left( \frac{t_i}{\beta} \right)^{-2\lambda} \right] \\ + \frac{2\lambda^2}{\alpha^2 \beta^2} \sum_{i=1}^n \left[ \left( \frac{t_i}{\beta} \right)^{2\lambda} + \left( \frac{t_i}{\beta} \right)^{-2\lambda} \right]$$

(5.8)

$$I_{33} = E \left[ -\frac{\partial^2 l}{\partial \lambda^2} \right] = \frac{n}{\lambda^2} + \sum_{i=1}^n \frac{2}{\alpha^2} \ln^2 \left( \frac{t_i}{\beta} \right) \left[ \left( \frac{t_i}{\beta} \right)^{2\lambda} + \left( \frac{\beta}{t_i} \right)^{2\lambda} \right] - \sum_{i=1}^n \frac{4 \ln^2 \left( \frac{t_i}{\beta} \right)}{\left[ \left( \frac{t_i}{\beta} \right)^\lambda + \left( \frac{\beta}{t_i} \right)^\lambda \right]^2} \quad (5.9)$$

$$I_{12} = I_{21} = E \left[ -\frac{\partial^2 l}{\partial \alpha \partial \beta} \right] = \frac{\lambda}{\beta} \frac{2}{\alpha^3} \sum_{i=1}^n \left[ \left( \frac{t_i}{\beta} \right)^{2\lambda} - \left( \frac{t_i}{\beta} \right)^{-2\lambda} \right]^2 \quad (5.10)$$

$$I_{13} = I_{31} = E \left[ -\frac{\partial^2 l}{\partial \alpha \partial \lambda} \right] = \frac{-2n}{\alpha^3} \sum_{i=1}^n \left[ \left( \frac{t_i}{\beta} \right)^{2\lambda} - \left( \frac{t_i}{\beta} \right)^{-2\lambda} \right] \ln \left( \frac{t_i}{\beta} \right) \quad (5.11)$$

$$\begin{aligned}
I_{23} = I_{32} = E \left[ -\frac{\partial^2 l}{\partial \lambda \partial \beta} \right] &= \frac{n}{\beta} \sum_{i=1}^n \frac{\left(\frac{t_i}{\beta}\right)^\lambda - \left(\frac{t_i}{\beta}\right)^{-\lambda}}{\left(\frac{t_i}{\beta}\right)^\lambda + \left(\frac{t_i}{\beta}\right)^{-\lambda}} + \frac{n\lambda}{\beta} \sum_{i=1}^n \frac{4 \ln \left(\frac{t_i}{\beta}\right)}{\left[\left(\frac{t_i}{\beta}\right)^\lambda + \left(\frac{t_i}{\beta}\right)^{-\lambda}\right]^2} - \frac{n}{\alpha^2 \beta} \sum_{i=1}^n \left[ \left(\frac{t_i}{\beta}\right)^{2\lambda} - \left(\frac{t_i}{\beta}\right)^{-2\lambda} \right] \\
&\quad - \frac{2n\lambda}{\alpha^2 \beta} \sum_{i=1}^n \ln \left(\frac{t_i}{\beta}\right) \left[ \left(\frac{t_i}{\beta}\right)^{2\lambda} + \left(\frac{t_i}{\beta}\right)^{-2\lambda} \right]
\end{aligned}$$

(5.12)

With the likelihood functions and the variance-covariance matrix, we theoretically obtain the point estimations of the mean and standard deviations of the parameters. However, in case of small sample size, MLE fails to exhibit clearly defined local maximum equations. Consequently, it is necessary to investigate other estimators for small samples.

## 5.2 Modified Maximum Likelihood Estimation (MMLE)

Cohen and Whitten (1980) present a modified estimation methodology (MMLE) by replacing one of the local MLE equations Eqs. (5.3)-(5.5) with

$$E(F(X_k)) = F(x_k) \quad (5.13)$$

Where  $E$  is the expectation symbol,  $X_k$  is the  $k$ th order statistics in a random sample of size  $n$  if we place the sample in order  $X_1 \leq X_2 \leq \dots \leq X_n$ .  $F(x_k)$  is the value of associated *cdf*.

Since  $E(F(X_k)) = \frac{k}{n+1}$ , for GB-S distribution, Eq. (5.13) can be rewritten as

$$E(F(X_k)) = \frac{k}{n+1} = F(x_k) = \Phi \left\{ \frac{1}{\alpha} \left[ \left( \frac{t_k}{\beta} \right)^\lambda - \left( \frac{\beta}{t_k} \right)^\lambda \right] \right\} \quad (5.14)$$

Here we replace Eq. (5.3)-(5.5) with (5.14) respectively. Accordingly, the estimation equations of MMLE-1 consist of Eqs. (5.4), (5.5) and (5.14); the estimation equations of MMLE-2 consist of Eqs. (5.3), (5.5) and (5.14); the estimation equations of MMLE-3 consist of Eqs. (5.3), (5.4) and (5.14).

More specifically, for MMLE-1, we obtain the estimation equations consisting of Eqs. (5.4), (5.5) and

$$\frac{\partial l}{\partial \alpha} = 1 - \frac{\alpha \Phi^{-1} \left( \frac{k}{n+1} \right)}{\left( \frac{t_k}{\beta} \right)^\lambda - \left( \frac{t_k}{\beta} \right)^{-\lambda}} \quad (5.15)$$

The elements of MMLE-1's Fisher information matrix  $\mathbf{I}_1$  are:

$$I_{111} = \frac{\Phi^{-1} \left( \frac{k}{n+1} \right)}{\left( \frac{t_k}{\beta} \right)^\lambda - \left( \frac{t_k}{\beta} \right)^{-\lambda}} \quad (5.16)$$

$$I_{112} = \frac{\lambda}{\beta} \alpha \Phi^{-1} \left( \frac{k}{n+1} \right) \frac{\left( \frac{t_k}{\beta} \right)^{\lambda} + \left( \frac{t_k}{\beta} \right)^{-\lambda}}{\left[ \left( \frac{t_k}{\beta} \right)^{\lambda} - \left( \frac{t_k}{\beta} \right)^{-\lambda} \right]^2} \quad (5.17)$$

$$I_{113} = \frac{-\alpha \ln \left( \frac{t_k}{\beta} \right) \Phi^{-1} \left( \frac{k}{n+1} \right)}{\left( \frac{t_k}{\beta} \right)^{\lambda} - \left( \frac{t_k}{\beta} \right)^{-\lambda}} \quad (5.18)$$

$$I_{121} = I_{21}, \quad I_{122} = I_{22}, \quad I_{123} = I_{23}, \quad I_{131} = I_{31}, \quad I_{132} = I_{32}, \quad I_{133} = I_{33}$$

Where  $I_{ij}$  represents the  $(ij)$ th element of MMLE-1's Fisher information matrix  $\mathbf{I}_1$ .

For MMLE-2, the estimation equations consist of Eq. (5.3), (5.5) and

$$\frac{\partial l}{\partial \beta} = 1 - \frac{\alpha \Phi^{-1} \left( \frac{k}{n+1} \right)}{\left( \frac{t_k}{\beta} \right)^{\lambda} - \left( \frac{t_k}{\beta} \right)^{-\lambda}} \quad (5.19)$$

Then the elements of MMLE-2's Fisher information matrix  $\mathbf{I}_2$  are:

$$I_{221} = \frac{1}{\alpha^2} \left[ \left( \frac{t_k}{\beta} \right)^{\lambda} - \left( \frac{t_k}{\beta} \right)^{-\lambda} \right] \quad (5.20)$$

$$I_{222} = \frac{\lambda}{\alpha\beta} \left[ \left( \frac{t_k}{\beta} \right)^\lambda + \left( \frac{t_k}{\beta} \right)^{-\lambda} \right] \quad (5.21)$$

$$I_{223} = -\frac{1}{\alpha} \ln \left( \frac{t_k}{\beta} \right) \left[ \left( \frac{t_k}{\beta} \right)^\lambda + \left( \frac{t_k}{\beta} \right)^{-\lambda} \right] \quad (5.22)$$

$$I_{211} = I_{11}, \quad I_{212} = I_{12}, \quad I_{213} = I_{13}, \quad I_{231} = I_{31}, \quad I_{232} = I_{32}, \quad I_{233} = I_{33}$$

Where  $I_{2ij}$  represents the  $(ij)$ th element of MMLE-2's Fisher information matrix  $\mathbf{I}_2$ .

For MMLE-3, the estimation equations consist of Eq. (5.3), (5.4) and

$$\frac{\partial l}{\partial \lambda} = 1 - \frac{\alpha \Phi^{-1} \left( \frac{k}{n+1} \right)}{\left( \frac{t_k}{\beta} \right)^\lambda - \left( \frac{t_k}{\beta} \right)^{-\lambda}} \quad (5.23)$$

Then the elements of MMLE-3's Fisher information matrix  $\mathbf{I}_3$  are:

$$I_{331} = \frac{\Phi^{-1} \left( \frac{k}{n+1} \right)}{\left( \frac{t_k}{\beta} \right)^\lambda - \left( \frac{t_k}{\beta} \right)^{-\lambda}} \quad (5.24)$$

$$I_{332} = \frac{\lambda}{\beta} \alpha \Phi^{-1} \left( \frac{k}{n+1} \right) \frac{\left( \frac{t_k}{\beta} \right)^\lambda + \left( \frac{t_k}{\beta} \right)^{-\lambda}}{\left[ \left( \frac{t_k}{\beta} \right)^\lambda - \left( \frac{t_k}{\beta} \right)^{-\lambda} \right]^2} \quad (5.25)$$

$$I_{333} = \frac{-\alpha \ln\left(\frac{t_k}{\beta}\right) \Phi^{-1}\left(\frac{k}{n+1}\right)}{\left(\frac{t_k}{\beta}\right)^\lambda - \left(\frac{t_k}{\beta}\right)^{-\lambda}} \quad (5.26)$$

$$I_{311} = I_{11}, I_{312} = I_{12}, I_{313} = I_{13}, I_{321} = I_{21}, I_{322} = I_{22}, I_{323} = I_{23}$$

Where  $I_{3ij}$  represents the  $(ij)$ th element of MMLE-3's Fisher information matrix  $\mathbf{I}_3$ .

It is clear that the Fisher information matrixes  $\mathbf{I}_1, \mathbf{I}_2, \mathbf{I}_3$  are not symmetric.

### 5.3 Simulation Study

In section 5.1 and 5.2, we show the estimation equations and variances of MLE and MMLE. Usually, the non-linear estimation equations can be solved by Newton's iterative method or the gradient of the likelihood method. In this section, we compare the performances of the two estimation methods with simulated failure data. We use MATLAB to generate the data with given distribution parameters.

#### 5.3.1 Computation Procedure

To make a comprehensive comparison between the two estimation methodologies, a simulation study for different sample sizes and for different values of the shape parameters is performed. We apply both estimation methods to several groups of



simulation failure data. Those groups of random data are generated with different values of shape parameters and different sample sizes. The simulation results are based on 1000 runs.

We take the sample size as  $n=10, 50, 100$  and the shape parameters as  $\alpha=1.8, \beta=1.5$  and  $\alpha=0.4, \lambda=0.3$  while  $\beta$  is kept fixed at 1.0 without loss of generality since it is a scale parameter. If  $\beta$  is not 1, the values of the bias and standard deviation of estimates of  $\beta$  should be multiplied by  $\beta$ . Estimations are based on the first order statistics. Table 5.1 summarizes the values of the shape parameters and each group's sample size.

Table 5.1 Sample sizes and values of the shape parameters

	$n$	$\alpha$	$\lambda$	$\beta$
Group1	100	1.8	1.5	1
Group2	50	1.8	1.5	1
Group3	10	1.8	1.5	1
Group4	100	0.3	0.4	1
Group5	50	0.3	0.4	1
Group6	10	0.3	0.4	1

Taking group 1 for example, we first generate 100 random failure data with

$\alpha=1.8$  ,  $\beta=1$  and  $\lambda=1.5$  , and then apply MLE and MMLE-1, 2, 3 to the 100 random failures data. Then we take the means and the deviations of the estimates over 1000 such runs. The same procedure is applied to other groups.

### 5.3.2 Simulation Result

Tables 5.2 to 5.7 report the results obtained from the simulation. It is clear that the sample size has significant impact on both bias and variances. When the sample is large, for example,  $n=100$ , the performances of MLE and MMLEs are almost identical in terms of the means of the estimates. However, the variances of MMLEs are smaller than MLE. When sample size decreases to a small number, the MLEs are highly biased and possess large variances while the MMLEs provide almost unbiased results and smaller deviations. The difference between the two methodologies is significant regardless of the value of the shape parameters. Thus, for GB-S distribution, the MMLE is recommended especially when the sample and the shape parameters are small.

Table 5.2 Means of the estimates of parameters when  $n=10$ 

$n=10$	$\alpha=1.8$	$\beta=1$	$\lambda=1.5$	$\alpha=0.3$	$\beta=1$	$\lambda=0.4$
MLE	2.4729	1.0270	2.0113	2.3300	1.2494	2.7790
MMLE-1	1.7310	1.0173	1.5895	.3094	1.2268	.3958
MMLE-2	1.6778	.9062	1.3565	.3158	1.0513	.3743
MMLE-3	2.0241	1.0217	1.7608	.3072	1.2268	.3919

Table 5.3 Means of the estimates of parameters when  $n=50$ 

$n=50$	$\alpha=1.8$	$\beta=1$	$\lambda=1.5$	$\alpha=0.3$	$\beta=1$	$\lambda=0.4$
MLE	1.2803	.9763	1.3389	.3020	.9568	.4224
MMLE-1	1.7276	.9723	1.6635	.3039	.9568	.4250
MMLE-2	1.3121	.9166	1.3555	.2618	1.0981	.3423
MMLE-3	1.6578	.9729	1.6288	.3017	.9568	.4221

Table 5.4 Means of the estimates of parameters when  $n=100$ 

$n=100$	$\alpha=1.8$	$\beta=1$	$\lambda=1.5$	$\alpha=0.3$	$\beta=1$	$\lambda=0.4$
MLE	1.9030	.9949	1.5134	.3083	.9554	.4035
MMLE-1	1.8788	.9943	1.5004	.3137	.9553	.4103
MMLE-2	1.8809	.9910	1.5013	.3067	1.0161	.3960

MMLE-3	1.8625	.9939	1.4908	.3101	.9553	.4058
--------	--------	-------	--------	-------	-------	-------

Table 5.5 Variances of the estimates of parameters when  $n=10$ 

$n=10$	$\alpha=1.8$	$\beta=1$	$\lambda=1.5$	$\alpha=0.3$	$\beta=1$	$\lambda=0.4$
MLE	6.5104	.0134	1.6594	5.8197	.0148	2.2577
MMLE-1	1.2577	.0157	.0342	.2876	.0224	.0062
MMLE-2	.9215	.3769	2.4345	.0170	.0017	.0329
MMLE-3	.1029	.0149	.8523	.0008	.0226	.03581

Table 5.6 Variances of the estimates of parameters when  $n=50$ 

$n=50$	$\alpha=1.8$	$\beta=1$	$\lambda=1.5$	$\alpha=0.3$	$\beta=1$	$\lambda=0.4$
MLE	.5947	.0030	.3989	1.0114	.0023	1.8908
MMLE-1	1.0904	.0026	.0066	.2700	..23	.0013
MMLE-2	.4556	.1216	.2519	.0328	.0085	.0045
MMLE-3	.0146	.0026	.7296	.0002	.0023	.3673

Table 5.7 Variances of the estimates of parameters when  $n=100$ 

$n=100$	$\alpha=1.8$	$\beta=1$	$\lambda=1.5$	$\alpha=0.3$	$\beta=1$	$\lambda=0.4$
MLE	.4361	.0020	.1273	.5258	.0013	.8587
MMLE-1	.8844	.0019	.0027	.2688	.0013	.0006
MMLE-2	.3392	.2476	.0912	.0346	.0693	.0371
MMLE-3	.0087	.0019	.4811	.0001	.0013	.3407

#### 5.4 Conclusion

In this chapter, we investigate the estimation of GB-S's parameters. We utilize MLE and MMLE to present the estimation equations and variances and compare the performances of MLE and MMLE under different sample sizes and different shape parameters. The simulation study indicates that MLE is highly biased and possesses large deviations in case of small samples for GB-S distribution especially when the shape parameters are small. By utilizing MMLE, we provide a satisfactory estimation of GB-S distribution's parameters.

## CHAPTER 6

### GB-S ACCELERATED LIFE MODELS

In the previous chapters, we investigate the properties, characteristics, the inference procedure and the hazard function of GB-S distribution. It is also worth noting that the B-S model is initially derived to describe the fatigue phenomenon and to predict the reliability and useful life of mechanical components which are subjected to fatigue due to random or constant amplitude loading. In this chapter, we investigate the application of the GB-S distribution to ALT models. More specifically, we utilize the observed accelerated failure data to predict the reliability under normal conditions with GB-S life distribution and compare the performance of GB-S ALT model with other ALT models. We also optimally design several ALT plans that meet different optimization criterion. In section 6.1, we propose an GB-S ALT model which utilizes inverse power law accelerated model. To validate the performance of the GB-S ALT model, we apply an exponential acceleration form which is more flexible and incorporate the inverse power law acceleration form as its special case. In section 6.2 we provide the likelihood functions and partial derivatives with respect to the ALT model's unknown parameters. In section 6.3, we compare the performances of those ALT models based on several experimental data sets. These data sets are utilized to obtain the parameters of the models which are then used for reliability prediction at any stress conditions. We also calculate the SSE of each model.

An appropriate ALT model is important since it reflects how the applied stresses affect the lifetime of a component or a system. On the other hand, a properly designed ALT plan makes the reliability estimation and prediction more efficient. In section 6.4, we design ALT plans based on the GB-S distribution to predict the reliability performances more accurately.

## 6.1 GB-S and Other Accelerated Models

Once a baseline lifetime distribution with scale parameter or mean is adopted and an appropriate acceleration form is selected according to the applied stress type, the unknown parameters can be estimated by observing failure times at elevated stress levels which are then used to predict reliability at normal operating conditions. In this section, we present the expressions of GB-S accelerated models, as well as Weibull and SB-S accelerated models, either in specific or general forms.

### 6.1.1 The Inverse Power Law Accelerated Models

The power law model has applications in fatigue testing of metals and the aging of multi-component systems, especially in components subject to non-thermal stresses:

$$h(V) = \gamma \cdot V^{-\eta}, \quad \gamma > 0, \eta > 0 \quad (6.1)$$

Where

$h(V)$  is a quantifiable life measure, such as mean life or characteristic life

$V$  represents the stress level

$\gamma, \eta$  are model parameters.

Typically,  $h(V)$  is substituted for a mean or scale parameter in a lifetime distribution.

By substituting the scale parameter  $\beta$  with the accelerated life model  $h(V)$ , the inverse power law accelerated GB-S model can be written as:

$$F(t; V) = \Phi \left\{ \frac{1}{\alpha} \left[ \left( \frac{t}{\gamma V^{-\eta}} \right)^{\lambda} - \left( \frac{t}{\gamma V^{-\eta}} \right)^{-\lambda} \right] \right\} \quad (6.2)$$

$$f(t; V) = \frac{\lambda}{\sqrt{2\pi}at} \left[ \left( \frac{t}{\gamma V^{-\eta}} \right)^{\lambda} + \left( \frac{\gamma V^{-\eta}}{t} \right)^{\lambda} \right] \exp \left\{ -\frac{1}{2a^2} \left[ \left( \frac{t}{\gamma V^{-\eta}} \right)^{2\lambda} + \left( \frac{t}{\gamma V^{-\eta}} \right)^{-2\lambda} - 2 \right] \right\} \quad (6.3)$$

Then the parameters can be estimated using the likelihood function and partial derivatives with respect to the parameters  $\alpha, \lambda, \gamma$  and  $\eta$  as described in section 6.2.

Compared with Weibull, lognormal and other distributions which fit failure data well especially within the central region of the distribution, B-S distribution has been shown to provide an accurate description of failure data especially under low stress



levels. In order to compare the performance of the GB-S accelerated model with other ALT models, we derive the inverse power law Weibull accelerated models as follows:

$$F(t;V) = 1 - e^{-\left(\frac{t}{\gamma V^{-\eta}}\right)^k} \quad (6.4)$$

$$f(t;V) = \left(\frac{t}{\gamma V^{-\eta}}\right)^{k-1} \frac{k}{\gamma V^{-\eta}} e^{-\left(\frac{t}{\gamma V^{-\eta}}\right)^k} \quad (6.5)$$

The inverse power law SB-S accelerated model is given by Owen and Padgett (2000) as:

$$F(t;V) = \Phi \left\{ \frac{1}{\alpha} \left[ \left(\frac{t}{\gamma V^{-\eta}}\right)^{\frac{1}{2}} - \left(\frac{t}{\gamma V^{-\eta}}\right)^{-\frac{1}{2}} \right] \right\} \quad (6.6)$$

The *pdf* of the model is

$$f(t;V) = \frac{V^{\frac{\eta}{2}}}{2\sqrt{2\pi\alpha}\sqrt{\gamma t}} \left(1 + \frac{\gamma}{tV^{-\eta}}\right) \exp \left[ -\frac{1}{2\alpha^2} \left( \frac{tV^{\eta}}{\gamma} - 2 + \frac{\gamma}{tV^{\eta}} \right) \right] \quad (6.7)$$

### 6.1.2 General Exponential Acceleration Form

The inverse power law accelerated model is usually limited to modeling the relationship between lifetime and mechanical stress. Here we consider a general exponential acceleration form of life-stress relationship:

$$h(Z) = \exp(a_0 + a_1 z_1) \quad (6.8)$$

Where

$Z$  is the stress vector (varied types of stress can be used)

$a_0$  and  $a_1$  are model parameters.

When  $\exp(a_0) = \gamma$ , and  $\exp(a_1 z) = V^{-\eta}$ , the exponential model yields the inverse-power accelerated model. Indeed, this exponential acceleration form yields other acceleration models such as Arrhenius, Temp-Non Thermal, Temp-Humidity, etc. Substituting the scale parameter of each life model, we obtain the general accelerated models for Weibull, SB-S and GB-S distributions respectively:

$$F_{Weibull}(t; z) = 1 - e^{-\left(\frac{t}{\exp(a_0 + a_1 z)}\right)^k} \quad (6.9)$$

$$F_{SB-S}(t; z) = \Phi \left\{ \frac{1}{\alpha} \left[ \left( \frac{t}{\exp(a_0 + a_1 z)} \right)^{\frac{1}{2}} - \left( \frac{t}{\exp(a_0 + a_1 z)} \right)^{\frac{1}{2}} \right] \right\} \quad (6.10)$$

$$F_{GB-S}(t; z) = \Phi \left\{ \frac{1}{\alpha} \left[ \left( \frac{t}{\exp(a_0 + a_1 z)} \right)^{\lambda} - \left( \frac{t}{\exp(a_0 + a_1 z)} \right)^{-\lambda} \right] \right\} \quad (6.11)$$

So far, we derive the accelerated models based on three baseline distributions and two acceleration forms. In the next section, we investigate the estimation of the model

parameters.

## 6.2 Parameter Estimation

### 6.2.1 Estimation of Inverse Power Law Accelerated Models' Parameters

The estimation of the unknown model parameters in above models can be obtained by maximizing the likelihood function for the observed accelerated failure data. Usually multilevel stresses are applied in the ALT test, here we assume two stress levels  $V_1$  and  $V_2$  are applied and the corresponding two failure time data sets are obtained, then the reliability under any stress level can be predicted with those estimated parameters. Generally, for the inverse power law GB-S accelerated model, the likelihood function is obtained as:

$$L(\gamma, \eta, \alpha, \lambda; t_{ij}, V_i) = \prod_{i=1}^2 \prod_{j=1}^{n_i} f(\gamma, \eta, \alpha, \lambda; t_{ij}, V_i) \quad (6.12)$$

Where

$i$  is the  $i$ th stress level

$j$  is the  $j$ th failure data in the corresponding data set

$n_i$  is the number of observations in  $i$ th data set

$t_{ij}$  represents the  $j$ th failure observation in the data set obtained under  $i$ th stress level

$V_i$  is the  $i$ th stress level

In this section, the data are obtained from the Instrument Development Unit of the Physical Research Staff, Boeing Aircraft Company, by subjecting metal-coupons to repeated alternating stresses and strains (Owen and Padgett 2000), the three data sets obtained under three stress levels are listed below:

Sample 1 (Stress/cycle:  $2.1 \times 10^4$  psi):

3.70, 7.06, 7.06, 7.46, 7.85, 7.97, 8.44, 8.55, 8.58, 8.86, 8.86, 9.30, 9.60, 9.88, 9.90, 10.00, 10.10, 10.16, 10.18, 10.20, 10.55, 10.85, 11.02, 11.02, 11.08, 11.15, 11.20, 11.34, 11.40, 11.99, 12.00, 12.00, 12.03, 12.22, 12.35, 12.38, 12.52, 12.58, 12.62, 12.69, 12.70, 12.90, 12.93, 13.00, 13.10, 13.13, 13.15, 13.30, 13.55, 13.90, 14.16, 14.19, 14.20, 14.20, 14.50, 14.52, 14.75, 14.78, 14.81, 14.85, 15.02, 15.05, 15.13, 15.22, 15.22, 15.30, 15.40, 15.60, 15.67, 15.78, 15.94, 16.02, 16.04, 16.08, 16.30, 16.42, 16.74, 17.30, 17.50, 17.50, 17.63, 17.68, 17.81, 17.82, 17.92, 18.20, 18.68, 18.81, 18.90, 18.93, 18.95, 19.10, 19.23, 19.40, 19.45, 20.23, 21.00, 21.30, 22.15, 22.68, 24.40

Sample 2 (Stress/cycle:  $2.6 \times 10^4$  psi):

2.33, 2.58, 2.68, 2.76, 2.90, 3.10, 3.12, 3.15, 3.18, 3.21, 3.21, 3.29, 3.35, 3.36, 3.38, 3.38, 3.42, 3.42, 3.42, 3.44, 3.49, 3.50, 3.50, 3.51, 3.51, 3.52, 3.52, 3.56, 3.58, 3.58, 3.60, 3.62, 3.63, 3.66, 3.67, 3.70, 3.70, 3.72, 3.72, 3.74, 3.75, 3.76, 3.79, 3.79, 3.80, 3.82, 3.89, 3.89, 3.95, 3.96, 4.00, 4.00, 4.00, 4.03, 4.04, 4.06, 4.08, 4.08, 4.10, 4.12, 4.14, 4.16, 4.16, 4.16, 4.20, 4.22, 4.23, 4.26, 4.28, 4.32, 4.32, 4.33, 4.33, 4.37, 4.38, 4.39, 4.39, 4.43, 4.45, 4.45, 4.52, 4.56, 4.56, 4.60, 4.64, 4.66, 4.68, 4.70, 4.70, 4.73, 4.74, 4.76, 4.76, 4.86, 4.88, 4.89, 4.90, 4.91, 5.03, 5.17, 5.40, 5.60

Sample 3 (Stress/cycle:  $3.1 \times 10^4$  psi):

0.7,0.9,0.96,0.97,0.99,1.00,1.03,1.04,1.04,1.05,1.07,1.08,1.08,1.08,1.09,1.09,1.12,  
 1.12,1.13,1.14,1.14,1.14,1.16,1.19,1.20,1.20,1.20,1.21,1.21,1.23,1.24,1.24,1.24,1.24,  
 1.24,1.28,1.28,1.29,1.29,1.30,1.30,1.30,1.31,1.31,1.31,1.31,1.31,1.32,1.32,1.32,1.33,  
 1.34,1.34,1.34,1.34,1.34,1.36,1.36,1.37,1.38,1.38,1.38,1.39,1.39,1.41,1.41,1.42,1.42,  
 1.42,1.42,1.42,1.42,1.44,1.44,1.45,1.46,1.48,1.48,1.49,1.51,1.51,1.52,1.55,1.56,1.57,  
 1.57,1.57,1.57,1.58,1.59,1.62,1.63,1.63,1.64,1.66,1.66, 1.68, 1.70,1.74,1.96,2.12

To examine the performance of inverse power law GB-S model, failure data from any two of the three samples are utilized to estimate the unknown parameters of the model and these estimated parameters are then used to predict the reliability under the third stress. The predicted reliability is then compared with the theoretical reliability (observed data set). To illustrate, we use data sets 1 and 2 to estimate the unknown parameters. The log-likelihood function of the inverse power law GB-S model can be written as:

$$\begin{aligned}
 l = & 203 \log \lambda - 203 \log \alpha \\
 & + \sum_{j=1}^{101} \log \left[ \left( \frac{t_{1j}}{\gamma W_1^{-\eta}} \right)^{\lambda} + \left( \frac{t_{1j}}{\gamma W_1^{-\eta}} \right)^{-\lambda} \right] + \sum_{j=1}^{102} \log \left[ \left( \frac{t_{2j}}{\gamma W_2^{-\eta}} \right)^{\lambda} + \left( \frac{t_{2j}}{\gamma W_2^{-\eta}} \right)^{-\lambda} \right] \\
 & - \sum_{j=1}^{101} \frac{\left[ \left( \frac{t_{1j}}{\gamma W_1^{-\eta}} \right)^{\lambda} - \left( \frac{t_{1j}}{\gamma W_1^{-\eta}} \right)^{-\lambda} \right]^2}{2\alpha^2} - \sum_{j=1}^{102} \frac{\left[ \left( \frac{t_{2j}}{\gamma W_2^{-\eta}} \right)^{\lambda} - \left( \frac{t_{2j}}{\gamma W_2^{-\eta}} \right)^{-\lambda} \right]^2}{2\alpha^2}
 \end{aligned} \quad (6.13)$$

Taking partial derivatives of the log-likelihood function with respect to  $\alpha, \lambda, \gamma$  and  $\eta$  yields the following four equations:

$$\frac{\partial l}{\partial \alpha} = -\frac{203}{\alpha} + \frac{1}{\alpha^3} \sum_{j=1}^{101} \left[ \left( \frac{t_{1j}}{\gamma \mathcal{W}_1^{-\eta}} \right)^{\lambda} - \left( \frac{t_{1j}}{\gamma \mathcal{W}_1^{-\eta}} \right)^{-\lambda} \right]^2 + \frac{1}{\alpha^3} \sum_{j=1}^{102} \left[ \left( \frac{t_{2j}}{\gamma \mathcal{W}_2^{-\eta}} \right)^{\lambda} - \left( \frac{t_{2j}}{\gamma \mathcal{W}_2^{-\eta}} \right)^{-\lambda} \right]^2 \quad (6.14)$$

$$\begin{aligned} \frac{\partial l}{\partial \lambda} = & \frac{203}{\lambda} + \sum_{j=1}^{101} \frac{\left( \frac{t_{1j}}{\gamma \mathcal{W}_1^{-\eta}} \right)^{\lambda} - \left( \frac{t_{1j}}{\gamma \mathcal{W}_1^{-\eta}} \right)^{-\lambda}}{\left( \frac{t_{1j}}{\gamma \mathcal{W}_1^{-\eta}} \right)^{\lambda} + \left( \frac{t_{1j}}{\gamma \mathcal{W}_1^{-\eta}} \right)^{-\lambda}} \log \left( \frac{t_{1j}}{\gamma \mathcal{W}_1^{-\eta}} \right) \\ & + \sum_{j=1}^{102} \frac{\left( \frac{t_{2j}}{\gamma \mathcal{W}_2^{-\eta}} \right)^{\lambda} - \left( \frac{t_{2j}}{\gamma \mathcal{W}_2^{-\eta}} \right)^{-\lambda}}{\left( \frac{t_{1j}}{\gamma \mathcal{W}_2^{-\eta}} \right)^{\lambda} + \left( \frac{t_{1j}}{\gamma \mathcal{W}_2^{-\eta}} \right)^{-\lambda}} \log \left( \frac{t_{2j}}{\gamma \mathcal{W}_2^{-\eta}} \right) \\ & - \sum_{j=1}^{101} \frac{\left( \frac{t_{1j}}{\gamma \mathcal{W}_1^{-\eta}} \right)^{2\lambda} - \left( \frac{t_{1j}}{\gamma \mathcal{W}_1^{-\eta}} \right)^{-2\lambda}}{\alpha^2} \log \left( \frac{t_{1j}}{\gamma \mathcal{W}_1^{-\eta}} \right) \\ & - \sum_{j=1}^{102} \frac{\left( \frac{t_{2j}}{\gamma \mathcal{W}_2^{-\eta}} \right)^{2\lambda} - \left( \frac{t_{2j}}{\gamma \mathcal{W}_2^{-\eta}} \right)^{-2\lambda}}{\alpha^2} \log \left( \frac{t_{2j}}{\gamma \mathcal{W}_2^{-\eta}} \right) \end{aligned} \quad (6.15)$$

$$\begin{aligned} \frac{\partial l}{\partial \gamma} = & -\frac{\lambda}{\gamma} \sum_{j=1}^{101} \frac{\left( \frac{t_{1j}}{\gamma \mathcal{W}_1^{-\eta}} \right)^{\lambda} - \left( \frac{t_{1j}}{\gamma \mathcal{W}_1^{-\eta}} \right)^{-\lambda}}{\left( \frac{t_{1j}}{\gamma \mathcal{W}_1^{-\eta}} \right)^{\lambda} + \left( \frac{t_{1j}}{\gamma \mathcal{W}_1^{-\eta}} \right)^{-\lambda}} - \frac{\lambda}{\gamma} \sum_{j=1}^{102} \frac{\left( \frac{t_{2j}}{\gamma \mathcal{W}_2^{-\eta}} \right)^{\lambda} - \left( \frac{t_{2j}}{\gamma \mathcal{W}_2^{-\eta}} \right)^{-\lambda}}{\left( \frac{t_{2j}}{\gamma \mathcal{W}_2^{-\eta}} \right)^{\lambda} + \left( \frac{t_{2j}}{\gamma \mathcal{W}_2^{-\eta}} \right)^{-\lambda}} \\ & + \frac{\lambda}{\alpha^2 \gamma} \sum_{j=1}^{101} \left[ \left( \frac{t_{1j}}{\gamma \mathcal{W}_1^{-\eta}} \right)^{2\lambda} - \left( \frac{t_{1j}}{\gamma \mathcal{W}_1^{-\eta}} \right)^{-2\lambda} \right] + \frac{\lambda}{\alpha^2 \gamma} \sum_{j=1}^{102} \left[ \left( \frac{t_{2j}}{\gamma \mathcal{W}_2^{-\eta}} \right)^{2\lambda} - \left( \frac{t_{2j}}{\gamma \mathcal{W}_2^{-\eta}} \right)^{-2\lambda} \right] \end{aligned} \quad (6.16)$$

$$\begin{aligned}
\frac{\partial l}{\partial \eta} = & \lambda \log V_1 \sum_{j=1}^{101} \frac{\left( \frac{t_{1j}}{\gamma V_1^{-\eta}} \right)^{\lambda} - \left( \frac{t_{1j}}{\gamma V_1^{-\eta}} \right)^{-\lambda}}{\left( \frac{t_{1j}}{\gamma V_1^{-\eta}} \right)^{\lambda} + \left( \frac{t_{1j}}{\gamma V_1^{-\eta}} \right)^{-\lambda}} \\
& + \lambda \log V_2 \sum_{j=1}^{102} \log \left[ \left( \frac{t_{2j}}{\gamma V_2^{-\eta}} \right)^{\lambda} + \left( \frac{t_{2j}}{\gamma V_2^{-\eta}} \right)^{-\lambda} \right] \\
& - \frac{\lambda \log V_1}{\alpha^2} \sum_{j=1}^{101} \left[ \left( \frac{t_{1j}}{\gamma V_1^{-\eta}} \right)^{2\lambda} - \left( \frac{t_{1j}}{\gamma V_1^{-\eta}} \right)^{-2\lambda} \right] \\
& - \frac{\lambda \log V_2}{\alpha^2} \sum_{j=1}^{102} \left[ \left( \frac{t_{2j}}{\gamma V_2^{-\eta}} \right)^{2\lambda} - \left( \frac{t_{2j}}{\gamma V_2^{-\eta}} \right)^{-2\lambda} \right]
\end{aligned} \tag{6.17}$$

Similarly, from Eq. (6.5), we take the logarithm of the likelihood function and partial derivatives with respect to the unknown parameters of inverse power law Weibull accelerated model:

$$\begin{aligned}
l = & 203 \log k - 203 \log \gamma + 101 \eta \log V_1 + 102 \log V_2 + (k-1) \sum_{i=1}^2 \sum_{j=1}^{n_i} t_{ij} \\
& - 203(k-1) \log \gamma + 101(k-1) \eta \log V_1 + 102(k-1) \eta \log V_2 \\
& - \sum_{j=1}^{101} \left( \frac{t_{1j}}{\gamma V_1^{-\eta}} \right)^k - \sum_{j=1}^{102} \left( \frac{t_{2j}}{\gamma V_2^{-\eta}} \right)^k
\end{aligned} \tag{6.18}$$

$$\begin{aligned}
\frac{\partial l}{\partial k} = & \frac{203}{k} + \sum_{i=1}^2 \sum_{j=1}^{n_i} t_{ij} - 203 \log \gamma \\
& + 101 \eta \log V_1 + 102 \log \eta \log V_2 \\
& - \sum_{j=1}^{101} \log \left( \frac{t_{1j} V_1^{\eta}}{\gamma} \right) \cdot \left( \frac{t_{1j} V_1^{\eta}}{\gamma} \right)^k - \sum_{j=1}^{102} \log \left( \frac{t_{2j} V_2^{\eta}}{\gamma} \right) \cdot \left( \frac{t_{2j} V_2^{\eta}}{\gamma} \right)^k
\end{aligned} \tag{6.19}$$

$$\begin{aligned} \frac{\partial l}{\partial \gamma} = & -\frac{203}{\gamma} - 203(k-1)\frac{1}{\gamma} \\ & + \sum_{j=1}^{101} \frac{k}{\gamma} \cdot \left( \frac{t_{1j}V_1^\eta}{\gamma} \right)^k + \sum_{j=1}^{102} \frac{k}{\gamma} \cdot \left( \frac{t_{2j}V_2^\eta}{\gamma} \right)^k \end{aligned} \quad (6.20)$$

$$\begin{aligned} \frac{\partial l}{\partial \eta} = & 101k \log V_1 + 102k \log V_2 \\ & - \sum_{j=1}^{101} \frac{k\eta}{V_1} \cdot \left( \frac{t_{1j}V_1^\eta}{\gamma} \right)^k - \sum_{j=1}^{102} \frac{k\eta}{V_2} \cdot \left( \frac{t_{2j}V_2^\eta}{\gamma} \right)^k \end{aligned} \quad (6.21)$$

The likelihood function of inverse power law SB-S accelerated model is given by Owen and Padgett (2000):

$$\begin{aligned} l = & \frac{101}{2}\eta \log V_1 + \frac{102}{2}\eta \log V_2 - 203 \log \alpha - \frac{203}{2} \log \gamma \\ & + \sum_{j=1}^{101} \log \left( 1 + \frac{\gamma}{t_{1j}V_1^\eta} \right) + \sum_{j=1}^{102} \log \left( 1 + \frac{\gamma}{t_{2j}V_2^\eta} \right) \\ & - \frac{1}{2\alpha^2} \left[ \sum_{j=1}^{101} \left( \frac{t_{1j}V_1^\eta}{\gamma} - 2 + \frac{\gamma}{t_{1j}V_1^\eta} \right) + \sum_{j=1}^{102} \left( \frac{t_{2j}V_2^\eta}{\gamma} - 2 + \frac{\gamma}{t_{2j}V_2^\eta} \right) \right] \end{aligned} \quad (6.22)$$

We obtain the partial derivatives with respect to each parameter as:

$$\frac{\partial l}{\partial \alpha} = -\frac{203}{\alpha} + \frac{1}{\alpha^3} \left[ \sum_{j=1}^{101} \left( \frac{t_{1j}V_1^\eta}{\gamma} - 2 + \frac{\gamma}{t_{1j}V_1^\eta} \right) + \sum_{j=1}^{102} \left( \frac{t_{2j}V_2^\eta}{\gamma} - 2 + \frac{\gamma}{t_{2j}V_2^\eta} \right) \right] \quad (6.23)$$



$$\begin{aligned} \frac{\partial l}{\partial \gamma} = & -\frac{203}{2\gamma} + \sum_{j=1}^{101} \frac{1}{t_{1j}V_1^\eta + \gamma} + \sum_{j=1}^{102} \frac{1}{t_{2j}V_2^\eta + \gamma} \\ & - \frac{1}{2\alpha^2} \left[ \sum_{j=1}^{101} \left( \frac{1}{t_{1j}V_1^\eta} - \frac{t_{1j}V_1^\eta}{\gamma^2} \right) + \sum_{j=1}^{102} \left( \frac{1}{t_{2j}V_2^\eta} - \frac{t_{2j}V_2^\eta}{\gamma^2} \right) \right] \end{aligned} \quad (6.24)$$

$$\begin{aligned} \frac{\partial l}{\partial \eta} = & \frac{101}{2} \log V_1 + \frac{102}{2} \log V_2 - \sum_{j=1}^{101} \frac{\mathcal{M}V_1^{-1}}{t_{1j}V_1^\eta + \gamma} - \sum_{j=1}^{102} \frac{\mathcal{M}V_2^{-1}}{t_{2j}V_2^\eta + \gamma} \\ & - \frac{\eta}{2\alpha^2} \left[ \sum_{j=1}^{101} \left( \frac{t_{1j}V_1^{\eta-1}}{\gamma} \frac{\gamma}{t_{1j}V_1^{\eta+1}} \right) + \sum_{j=1}^{102} \left( \frac{t_{2j}V_2^{\eta-1}}{\gamma} \frac{\gamma}{t_{2j}V_2^{\eta+1}} \right) \right] \end{aligned} \quad (6.25)$$

Newton's iterative method is applied to solve the partial derivatives of the log likelihood functions. The iteration ends when the estimate converges. Usually for a nonlinear equation, there exists more than one local optimal solution. These solutions are returned to the likelihood function and the global optimal value is obtained accordingly.

### 6.2.2 Estimation of General Accelerated Models' Parameters

From Eq. (6.9)-(6.11), we obtain the likelihood functions of the three general accelerated models, then the partial derivatives with respect to each model's parameters can be obtained with the same procedure that stated in 6.2.1.

### 6.3 ALT Models Comparison

An ALT model is usually used to estimate reliability performance under the desired stress level by utilizing failure data obtained at different stress levels to estimate the

parameters of the model. In this section, we consider all the scenarios where any two of the data sets are utilized to estimate the parameters of each proposed model and the predicted reliabilities are compared with the theoretical ones.

Applying data sets 1 and 2 to each model and comparing with the third data set, each model's estimated parameters and sum of squared errors (SSE) are obtained as summarized in Table 6.1. Figures 6.1 and 6.2 plot the *cdf* predicted by each model and *cdf* of the observed data (set 3):

Table 6.1 Estimated Parameters and SSEs of each accelerated model (Sets 1&2)

Inverse power law Weibull accelerated model	
$\hat{k} = 0.347, \hat{\gamma} = 1775.6, \hat{\eta} = 1.756$	SSE=19.918
Inverse power law SB-S accelerated model	
$\hat{\alpha} = 0.249, \hat{\gamma} = 821.186, \hat{\eta} = 5.548$	SSE=5.089
Inverse power law GB-S accelerated model	
$\hat{\alpha} = 0.164, \hat{\lambda} = 0.333, \hat{\gamma} = 1045.834, \hat{\eta} = 5.855$	SSE=1.003
General Weibull accelerated model	
$\hat{k} = 2.618, \hat{a}_0 = 3.852, \hat{a}_1 = -1.868$	SSE=30.328
General SB-S accelerated model	
$\hat{\alpha} = 0.248, \hat{a}_0 = 6.674, \hat{a}_1 = -5.533$	SSE=4.032
General GB-S accelerated model	
$\hat{\alpha} = 0.258, \hat{\lambda} = 0.522, \hat{a}_0 = 6.758, \hat{a}_1 = -5.629$	SSE=2.896

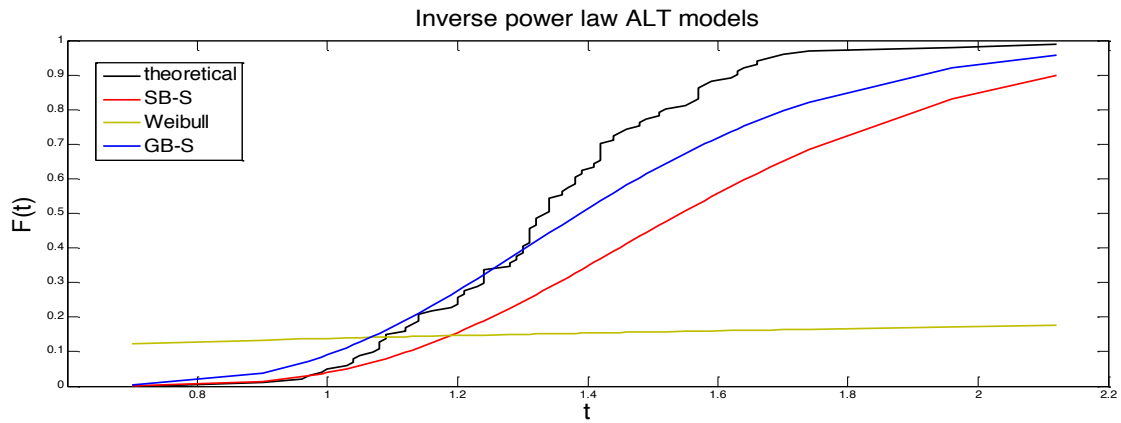


Figure 6.1 Predicted *cdf* (Data sets 1&2) of three inverse power law models and theoretical *cdf*

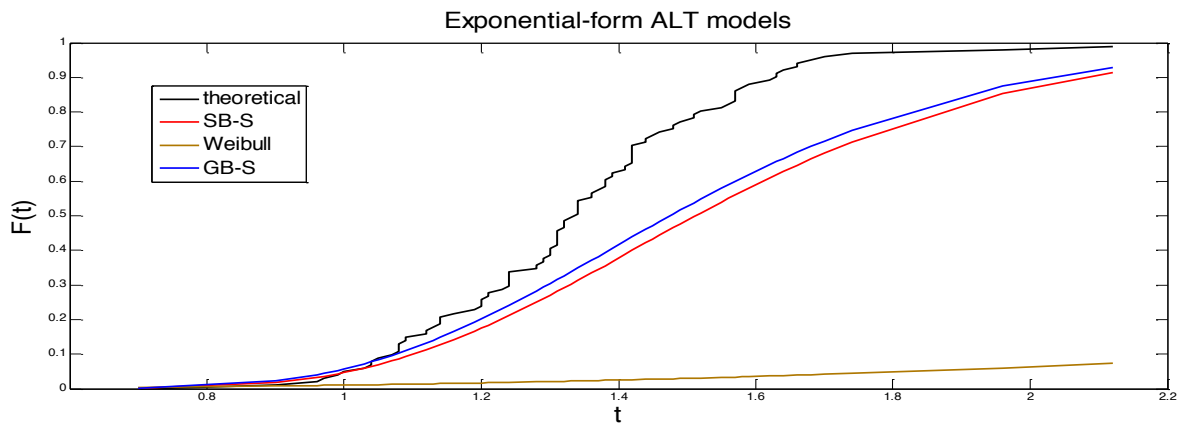


Figure 6.2 Predicted *cdf* (Data sets 1&2) of three general models and theoretical *cdf*

The Weibull accelerated model results in the largest SSEs for all scenarios implying that its prediction as an Accelerated Failure Time (AFT) model for these fatigue data is inaccurate. The GB-S accelerated model has the smallest SSEs for both inverse power law and the general cases.

For the general accelerated models, the estimates of the SB-S and GB-S's shape parameters are almost identical (estimates of  $\lambda$  are close to 0.5). For the inverse power law accelerated models, there exist significant differences among the three models in terms of SSE and the estimates of parameters. Clearly, GB-S model provides the most accurate prediction among all models.

Now we use data sets 2 and 3 to conduct similar estimation procedure. Table 6.2 provides the estimation of the parameters as well as SSEs. Figures 6.3 and 6.4 plot the predicted *cdf* of each accelerated model and theoretical *cdf*:

Table 6.2 Estimated Parameters and SSEs of each accelerated model (Sets 2&3)

Inverse power law Weibull accelerated model	
$\hat{k} = 4.950, \hat{\gamma} = 323.241, \hat{\eta} = 4.552$	SSE=11.407
Inverse power law SB-S accelerated model	
$\hat{\alpha} = 0.166, \hat{\gamma} = 1496.527, \hat{\eta} = 6.211$	SSE=1.754
Inverse power law GB-S accelerated model	
$\hat{\alpha} = 0.029, \hat{\lambda} = 0.089, \hat{\gamma} = 1496.527, \hat{\eta} = 6.211$	SSE=1.628
General Weibull accelerated model	
$\hat{k} = 4.393, \hat{a}_0 = 5.169, \hat{a}_1 = -4.043$	SSE=22.890
General SB-S accelerated model	
$\hat{\alpha} = 0.166, \hat{a}_0 = 7.299, \hat{a}_1 = -6.207$	SSE=1.573
General GB-S accelerated model	
$\hat{\alpha} = 0.160, \hat{\lambda} = 0.482, \hat{a}_0 = 7.299, \hat{a}_1 = -6.207$	SSE=1.571

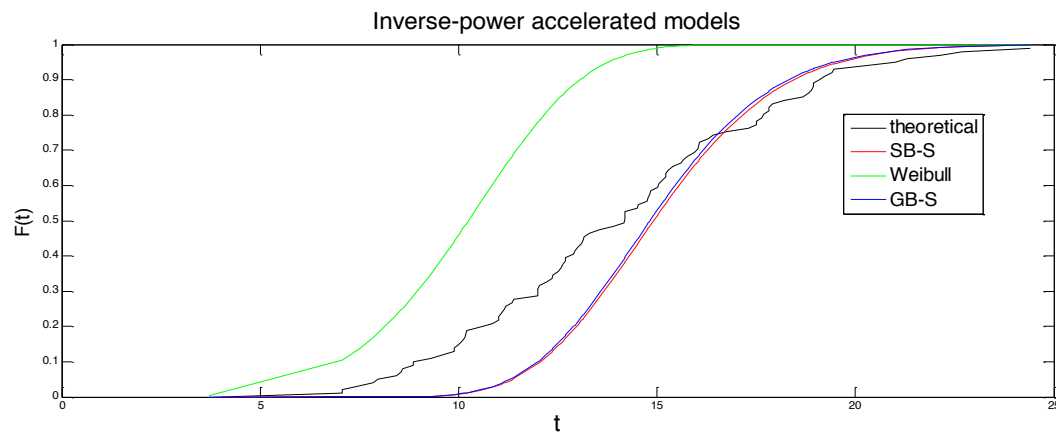


Figure 6.3 Predicted *cdf* (Data sets 2&3) three inverse power law models and theoretical *cdf*

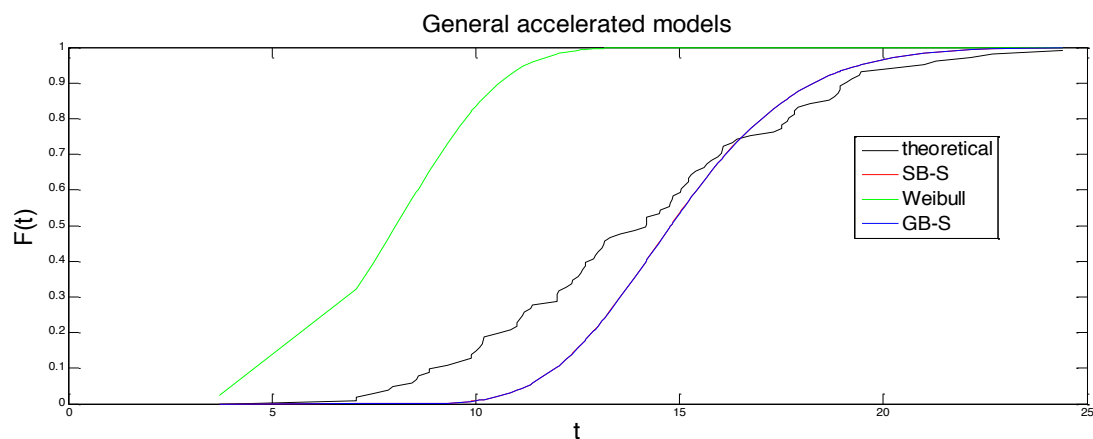


Figure 6.4 Predicted *cdf* (Data sets 2&3) of three general models and theoretical *cdf*

Apparently, if we use data sets 2 and 3 to estimate the parameters, GB-S accelerated model still has the smallest SSEs for both inverse power law and general models. Weibull accelerated model fails to provide accurate predictions.

For the general accelerated models, the estimates of the SB-S and GB-S's parameters  $\hat{a}_0$ ,  $\hat{a}_1$  coincide up to three decimal places. It is also worth noting that SB-S and GB-S exhibit almost identical values in terms of SSEs and shape parameters (estimate of

GB-S's  $\lambda$  is closed to 0.5), Fig. 6.4 shows that the *cdf* of SB-S and GB-S overlap.

For the inverse power law accelerated models, GB-S model performs slightly better than SB-S model in terms of SSE. The estimates of the shape parameters  $\alpha$  and  $\lambda$  have significant difference; however, the ratios of  $\hat{\alpha} / \hat{\lambda}$  of SB-S and GB-S models are close.

When applying data sets 1 and 3 to the models, the results are also similar. We now conclude that Weibull accelerated models are not suitable for this group of data while GB-S accelerated model performs best among the three models.

#### 6.4 Accelerated Life Testing Plan

In order to increase the accuracy of reliability prediction at normal operating conditions, a carefully designed ALT plan is required. The test plan is designed to optimize a specified criterion under the design stress level, for example, minimizing the variance of a reliability-related estimate, such as reliability function, or maximizing mean time to first failure or a percentile of failure time, under specific time and cost constraints. In this section, we investigate the design of GB-S based ALT plans for several objectives under both constant stress and step stress cases. We only consider a single type of stress application.

#### 6.4.1 GB-S ALT Plan with Constant Stress

When designing an ALT plan with single constant stress, we need to select the stress types to be used in the experiment, determine the stress levels and the proportion of test units to be allocated to each stress level. Figure 6.5 shows the stress condition of constant stress test.

In this section, we select the temperature as the applying stress; the goal is to determine the selection of the stress level  $z_i$  and the proportion of units  $p_i$  to allocate for each  $z_i$  such that an optimization criterion can be achieved. Of course, the test duration might be predetermined or a decision variable. The following assumptions are necessary:

1. Test is run at three levels of stresses.
2. Total test time is limited to  $\tau$  units of time.
3. A total of  $N$  units are available for testing.
4. The highest level of stress, denoted by  $z_U$ , at which the failure mechanisms remain the same as those at normal operating conditions
5. The operating or design stress condition is denoted by  $z_D$ .

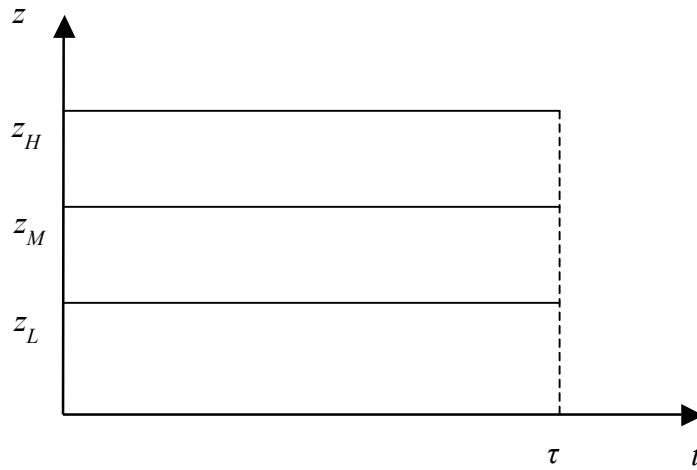


Figure 6.5 Constant-stress test

#### 6.4.1.1 Variance of Reliability Estimate

For GB-S ALT model with exponential acceleration form, we have:

$$R(t; z) = 1 - \Phi \left\{ \frac{1}{\alpha} \left[ \left( \frac{t}{\exp(a_0 + a_1 z)} \right)^\lambda - \left( \frac{t}{\exp(a_0 + a_1 z)} \right)^{-\lambda} \right] \right\} \quad (6.26)$$

$$f(t; z) = \frac{\lambda}{\sqrt{2\pi}at} \left[ \left( \frac{t}{\exp(a_0 + a_1 z)} \right)^\lambda + \left( \frac{\exp(a_0 + a_1 z)}{t} \right)^\lambda \right] \exp \left\{ -\frac{1}{2a^2} \left[ \left( \frac{t}{\exp(a_0 + a_1 z)} \right)^{2\lambda} + \left( \frac{t}{\exp(a_0 + a_1 z)} \right)^{-2\lambda} - 2 \right] \right\} \quad (6.27)$$



Define the indicator function  $I = I(t \leq \tau)$  in terms of the censoring time  $\tau$  as:

$$I = I(t \leq \tau) = \begin{cases} 1 & \text{if } t \leq \tau, \text{ failure observed before time } \tau, \\ 0 & \text{if } t > \tau, \text{ censored at time } \tau. \end{cases}$$

The log likelihood of a single observation with failure time  $t_i$  from Type I censored data at a stress  $z_i$  is:

$$l_i = \ln L(t_i; z_i) = I \ln f(t_i; z_i) + (1 - I) \ln R(t_i; z_i) \quad (6.28)$$

Then the sample log likelihood  $l$  for  $n$  independent observations is:

$$l = \sum_{i=1}^n l_i \quad (6.29)$$

Taking the first partial derivatives with respect to the model parameters, we obtain:

$$\begin{aligned} \frac{\partial l}{\partial \alpha} = & \sum_{i=1}^n I_i \left\{ -\frac{1}{\alpha} + \frac{1}{\alpha^3} \left[ \left( \frac{t_i}{e^{a_0 + a_1 z}} \right)^\lambda - \left( \frac{t_i}{e^{a_0 + a_1 z}} \right)^{-\lambda} \right]^2 \right\} \\ & + \sum_{i=1}^n (1 - I_i) \left\{ \frac{\frac{1}{\sqrt{2\pi}\alpha^2} \exp \left\{ -\frac{1}{2\alpha^2} \left[ \left( \frac{t_i}{\exp(a_0 + a_1 z)} \right)^\lambda - \left( \frac{t_i}{\exp(a_0 + a_1 z)} \right)^{-\lambda} \right] \right\}}{1 - \Phi \left\{ \frac{1}{\alpha} \left[ \left( \frac{t_i}{\exp(a_0 + a_1 z)} \right)^\lambda - \left( \frac{t_i}{\exp(a_0 + a_1 z)} \right)^{-\lambda} \right] \right\}} \right. \\ & \cdot \left. \left[ \left( \frac{t_i}{\exp(a_0 + a_1 z)} \right)^\lambda - \left( \frac{t_i}{\exp(a_0 + a_1 z)} \right)^{-\lambda} \right] \right\} \end{aligned} \quad (6.30)$$

$$\begin{aligned}
\frac{\partial l}{\partial a_1} = & \sum_{i=1}^n I \lambda z \left\{ - \frac{\left[ \left( \frac{t}{\exp(a_0 + a_1 z)} \right)^\lambda - \left( \frac{t}{\exp(a_0 + a_1 z)} \right)^{-\lambda} \right]}{\left[ \left( \frac{t}{\exp(a_0 + a_1 z)} \right)^\lambda + \left( \frac{t}{\exp(a_0 + a_1 z)} \right)^{-\lambda} \right]} \right. \\
& \left. + \frac{\left[ \left( \frac{t}{\exp(a_0 + a_1 z)} \right)^{2\lambda} - \left( \frac{t}{\exp(a_0 + a_1 z)} \right)^{-2\lambda} \right]}{\alpha^2} \right\} \\
& + \sum_{i=1}^n (1 - I_i) \left\{ \frac{\frac{\lambda z}{\sqrt{2\pi\alpha}} \exp \left\{ -\frac{1}{2\alpha^2} \left[ \left( \frac{t_i}{\exp(a_0 + a_1 z)} \right)^\lambda - \left( \frac{t_i}{\exp(a_0 + a_1 z)} \right)^{-\lambda} \right] \right\}}{1 - \Phi \left\{ \frac{1}{\alpha} \left[ \left( \frac{t_i}{\exp(a_0 + a_1 z)} \right)^\lambda - \left( \frac{t_i}{\exp(a_0 + a_1 z)} \right)^{-\lambda} \right] \right\}} \right\} \\
& \cdot \left[ \left( \frac{t_i}{\exp(a_0 + a_1 z)} \right)^\lambda - \left( \frac{t_i}{\exp(a_0 + a_1 z)} \right)^{-\lambda} \right] \quad (6.31)
\end{aligned}$$

$$\begin{aligned}
\frac{\partial l}{\partial \lambda} = & \sum_{i=1}^n I \left\{ \frac{1}{\lambda} + \frac{\log \left( \frac{t}{\exp(a_0 + a_1 z)} \right) \left[ \left( \frac{t}{\exp(a_0 + a_1 z)} \right)^\lambda - \left( \frac{t}{\exp(a_0 + a_1 z)} \right)^{-\lambda} \right]}{\left[ \left( \frac{t}{\exp(a_0 + a_1 z)} \right)^\lambda + \left( \frac{t}{\exp(a_0 + a_1 z)} \right)^{-\lambda} \right]} \right\} \\
& - \frac{\log \left( \frac{t}{\exp(a_0 + a_1 z)} \right) \left[ \left( \frac{t}{\exp(a_0 + a_1 z)} \right)^{2\lambda} - \left( \frac{t}{\exp(a_0 + a_1 z)} \right)^{-2\lambda} \right]}{\alpha^2} \right\} \\
& + \sum_{i=1}^n (1 - I_i) \left\{ \frac{\frac{1}{\sqrt{2\pi\alpha}} \exp \left\{ -\frac{1}{2\alpha^2} \left[ \left( \frac{t_i}{\exp(a_0 + a_1 z)} \right)^\lambda - \left( \frac{t_i}{\exp(a_0 + a_1 z)} \right)^{-\lambda} \right] \right\}}{1 - \Phi \left\{ \frac{1}{\alpha} \left[ \left( \frac{t_i}{\exp(a_0 + a_1 z)} \right)^\lambda - \left( \frac{t_i}{\exp(a_0 + a_1 z)} \right)^{-\lambda} \right] \right\}} \right\} \\
& \cdot \log \left( \frac{t}{\exp(a_0 + a_1 z)} \right) \left[ \left( \frac{t_i}{\exp(a_0 + a_1 z)} \right)^\lambda - \left( \frac{t_i}{\exp(a_0 + a_1 z)} \right)^{-\lambda} \right] \quad (6.32)
\end{aligned}$$

Setting these four equations equal to zero and solving them simultaneously, we obtain the maximum likelihood estimates for the model parameters.

The elements of the Fisher information matrix for an observation are the negative

expectations of the second-partial derivatives with respect to the model parameters as shown below:

$$F = \begin{pmatrix} E\left(-\frac{\partial^2 l}{\partial \alpha^2}\right) & E\left(-\frac{\partial^2 l}{\partial \alpha \partial a_0}\right) & E\left(-\frac{\partial^2 l}{\partial \alpha \partial a_1}\right) & E\left(-\frac{\partial^2 l}{\partial \alpha \partial \lambda}\right) \\ E\left(-\frac{\partial^2 l}{\partial \alpha \partial a_0}\right) & E\left(-\frac{\partial^2 l}{\partial a_0^2}\right) & E\left(-\frac{\partial^2 l}{\partial a_0 \partial a_1}\right) & E\left(-\frac{\partial^2 l}{\partial a_0 \partial \lambda}\right) \\ E\left(-\frac{\partial^2 l}{\partial \alpha \partial a_1}\right) & E\left(-\frac{\partial^2 l}{\partial a_0 \partial a_1}\right) & E\left(-\frac{\partial^2 l}{\partial a_1^2}\right) & E\left(-\frac{\partial^2 l}{\partial a_1 \partial \lambda}\right) \\ E\left(-\frac{\partial^2 l}{\partial \alpha \partial \lambda}\right) & E\left(-\frac{\partial^2 l}{\partial a_0 \partial \lambda}\right) & E\left(-\frac{\partial^2 l}{\partial a_1 \partial \lambda}\right) & E\left(-\frac{\partial^2 l}{\partial \lambda^2}\right) \end{pmatrix}$$

If  $Np_1$  of the test units are tested at the low stress level  $z_L$ , and  $F_L$  is the Fisher information matrix for a test unit, similarly,  $Np_2$  units and  $N(1 - p_1 - p_2)$  units are tested at medium stress level  $z_M$  and high stress level  $z_H$ ,  $F_M$  and  $F_H$  are the corresponding Fisher information matrix for a test unit, then the Fisher information matrix for the entire sample is

$$F = Np_1 F_L + Np_2 F_M + N(1 - p_1 - p_2) F_H$$

Then we obtain the variance covariance matrix  $\Sigma$  of the maximum likelihood estimates  $\hat{\alpha}, \hat{\lambda}, \hat{a}_0, \hat{a}_1$ , which is the inverse of the corresponding Fisher information matrix.

With the optimal criterion to minimize the asymptotic variance of the reliability estimate over a prespecified period of time  $T$  at the design stress  $z_D$ , we formulate the objective function:

$$\text{Min } \int_0^T \text{Var}[\hat{R}(t; z_D)] dt.$$

Decision variables:

$z_L, z_M, z_H$ : low, medium, high stress levels respectively

$p_1, p_2, p_3$ : proportion of test units allocated to  $z_L, z_M, z_H$ , respectively

Constraints:

$$0 \leq p_i \leq 1, \quad i = 1, 2, 3$$

$$\sum_{i=1}^3 p_i = 1$$

$$z_D \leq z_L \leq z_M \leq z_H \leq z_U$$

$$z_M = \frac{z_L + z_H}{2}$$

$$Np_i \Pr[t \leq \tau | z_i] \geq MNF, \quad i = 1, 2, 3$$

Where  $MNF$  is the minimum numbers of failures at each stress level  $z_i$ .

### 6.4.1.2 Mean Time to First Failure or Quantile Failure

Early failures increase the warranty cost significantly. Therefore estimation of low quantile failures at design stress using accelerated life testing data is important. Also, the time of the first failure in a batch of  $N$  devices is the specific case of lower life quantile. Therefore, we propose to determine the optimal test plan with respect to maximize the mean time of the first failure in a group of  $N$  units at normal operating conditions. Also we consider another optimal criterion that maximizing the lower quantile failure at normal operating conditions.

#### 6.4.1.2.1 Quantile Failure

Let  $t_p$  be the  $p$ -th quantile of the failure time at normal operating conditions, then:

$$F(t_p; z_D) = \Phi \left\{ \frac{1}{\alpha} \left[ \left( \frac{t_p}{\exp(a_0 + a_1 z_D)} \right)^\lambda - \left( \frac{t_p}{\exp(a_0 + a_1 z_D)} \right)^{-\lambda} \right] \right\} = p \quad (6.33)$$

We solve:

$$t_p = e^{a_0 + a_1 z_D} \cdot \left( \frac{\alpha \Phi^{-1}(p) + \sqrt{[\alpha \Phi^{-1}(p)]^2 + 4}}{2} \right)^{\frac{1}{\lambda}} \quad (6.34)$$

Now we formulate the optimization problem with the objective to maximize the time of the  $p$ -th percentile of the failures under normal operating conditions, that is:

$$\text{Max } t_p$$

Constraint:

$$0 \leq p_i \leq 1, \quad i = 1, 2, 3$$

$$\sum_{i=1}^3 p_i = 1$$

$$z_D \leq z_L \leq z_M \leq z_H \leq z_U$$

$$z_M = \frac{z_L + z_H}{2}$$

$$Np_i \Pr[t \leq \tau \mid z_i] \geq MNF_i, \quad i = 1, 2, 3$$

Here we have the decision variable  $x_{\%}$  where

$$x_{\%} = \begin{bmatrix} z_L \\ z_M \\ z_H \\ p_1 \\ p_2 \\ p_3 \end{bmatrix}$$

We maximize the  $p$ -th percentile of the failures by searching a group of most satisfying model parameters. Those parameters are estimated base on the accelerated data. Obviously, different allocation of accelerated stress and proportion of test units provide different experimental data.

#### 6.4.1.2.2 Mean Time to First Failure

To determine the optimal test plan based on the criterion of maximizing the mean time to first failure in a group of  $N$  units at normal operating conditions, we first derive the analytic expression of the time of first failure for  $N$  units as follows:

Assuming the failure time of a single unit follows a GB-S distribution. Then we have:

$$\frac{dF(t|z_D)}{dt} = Nf(t|z_D) \left( \int_t^\infty f(t'|z_D) dt' \right)^{N-1}$$

We now determine the  $\frac{dF_1(t|z_D)}{dt}$  that the first failure of  $N$  devices occurs in  $[t, t + dt]$ . This can be expressed as:

$$f_1(t|z_D) = \frac{dF_1(t|z_D)}{dt} = Nf(t|z_D) \left[ \int_t^\infty f(t'|z_D) dt' \right]^{N-1} \quad (6.35)$$

Then the mean time to first failure is:

$$\begin{aligned}
 E[t_1] &= \int_0^\infty t \cdot \left[ \frac{dF_1(t|z_D)}{dt} \right] \cdot dt = \int_0^\infty t \cdot \left[ \frac{dF_1(t|z_D)}{dt} \right] \cdot dt \\
 &= \int_0^\infty t Nf(t|z_D) \cdot R(t|z_D)^{N-1} dt
 \end{aligned} \tag{6.36}$$

Then we formulate the optimal problem as:

$$\begin{aligned}
 \text{Max } E[t_1] &= \int_0^\infty t \cdot \left[ \frac{dF_1(t|z_D)}{dt} \right] \cdot dt = \int_0^\infty t \cdot \left[ \frac{dF_1(t|z_D)}{dt} \right] \cdot dt \\
 &= \int_0^\infty t Nf(t|z_D) \cdot R(t|z_D)^{N-1} dt
 \end{aligned}$$

Constraints:

$$0 \leq p_i \leq 1, \quad i=1,2,3$$

$$\sum_{i=1}^3 p_i = 1$$

$$z_D \leq z_L \leq z_M \leq z_H \leq z_U$$

$$z_M = \frac{z_L + z_H}{2}$$

$$Np_i \Pr[t \leq \tau | z_i] \geq MNF_i, \quad i=1,2,3$$



### 6.4.1.3 Numerical Example

An accelerated life test is to be conducted at three temperature levels in order to estimate the life distribution of the units at design temperature of 50°C. The test needs to be completed in 250 hours. The total number of units to be placed under test is 200 units. To avoid the introduction of failure mechanisms other than those expected at the design temperature, the testing temperature cannot exceed 250°C. The minimum number of failures for each of the three temperatures is specified as 20.

We use  $1/(\text{Absolute Temperature})$  as the covariate  $z$  in the ALT model, i.e., the design stress level  $z_D = 1/323.16\text{K}$ , and the highest stress level  $z_U = 1/523.16\text{K}$ . Also, a baseline experiment is conducted to obtain initial values for the GB-S accelerated model. These values are:

$$\hat{\alpha} = 0.5, \hat{\lambda} = 0.6, \hat{a}_0 = 0.001, \hat{a}_1 = -3000$$

We use the initial baseline values for the model parameters, the design stress level  $z_D$  and highest stress level  $z_U$  as well as total test units  $N$ , test duration  $\tau$  and minimum number of failures for each stress level. The optimum plans derived that optimize the objective function and meet the constraints are shown in Table 6.3:

Table 6.3 Optimal solutions to different objectives with constant stress

Objective (Max)	Solution
25% quantile failure	$p_1 = 0.56, p_2 = 0.28, p_3 = 0.16$ $z_L = 89, z_M = 158, z_H = 227$
Mean time to first failure	$p_1 = 0.58, p_2 = 0.29, p_3 = 0.13$ $z_L = 101.7, z_M = 175.8, z_H = 239.9$

#### 6.4.2 GB-S ALT Plan with Step Stress

A step-stress ALT plan allows test conditions to change during the testing time. The stress on each unit is not constant but increases by planned steps at specified times. The test starts at a low stress. At the specified stress change time, the stress increases and holds constant for a specified time. Such step is repeated until all the test units fail. The step-stress assures that failures occur more quickly.

A simple step-stress tests use only two stress levels (Figure 6.6). In a simple time-step test, units are initially placed on test at low stress level and run until a specified time. Then the stress changes to the high stress level and the test is continued until a predetermined censoring time. In this section we present the optimum simple time-step tests which are defined by optimal low stress level  $z_1$  and optimal stress change point  $\tau_1$ .

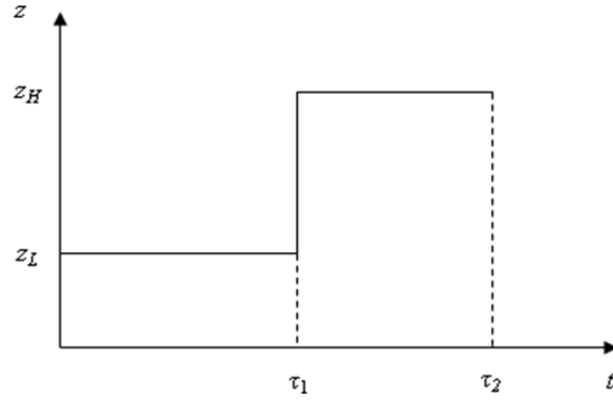


Figure 6.6 Simple step-stress test

#### 6.4.2.1 Cumulative Damage Model

Let  $F_i(t)$  denote *cdf* of time to failure for units run at constant stress  $z_i$ ,  $i=1,2$ .

Suppose step 1 at stress  $z_1$  runs to time  $\tau_1$ . The population *cdf* of units failed by time  $t$  in step 1 is:  $F_0(t) = F_1(t)$ . Step 2 has an equivalent start time  $\tau_1'$  which is the solution of  $F_2(\tau_1') = F_1(\tau_1)$ . More specifically, for the GB-S model:

$$F_{GB-S}(\tau_1; z_1) = F_{GB-S}(\tau_1'; z_2)$$

That is:

$$\begin{aligned} & \Phi \left\{ \frac{1}{\alpha} \left[ \left( \frac{\tau_1}{\exp(a_0 + a_1 z_1)} \right)^\lambda - \left( \frac{\tau_1}{\exp(a_0 + a_1 z_1)} \right)^{-\lambda} \right] \right\} \\ &= \Phi \left\{ \frac{1}{\alpha} \left[ \left( \frac{\tau_1'}{\exp(a_0 + a_1 z_2)} \right)^\lambda - \left( \frac{\tau_1'}{\exp(a_0 + a_1 z_2)} \right)^{-\lambda} \right] \right\} \\ &\Rightarrow \tau_1' = \frac{e^{a_0 + a_1 z_2}}{e^{a_0 + a_1 z_1}} \tau_1 \end{aligned}$$

The *cdf* of units failing by time  $t > \tau_1$  is:

$$F_{GB-S}(t) = F_{GB-S}(t - \tau_1 + \tau'_1; z_2)$$

#### 6.4.2.2 Likelihood Function

A test unit may either fail under stress level  $z_1$  before the stress changes at time  $\tau_1$  or does not fail by time  $\tau_1$  and continues to run either to failure or to censoring time  $\tau_2$  at stress level  $z_2$ . First, we define the indicator function  $I_1 = I_1(t \leq \tau_1)$  in terms of the stress change point  $t_1$  and the indicator function  $I_2 = I_2(t \leq \tau_2)$  in terms of the censoring time  $\tau_2$  by:

$$I_1 = I_1(t \leq \tau_1) = \begin{cases} 1 & \text{if } t \leq \tau_1, \text{ failure observed before time } \tau_1, \\ 0 & \text{if } t > \tau_1, \text{ failure observed after time } \tau_1. \end{cases}$$

$$I_2 = I_2(t \leq \tau_2) = \begin{cases} 1 & \text{if } t \leq \tau_2, \text{ failure observed before time } \tau_2, \\ 0 & \text{if } t > \tau_2, \text{ censored at time } \tau_2. \end{cases}$$

Where  $\tau_1 \leq \tau_2$ .

The log likelihood of the single observation  $t$  is expressed as:

$$\ln L(t; z) = I_2 \{I_1[\ln f(t; z_1)] + (1 - I_1)[\ln f(t'; z_2)]\} + (1 - I_2)[- \Lambda(t'; z_2)] \quad (6.37)$$

Where,  $t' = t - \tau_1 + \tau'_1$  and  $\Lambda(t'; z_2)$  is the cumulative hazard function. Then we can obtain the first partial derivatives with respect to each parameter and construct the variance covariance matrix.

### 6.4.2.3 Formulating Optimal Problems

We optimally design a simple step-stress ALT plan under the constraints of available test units  $N$ , censoring time  $\tau_2$  and specification of minimum number of failures  $MNF$  at low stress level  $z_1$ . The optimal decision variables – low stress level  $z_1^*$  and stress change time  $\tau_1^*$  are determined by solving the nonlinear optimization problem.

#### 6.4.2.3.1 Variance of Reliability Estimate

To design a simple step-stress ALT plan such that the variance of the reliability estimate at design stress is minimized over a prespecified period of time  $T$ . we formulate the problem as:

Objective function:

$$\text{Min} \quad \int_0^T \text{Var}[\hat{R}(t; z_D)] dt$$

Constraint:

$$N \cdot \Pr(t \leq \tau_1; z_1) \geq MNF_1$$

$$z_D \leq z_1 \leq z_2 = z_H$$

The decision variables are the low stress level  $z_L$  and time to change the stress level  $\tau_1$

represented by  $\begin{bmatrix} z_L \\ \tau_1 \end{bmatrix}$ . In all the following formulations for step-stress test plans the

decision variables are  $\begin{bmatrix} z_L \\ \tau_1 \end{bmatrix}$ .

#### 6.4.2.3.2 Quantile Failure and Mean Time to First Failure

If we optimally design the test such that the time of the  $p$ -th percentile of the failures under normal operating conditions is maximized, the problem can be formulated as:

$$\text{Max } t_p$$

Constraint:

$$N \cdot \Pr(t \leq \tau_1; z_1) \geq MNF_1$$

$$z_D \leq z_1 \leq z_2 = z_H$$

Also, if the objective is to maximize the mean time to first failure, we formulate the problem as:

$$\begin{aligned} \text{Max } E[t_1] &= \int_0^\infty t \cdot \left[ \frac{dF_1(t|z_D)}{dt} \right] \cdot dt = \int_0^\infty t \cdot \left[ \frac{dF_1(t|z_D)}{dt} \right] \cdot dt \\ &= \int_0^\infty t N f(t|z_D) \cdot R(t|z_D)^{N-1} dt \end{aligned}$$

Constraints:

$$N \cdot \Pr(t \leq \tau_1; z_1) \geq M N F_1$$

$$z_D \leq z_1 \leq z_2 = z_H$$

Here we also assume that pre-estimates  $(\hat{\alpha}, \hat{a}_0, \hat{a}_1, \hat{\lambda})$  are available through either the baseline experiments or engineering experience.

#### 6.4.2.4 Numerical Example

A simple step stress accelerated life test is conducted in order to estimate the performance of units at design temperature of 50°C. The test needs to be completed in 250 hours. The total number of test units placed under test is 200 units. To avoid the introduction of failure mechanisms other than those expected at the design

temperature, the testing temperature cannot exceed  $250^{\circ}\text{C}$ . The minimum number of failures for low temperature is specified as 40. Again, the initial values of parameters for the GB-S accelerated model are:  $\hat{\alpha} = 0.5, \hat{\lambda} = 0.6, \hat{a}_0 = 0.001, \hat{a}_1 = -3000$

We use the initial baseline values for the model parameters, the design stress level  $z_D$  and highest stress level  $z_U$  as well as total test units  $N$ , test duration  $\tau$  and minimum number of failures for low stress level  $MNF$ . The solutions that optimize the objective functions and meet the constraints are shown in Table 6.4:

Table 6.4 Optimal solutions to different objectives with step stress

Objective (Max)	Solution
25% percentile of failures	$z_L = 161.1^{\circ}\text{C}, \quad \tau_1 = 143.0$
Mean time to first failure	$z_L = 177.5^{\circ}\text{C}, \quad \tau_1 = 129.1$

## 6.5 Conclusion

In this chapter, we investigate the GB-S accelerated model in details. We start with developing GB-S based ALT models, followed by the parameter estimation. Then we compare the performance of GB-S accelerated model with SB-S and Weibull based ALT models. The GB-S accelerated model is validated by fitting the model to several data sets at accelerated conditions to obtain the parameters of the model which are



then used for reliability prediction at normal operating conditions. We also develop the GB-S based accelerated life testing plans for reliability performance prediction. The constant stress ALT plans determine the levels for each stress type and the number of test units allocated to each level in order to optimize different objectives at normal operating conditions. Similar plans for simple step stress which determine the lower stress level and stress changing time are also developed.

## CHAPTER 7

### CONCLUSION AND FUTURE WORK

#### 7.1 Conclusion

In this thesis, we investigate a general Birnbaum-Saunders (GB-S) distribution in details. After briefly review previous and current research on B-S distribution in chapter 2 and 3, we obtain several conclusions from our research.

In chapter 4, we investigate the GB-S distribution and obtain its characteristics and properties. We mention that the moments of GB-S distribution does not exist for some conditions. We also overcome the limitation of the SB-S distribution in modeling different types of failure rates by presenting the sufficient and necessary conditions that enable GB-S distribution to model multiple failure conditions. More specifically, by introducing a new shape parameter, the shape of GB-S distribution can be increasing, upside-down and roller coaster. In addition, extensive simulation verifies that GB-S hazard function is more flexible than SB-S distribution in modeling failure data.

In chapter 5, we investigate the estimation of GB-S's parameters. We utilize MLE and MMLE to present the estimation equations and variances and compare the

performances of the two parameter estimation methods. Simulation study shows that MMLE provides a satisfactory estimation of GB-S distribution's parameters under most of the conditions, especially when MLE is highly biased as sample size is small

There is research in the literature that deals with the application of SB-S distribution to ALT. However, the GB-S ALT has not been investigated. In chapter 6, we develop the first GB-S based accelerated model. We also develop other ALT models with known failure time distribution and life-stress relationship. Comparison shows that the GB-S accelerate model is most suitable in modeling accelerated fatigue data. Besides, we optimally design the GB-S ALT plan that result in accurate reliability performances estimate at normal operating conditions.

## **7.2 Future Work**

Currently, we investigate the accelerated GB-S model and design the ALT plan based on the GB-S model with the simplest stress condition (single stress type). The research can be extended to the multiple stresses ALT plan that investigates the best combination of different stress types and their stress levels, which is much more complicated because of the uncertainty of interaction of the stresses and other factors.

Also, the research on the GB-S life model can be extended to the accelerated degradation life testing (ADT) or degradation modeling at normal conditions. Combining ALT data and degradation data to provide better estimates of reliability at

normal conditions is another challenging research topic.

## Reference

- Bhattacharyya, G.K. and Fries, A., 1980. Fatigue failure models: Birnbaum-Saunders vs Inverse Gaussian. *IEEE Transaction on Reliability*, 31(5), 439-440.
- Birnbaum, Z.W. and Saunders, S.C., 1968. A new family of life distribution. *Applied Probability*, 52(6), 319-327.
- Chang, D.S. and Tang, L.C., 1993. Reliability bounds and critical time for the Birnbaum-Saunders distribution. *IEEE Transaction on Reliability*, 42 (3), 464-469.
- Cohen, A.C. and Whitten, B.J., 1980. Estimation in the three-parameter log-normal distribution. *American Statistical Association*, 75 (370), 399-404.
- Cordeiro, G.M. and Lemonte, A.J., 2011. The  $\beta$ -Birnbaum-Saunders distribution: An improved distribution for fatigue life modeling. *Computational Statistics & Data Analysis*, 55 (3), 1145-1461.
- Desmond, A.F., 1985. Stochastic models of failure in random environments. *The Canadian Journal of Statistics*, 13 (2), 171-183.
- Desmond, A.F., 2012. A mixed effects log-linear model based on the Birnbaum-Saunders distribution. *Computational Statistics & Data Analysis*. 56 (2), 399-407.
- Díaz-García, J.A. and Dominguez-Molina, J.R., 2005. Generalized Birnbaum-Saunders and sinh-normal distributions. *Comunicación Técnica*, 5(1), 1-19.
- Díaz-García, J.A. and Leiva-Sánchez, V., 2002. A new family of life distribution based on Birnbaum-Saunders distribution. *Comunicación Técnica*, 2(1), 1-16.
- Dupuis, D.J. and Mills, J.E., 1998. Robust estimation of Birnbaum-Saunders distribution. *IEEE Transaction on Reliability*, 47 (1), 88-95.
- Elsayed, E.A., 2012. *Reliability Engineering*. 2<sup>nd</sup> ed. New Jersey: John Wiley & Sons.
- Engelhardt, M., Bain, L.J. and Wright, F.T., 1981. Inferences on the Parameters of the Birnbaum-Saunders Fatigue Life Distribution Based on Maximum Likelihood Estimation. *American Statistical Association*, 23 (3), 251-255.

- Escobar, L.A. and Meeker, W.Q., 2006. A review of accelerated testing models. *Statistical Science*, 21 (4), 552-577.
- Glaser, R.E., 1980. Bathtub and related failure rate characterizations. *Journal of the American Statistical Association*, 75 (371), 667-672.
- Kundu, D., Kannan, N. and Balakrishnan, D., 2008. On the hazard function of Birnbaum-Saunders distribution and associated inference. *Computational Statistics & Data Analysis*, 52(5), 2692-2702.
- Mann, N.R., Schafer, R.E. and Singpurwalla, N.D., 1974. *Methods for Statistical Analysis of Reliability and Life Data*. New York: John Wiley & Sons.
- Meintains, S.G., 2010. Inference procedures for the Birnbaum-Saunders distribution and its generalizations. *Computational Statistics & Data Analysis*, 54 (2), 367-373.
- Ng, H.K.T, Kundu, D. and Balakrishnan, D., 2003. Modified moment estimation for the two-parameter Birnbaum-Saunders distribution. *Computational Statistics & Data Analysis*, 43 (2003), 283-298.
- Owen, W.J., 2004. Another look at the Birnbaum-Saunders distribution. Available from: <http://www.stat.lanl.gov/MMR2004/Extended%20Abstract/WOwonn.pdf>.
- Owen, W.J., 2006. A new three-parameter extension to the Birnbaum-Saunders distribution. *IEEE Transactions on Reliability*, 55 (3), 457-479.
- Rieck, J.R., 1999. A Moment-generating Function with Application to the Birnbaum-Saunders Distribution. *Communications in Statistics-----Theory and Method*, 28 (9), 2213-2222.
- Santos-Neto, M., 2012. On new parameterizations of the Birnbaum-Saunders distribution. *Pak. J. Statist*, 28 (1), 1-26.
- Sen, D., 1999. *Accelerated life testing: concepts and models*. Thesis (MS), Concordia University.
- Wang, B.X., 2012. Generalized interval estimation for the Birnbaum-Saunders distribution. *Computational Statistics & Data Analysis*, 56 (12), 4320-4326.
- Wang, Z., Desmond, A.F. and Lu, X., 2006. Modified censored moment estimation for the two-parameter Birnbaum-Saunders distribution. *Computational Statistics & Data Analysis*, 50 (4), 1033-1051.

Wong, L.K. and Lindstrom, D.L., 1989. Off the bathtub onto the roller-coaster curve [electronic equipment failure]. *Reliability and Maintainability Symposium, 1988. Proceedings., Annual*, 356-363

Zaindin, M., 2009. Parameter estimation of the modified Weibull distribution. *Applied Mathematical Sciences*, 3(11), 541-550.

Zhang, H., 2005. *Modeling and planning accelerated testing with proportional odds*. Dissertation (PHD), Rutgers University.

## Appendix A

### Derivatives of Moments of GB-S Distribution

According to Newton's generalized binomial theorem:

If  $x$  and  $y$  are real numbers with the absolute value of  $x$  is larger than the absolute value of  $y$ ,  $r$  is any complex number, then

$$(x+y)^r \sum_{k=0}^{\infty} \binom{r}{k} x^{r-k} y^k = x^r + rx^{r-1}y + \frac{r(r-1)}{2} x^{r-2}y^2 + \frac{r(r-1)(r-2)}{3!} x^{r-3}y^3 + \dots$$

The relationship between  $T$  and  $Z$  (Eq. (4.4)) can be written as:

$$\left(\frac{T}{\beta}\right)^r = \left(\sqrt{\left(\frac{\alpha Z}{2}\right)^2 + 1} + \frac{\alpha Z}{2}\right)^{\frac{r}{\lambda}} = \sum_{k=0}^{\infty} \binom{\frac{r}{\lambda}}{k} \left[\left(\frac{\alpha Z}{2}\right)^2 + 1\right]^{\frac{r}{2\lambda} - \frac{k}{2}} \left(\frac{\alpha Z}{2}\right)^k$$

Then if  $-\frac{2}{\alpha} < Z < \frac{2}{\alpha}$ , that is  $\left(\frac{\alpha Z}{2}\right)^2 < 1$



$$\begin{aligned}
\left(\frac{T}{\beta}\right)^\gamma &= \sum_{k=0}^{\infty} \binom{\frac{r}{\lambda}}{k} \sum_{s=0}^{\infty} \binom{\frac{r}{2\lambda} - \frac{k}{2}}{s} \left(\frac{\alpha Z}{2}\right)^{2s} \left(\frac{\alpha Z}{2}\right)^k \\
&= \sum_{k=0}^{\infty} \sum_{s=0}^{\infty} \binom{\frac{r}{\lambda}}{k} \binom{\frac{r}{2\lambda} - \frac{k}{2}}{s} \left(\frac{\alpha}{2}\right)^{2s+k} Z^{2s+k}
\end{aligned}$$

If  $Z < -\frac{2}{\alpha}$  or  $Z > \frac{2}{\alpha}$ , that is  $\left(\frac{\alpha Z}{2}\right)^2 > 1$

$$\begin{aligned}
\left(\frac{T}{\beta}\right)^\gamma &= \sum_{k=0}^{\infty} \binom{\frac{r}{\lambda}}{k} \sum_{s=0}^{\infty} \binom{\frac{r}{2\lambda} - \frac{k}{2}}{s} \left(\frac{\alpha Z}{2}\right)^{\frac{r}{\lambda} - 2s - k} \left(\frac{\alpha Z}{2}\right)^k \\
&= \sum_{k=0}^{\infty} \sum_{s=0}^{\infty} \binom{\frac{r}{\lambda}}{k} \binom{\frac{r}{2\lambda} - \frac{k}{2}}{s} \left(\frac{\alpha}{2}\right)^{\frac{r}{\lambda} - 2s} Z^{\frac{r}{\lambda} - 2s}
\end{aligned}$$

If  $Z = -\frac{2}{\alpha}$  or  $\frac{2}{\alpha}$ , that is  $\left(\frac{\alpha Z}{2}\right)^2 = 1$

$$\left(\frac{T}{\beta}\right)^\gamma = \sum_{k=0}^{\infty} \binom{\frac{r}{\lambda}}{k} 2^{\frac{r}{2\lambda} - \frac{k}{2}} \left(\frac{\alpha Z}{2}\right)^k$$

Then we obtain the  $r$ th moment of  $T$  as Eq. (4.11).

## AppendixB

### Roots and Discriminant of Cubic Polynomials

For a cubic polynomial, its roots conditions are determined by its discriminant  $\Delta$ .

According to Shengjin's formula, a cubic polynomial

$$s'(x) = 4ax^3 + 3bx^2 + 2cx + d = Ax^3 + Bx^2 + Cx + D, \quad \text{with discriminant}$$

$\Delta = B'^2 - 4A'C' = -3B^2C^2 - 54ABCD + 81A^2D^2 + 12AC^3 + 12B^3D$ , has the following root conditions:

When  $\Delta < 0$ ,  $s'(x)$  has three roots which we place in order of  $x_{31}' < x_{32}' < x_{33}'$ :

$$x_{31}' = \min \{x_{31}, x_{32}, x_{33}\} = \min \left\{ \begin{array}{l} \frac{(-3b - 2\sqrt{9b^2 - 24ac}) \cos \left( \frac{\arccos(6b(9b^2 - 24ac) - 12a(6bc - 36ad))}{3} \right)}{12a}, \\ \frac{(-3b + \sqrt{9b^2 - 24ac}) \left\{ \cos \left( \frac{\arccos(6b(9b^2 - 24ac) - 12a(6bc - 36ad))}{3} \right) + \sqrt{3} \sin \left( \frac{\arccos(6b(9b^2 - 24ac) - 12a(6bc - 36ad))}{3} \right) \right\}}{12a}, \\ \frac{(-3b + \sqrt{9b^2 - 24ac}) \left\{ \cos \left( \frac{\arccos(6b(9b^2 - 24ac) - 12a(6bc - 36ad))}{3} \right) - \sqrt{3} \sin \left( \frac{\arccos(6b(9b^2 - 24ac) - 12a(6bc - 36ad))}{3} \right) \right\}}{12a} \end{array} \right\}$$

$$x_{33}' = \max \{x_{31}, x_{32}, x_{33}\} = \max \left\{ \begin{array}{l} \frac{(-3b - 2\sqrt{9b^2 - 24ac}) \cos \left( \frac{\arccos(6b(9b^2 - 24ac) - 12a(6bc - 36ad))}{3} \right)}{12a}, \\ \frac{(-3b + \sqrt{9b^2 - 24ac}) \left\{ \cos \left( \frac{\arccos(6b(9b^2 - 24ac) - 12a(6bc - 36ad))}{3} \right) + \sqrt{3} \sin \left( \frac{\arccos(6b(9b^2 - 24ac) - 12a(6bc - 36ad))}{3} \right) \right\}}{12a}, \\ \frac{(-3b + \sqrt{9b^2 - 24ac}) \left\{ \cos \left( \frac{\arccos(6b(9b^2 - 24ac) - 12a(6bc - 36ad))}{3} \right) - \sqrt{3} \sin \left( \frac{\arccos(6b(9b^2 - 24ac) - 12a(6bc - 36ad))}{3} \right) \right\}}{12a} \end{array} \right\}$$

$$x_{32}' \in \{x_{31}, x_{32}, x_{33}\} \text{ and } x_{31}' < x_{32}' < x_{33}'.$$

When  $\Delta = 0$ ,  $s'(x)$  has two roots  $x_{21}' < x_{22}'$ :

$$x_{21}' = \min\{x_{21}, x_{22}\} = \min\left\{-\frac{3b}{4a} + \frac{6bc - 36ad}{9b^2 - 24ac}, \frac{6bc - 36ad}{2(9b^2 - 24ac)}\right\}$$

$$x_{22}' = \max\{x_{21}, x_{22}\} = \max\left\{-\frac{3b}{4a} + \frac{6bc - 36ad}{9b^2 - 24ac}, \frac{6bc - 36ad}{2(9b^2 - 24ac)}\right\}$$

When  $\Delta > 0$ ,  $s'(x)$  has only one root  $x_{11}$ :

$$x_{11} = \frac{-3b - \sqrt[3]{3b(9b^2 - 24ac) + 6a\left[-(6bc - 36ad)^2 + \sqrt{(6bc - 36ad)^2 - 4(9b^2 - 24ac)(4c^2 - 9bd)}\right]} - \sqrt[3]{3b(9b^2 - 24ac) + 6a\left[-(6bc - 36ad)^2 - \sqrt{(6bc - 36ad)^2 - 4(9b^2 - 24ac)(4c^2 - 9bd)}\right]}}{12a}$$